CHARACTERIZATION OF ULTRA AND NANOFILTRATION COMMERCIAL FILTERS BY LIQUID-LIQUID DISPLACEMENT POROSIMETRY

RENÉ PEINADOR DÁVILA

CHARACTERIZATION OF ULTRA AND NANOFILTRATION COMMERCIAL FILTERS BY LIQUID-LIQUID DISPLACEMENT POROSIMETRY

UNIVERSIDAD DE VALLADOLID

Cover Picture: SEM image from a UF Polyethersulfone Membrane

Universidad de Valladolid

FACULTAD DE CIENCIAS

DEPARTAMENTO DE FÍSICA APLICADA

TESIS DOCTORAL

CHARACTERIZATION OF ULTRA AND NANOFILTRATION COMMERCIAL FILTERS BY LIQUID-LIQUID DISPLACEMENT POROSIMETRY

MEMORIA PARA OPTAR AL GRADO DE DOCTOR
PRESENTADO POR

René Israel Peinador Dávila

Dirigida por:
Dr. José Ignacio Calvo Díez

UNIVERSITY OF VALLADOLID

Universidad de Valladolid

AUTORIZACIÓN DEL DIRECTOR DE TESIS

(Art. 2.1. c de la Normativa para la presentación y defensa de la Tesis Doctoral en la UVa)

D. José Ignacio Calvo Díez, profesor del Departamento de Física Aplicada de la Facultad de Ciencias, como Director de la Tesis Doctoral titulada:
CHARACTERIZATION OF ULTRA AND NANOFILTRATION COMMERCIAL FILTERS BY LIQUID-LIQUID DISPLACEMENT POROSIMETRY.
presentada por D. René Israel Peinador Dávila, alumno del programa de Doctorado en Física, impartido por el departamento de Física Aplicada,

Considero que dicha tesis recoge el trabajo realizado por el interesado a lo largo de varios años, conteniendo aspectos novedosos de investigación sobre la técnica de desplazamiento de fluidos, aplicada a membranas sintéticas, que la hacen merecedora de su defensa y aprobación.

Por todo ello, autorizo la presentación y defensa de la misma.

Valladolid, 15 de mayo de 2013

El Director de la Tesis,

Fdo.: José Ignacio Calvo

SR. PRESIDENTE DE LA COMISIÓN DE DOCTORADO

No basta saber, se debe también aplicar:
No es suficiente querer, se debe también hacer:
Goethe
Poeta, dramaturgo y científico alemán
(1749- 1832)

A mis padres
y especialmente
a Ana

AGRADECIMIENTOS

Al finalizar un trabajo tan arduo y lleno de dificultades como el desarrollo de una tesis doctoral es inevitable padecer un muy humano egocentrismo que te lleva a concentrar la mayor parte del mérito en el aporte que has realizado, pero en cambio si lo analizamos objetivamente te demuestras inmediatamente que la magnitud de este aporte hubiese sido *imposible* sin la participación de muchas personas e instituciones que han facilitado mi evolución para que este trabajo llegue a un feliz término. Por ello, es para mí un verdadero placer utilizar este espacio para ser justo y consecuente con todos ellos, expresándoles mis agradecimientos.

Debo agradecer de manera especial y sincera a mi director de tesis el *Dr José Ignacio Calvo Díez* por haberme dado la oportunidad de aceptarme bajo su dirección. Su apoyo y confianza en mi trabajo y su capacidad para guiar mis ideas, ha sido un aporte incalculable, no solamente en el desarrollo de este trabajo, sino también en mi formación como investigador. Orientación, flexibilidad y rigurosidad en el campo científico, han sido clave del buen trabajo que hemos realizado juntos, el cual no se puede concebir sin su siempre oportuna participación, agradeciéndole en todo momento el haberme facilitado siempre los medios suficientes para llevar a cabo todas las actividades propuestas durante el desarrollo de esta tesis.

Quisiera extender también este agradecimiento a los Dres Antonio Hernández Jiménez, Laura Palacio Martínez y Pedro Prádanos del Pico, todos ellos "cabezas" indiscutibles del SMAP y docentes de la Universidad de Valladolid, con quienes he compartido estos buenos años de trabajo y quienes han estado a mi lado en todo momento.

A todos mis "colegas" de laboratorio, a los que siguen y a los que ya no están, les doy las gracias por haberme apoyado y hecho pasar excelentes momentos: Alberto, Álvaro, Andrea, Blanca, Fernando, Gloria, Liliana, Miguel, Noemí, Raquel, Roberto, Sara, Youssef.

Mis más sinceros agradecimientos a todo el personal del departamento de Física Aplicada, José Carlos, Isaías, Felipe.... y, en especial a Isma, agradecerles sinceramente su apoyo.

También quiero agradecer este trabajo a Juan Marcos Sánz Casado, compañero de estudios y exponente fundamental de esta técnica, dejándome un impresionante legado, siendo el hilo conductor en su implementación y desarrollo, junto a Pablo y Valeriano en las arduas tareas de programación.

Me gustaría además expresar mi gratitud a todo los tutores responsables, personal técnico, profesores, estudiantes y compañeros en mis estancias "fuera de casa" entre ellos al grupo de biorreactores encabezado por los doctores Emilia Mª Guadix Escobar y Antonio Mª Guadix del Departamento de Ingeniería Química de la Universidad de Granada,

y en especial a Mari Carmén Almécija, compañera de trabajo en diferentes estancias, así como en lo personal.

A mis compañeros de laboratorio de investigación y desarrollo, en mi estancia en Sartorius Stedim Biotech® en Göttingen, entre ellos, Celia, Pedro, Thobias, Jan, Roberto, Verónica, ...

A los miembros del Departamento de Química y Química Industrial de la Universidad de Génova, entre los que destaco afectuosamente a Giorgio, Antonio Comite, Silvia, Rafaella por su cálida acogida y especialmente a los Profesores Capanelli y Bottino, por su infinita ayuda, profesionalidad y experiencia en esta técnica, siendo ellos los auténticos pioneros en este campo.

Grazie mile con tutto il cuore

I would like to acknowledge Dr. Volkmar Thom and Kuong To-Vinh, from the R&D Departament of Sartorius-Stedim Biotech®, at Göttingen, for the opportunity they gave me to introduce in research through a collaboration with them, and for the kindness they offered me, which I would never forget.

Ich danke Ihnen sehr

Para todos aquellos que omito por falta de memoria, sin intención de restarles importancia, les agradezco enormemente su apoyo también.

Por último, quiero agradecer a todos mis amigos, que me han brindado su cariño y comprensión en todo momento, siempre atentos a mi evolución, Ángel, Héctor, Gabi, Rubén, Luis Carlos, Fernan, Patri, Jaime, Guty y por supuesto a toda mi *familia*, quienes me han apoyado con cualquier decisión que he tomado y quienes continuamente me animan a continuar en este intenso, pero apasionante camino de la investigación científica.

Muchas Gracias

Acknowledgements

Sartorius-Stedim Biotech® is acknowledged for funding through contract *061/074251* with the Fundación General de la Universidad de Valladolid, including a grant for the author during the period of the experimental work of this thesis.

Universidad de Valladolid, through its program "Ayudas para estancias breves en el desarrollo de tesis doctorales" is acknowledged for the funding of visits to the labs of Sartorius (Göttingen, Germany), Universidad de Génova (Italia) and Universidad de Granada (España).

Contents

RESUMEN

La tecnología de membranas aplicada, entre otros, en procesos como la Ultrafiltración (UF) y la Nanofiltración (NF), se ha convertido en una importante parte de los procesos biotecnológicos de separación en los últimos decenios. Su principal característica, la morfología porosa de los filtros, conducente a un "mecanismo de criba", permite una separación efectiva con altas características de selectividad y realizada en condiciones medioambientales y energéticas muy interesantes.

Ante el desarrollo ingente de los filtros de membrana, se hace necesario un crecimiento en paralelo de las técnicas de caracterización de dicho filtros, como herramientas fundamentales tanto para fabricantes, como usuarios o investigadores.

En este sentido necesitamos conocer de primera mano tanto los parámetros funcionales como los estructurales de la membrana, necesarios para una adecuada elección de la misma con vistas a una determinada aplicación.

La cuestión que se nos plantea es la siguiente: ¿Existe algún método de caracterización que, por sí sólo, nos de una visión clara y fácilmente interpretable de la verdadera estructura y funcionalidad del filtro?.

La respuesta a esta pregunta, evidentemente, es nula. Son tantos los parámetros estructurales y funcionales que contribuyen al conocimiento exacto de la membrana, que no hay ninguna técnica que pueda aportarnos toda esta cantidad de información.

Desde el punto de vista industrial y comercial, el parámetro más utilizado y requerido, con vistas a posibles aplicaciones de los filtros, es el peso molecular de corte (MWCO), aunque es evidente que por sí sólo no constituye una herramienta definitiva para la elección de un filtro de membrana.

La larga experiencia del SMAP en caracterización de membranas nos permite concluir que las técnicas porosimétricas dan información muy interesante, relacionada con el tamaño y la distribución de tamaños presentes en una membrana, información que puede ser convenientemente cotejada con aspectos funcionales de la misma.

En ese sentido, la técnica porosimétrica que podemos considerar más prometedora y completa en el rango de Ultrafiltración, es la Porosimetría de Desplazamiento Líquido-líquido (LLDP), la cual nos da información muy importante sobre este tipo de filtros.

Ahora bien, varios problemas se plantean en cuanto a la mejor aplicación de la técnica LLDP:
a) mejorar las condiciones operativas de la técnica, considerada por muchos investigadores como poco reproducible y complicada desde el punto de vista operativo.
b) extender el rango de aplicación de dicha técnica a membranas de Nanofiltración, en las

que los poros existentes van a estar en el rango cercano al nanómetro.
c) relacionar la información estructural obtenida con datos funcionales, especialmente con el MWCO, a fin de utilizar la técnica LLDP para estimar la aplicabilidad de una membrana a un proceso de separación dado.

A la mejora de estas cuestiones pretende contribuir la tesis presentada, mediante la mejora de la técnica LLDP, automatizando el equipo LLDP desarrollado en el SMAP, optimizando su forma de trabajo y operación y finalmente, extendiendo al máximo su rango de trabajo, a fin de que pueda cubrir tanto el rango de UF como buena parte de las membranas comerciales de NF.

Finalmente se ha buscado correlacionar la información estructural obtenida con el MWCO de las membranas analizadas, de forma que podamos asegurar una fiable estimación de las prestaciones operativas de las membranas en procesos industriales.

ABSTRACT

Membrane Technology applied, among others, in processes such as Ultrafiltration (UF) and Nanofiltration (NF), has become an important part of biotechnological separation processes in recent decades. Its main feature, the morphology of the porous filters, leading to a "sieving mechanism" allows effective separation with high selectivity features and made in energy and environmental conditions very interesting.

Given the enormous development of membrane filters, it becomes necessary the growth in parallel of characterization techniques applied to such filters, as essential tools for both manufacturers and end-users or researchers.

In this sense we need to know most exactly possible, both functional and structural parameters of the membrane, all necessary for a proper choice of that with a view to a particular application.

The question we must face is: Is there a characterization method, by itself, giving us a clear and easily interpretable picture of the true structure and functionality of the filter?.

The answer to this question is obviously no. There are so many structural and functional parameters that contribute to the exact knowledge of the membrane, that there is no technique that can bring us all this wealth of information.

From the industrial and commercial standpoints, the parameter most used and required, in view of possible applications of the filters, it is the molecular weight cut-off (MWCO), although it is clear that by itself is not a definitive tool for choosing a membrane filter.

SMAP group long experience in membrane characterization allows us to conclude that porosimetric techniques give interesting information related to the size and size distribution of the pores present in a membrane, information that can be conveniently checked against functional aspects of it.

In this sense, we can consider that Liquid-liquid displacement porosimetry (LLDP) is the most promising porosimetric technique in the range of Ultrafiltration, thus giving us important information about these filters.

However, several problems arise regarding the best application of the LLDP technique:
a) improvement of the operating conditions of the technique, considered by many researchers to be poorly reproducible and difficult from the standpoint of operating,
b) extension of the application range of this technique to Nanofiltration membranes, in which the pores are mostly in the range close to nanometer,

c) connection of the structural information obtained with functional data, especially with the MWCO, to use the LLDP technique for estimating applicability of a membrane to a given separation process.

To improve these issues, the present thesis aims to contribute by improving the LLDP technique, automating the LLDP equipment developed in the SMAP, optimizing the way they work and operates, and finally, extending at the maximum the working range, so that it can cover both the range of UF and most of commercial NF membranes.

Finally it has been sought to correlate structural information obtained from tested membranes, with their MWCO, so that we can ensure a reliable estimate of the operating performance of the membranes in industrial processes.

ORGANIZACIÓN DE LA MEMORIA

De acuerdo con la normativa vigente (Ejecución de Acuerdos de la Comisión de Doctorado de la Universidad de Valladolid de fecha 10 de mayo de 2010), esta Tesis Doctoral se presenta como compendio de publicaciones.

Además de incluir los diversos artículos publicados (*Capítulos 3-6*) como consecuencia del trabajo doctoral, se introduce mediante una síntesis de los conceptos téorico-experimentales mediante una extensa revisión ("state of the art") de las membranas, los procesos de membranas y las diversas técnicas de caracterización, con especial atención a la técnica de desplazamiento líquido-líquido (*capítulo 2*). Ambos capítulos introductorios permiten situar y enmarcar los contenidos de los artículos publicados en relación con los objetivos generales perseguidos al comienzo de esta tesis.

Los trabajos incluidos en este documento son los siguientes:

1. **Characterization of UF membranes by liquid–liquid displacement porosimetry.**
J.M. Sanz, R. Peinador, J.I. Calvo, A. Hernández, A.Bottino, G. Capannelli.
Desalination, 245 (2009) 546-553.

2. **Characterisation of polymeric UF membranes by liquid–liquid displacement porosimetry.**
René Israel Peinador, José Ignacio Calvo, Pedro Prádanos, Laura Palacio, Antonio Hernández.
Journal of Membrane Science, 348 (2010) 238-244.

3. **Liquid-liquid displacement porosimetry for the characterization of virus retentive membranes.**
René Israel Peinador, José Ignacio Calvo, Khuong ToVinh, Volkmar Thom, Pedro Prádanos and Antonio Hernández.
Journal of Membrane Science, 372 (2011) 366-372.

4. **Liquid-liquid displacement porometry to estimate the molecular weight cut-off of ultrafiltration membranes.**
José Ignacio Calvo, René Israel Peinador, Pedro Prádanos, Laura Palacio, Aldo Bottino, Gustavo Capannelli, Antonio Hernández.
Desalination, 268 (2011) 174-181.

No se incluyen en esta memoria aquellos trabajos o resultados que, siendo realizados en el marco de la financiación del proyecto conjunto entre el SMAP® y la empresa Sartorius-Stedim Biotech®, estén sujetos a propiedad industrial o consistan en información sensible para los competidores de dicha empresa.

THESIS OUTLINE

In accordance with current regulations (from the Doctoral Committee of the University of Valladolid, dated May 10, 2010), this PhD Thesis is presented as a compendium of publications.

Besides including various published articles (Chapters 3-6) as a result of doctoral work, it is introduced by an overview of both theoretical and experimental concepts through an extensive review ("state of the art") of the membranes, membrane processes and various characterization techniques (Chapter 1), with special attention to the technique of liquid-liquid displacement (Chapter 2). Both introductory chapters situate and frame the contents of the articles published in relation to the general objectives pursued at the beginning of this thesis.

The papers included in this document are:

1. **Characterization of UF membranes by liquid–liquid displacement porosimetry.**
J.M. Sanz, R. Peinador, J.I. Calvo, A. Hernández, A.Bottino, G. Capannelli.
Desalination, 245 (2009) 546-553.

2. **Characterisation of polymeric UF membranes by liquid–liquid displacement porosimetry.**
René Israel Peinador, José Ignacio Calvo, Pedro Prádanos, Laura Palacio, Antonio Hernández.
Journal of Membrane Science, 348 (2010) 238-244.

3. **Liquid-liquid displacement porosimetry for the characterization of virus retentive membranes.**
René Israel Peinador, José Ignacio Calvo, Khuong ToVinh, Volkmar Thom, Pedro Prádanos and Antonio Hernández.
Journal of Membrane Science, 372 (2011) 366-372.

4. **Liquid-liquid displacement porometry to estimate the molecular weight cut-off of ultrafiltration membranes.**
José Ignacio Calvo, René Israel Peinador, Pedro Prádanos, Laura Palacio, Aldo Bottino, Gustavo Capannelli, Antonio Hernández.
Desalination, 268 (2011) 174-181.

Not included in this report are those works or results, being conducted under the joint project between SMAP® and Sartorius-Stedim Biotech®, which are subjected to industrial property or consist of sensitive information to competitors of that company.

OBJETIVOS

El objetivo principal de este trabajo experimental es la mejora de la técnica de Porosimetría de Desplazamiento Líquido-líquido y su mejor aplicación al análisis de filtros porosos comerciales.

Para la consecución de este objetivo, diversas líneas simultáneas y complementarias se han seguido:

a) automatización del equipo LLDP existente en el SMAP de la Universidad de Valladolid, equipo desarrollado en cercana colaboración con los Dres. Bottino y Capannelli de la Universidad de Génova,
b) comprobación de las condiciones óptimas de trabajo de las diversas mezclas porosimétricas, de forma que estas puedan ser convenientemente elegidas en función del rango de poros a analizar o de la interacción de dichos líquidos con las membranas estudiadas,
c) estudio teórico de la correlación entre parámetros estructurales y funcionales de los filtros de membrana, buscando conectar la información obtenida de nuestro equipo, con datos funcionales de interés en la aplicación industrial de estos filtros.

Trabajando siempre en dichas líneas, se han realizado varias etapas, que han conducido a la publicación de los diversos artículos relacionados en esta memoria. Estas etapas se pueden resumir como sigue:

1) estudio de varias membranas de UF (tanto abiertas y como de poros más cercanos a NF) y análisis de su información porosimétrica,
2) estudio de varias membranas de NF, con diversas mezclas porosimétricas, en condiciones extremas de incompatibilidad química con los líquidos habituales,
3) estudio de membranas diseñadas para la retención de virus y correlación de la información porosimétrica con información funcional obtenida por variadas técnicas,
4) elaboración de un procedimiento de estimación del peso molecular de corte en membranas de UF y NF y comprobación de su validez en un amplio rango de membranas comerciales.

Todas estas etapas, y su exitosa culminación, deberían permitirnos avanzar en lo que consideramos un objetivo primordial de este trabajo y de la línea de investigación del SMAP que lo sustenta:

Contribuir a la extensión de la técnica LLDP aplicada a la caracterización estructural de membranas sintéticas en el rango de UF-NF, así como su posible estandarización como técnica de referencia en el estudio estructural y funcional de dichas membranas.

SCOPES

The main objective of this experimental work is the improvement of the Liquid-liquid displacement porosimetry and the best application of this technique to the analysis of commercial porous filters.

To achieve this goal, various simultaneous and complementary lines have been followed:

a) automatization of existing LLDP setup, built-up in the SMAP at the University of Valladolid, equipment developed in close collaboration with Drs. Capannelli and Bottino from the University of Genoa,
b) verification of the optimum working conditions of the various porosimetric mixtures, so that they can be suitably chosen according to the range of pores to be analyzed or the interaction of these fluids with the membranes studied,
c) theoretical study of the correlation between structural and functional parameters of the membrane filters, seeking to connect the information obtained from our setup, with functional data of interest in the industrial application of these filters.

Always working on these lines, there have been followed several steps, which led to the publication of several articles herein. These steps can be summarized as follows:

1) study of various UF membranes (both open and those with pores close to NF) and analysis of their porosimetric information,
2) study of various NF membranes by using several porosimetric mixtures, in extreme conditions of chemical incompatibility with the usual liquid pairs,
3) studying membranes designed for retention of viruses and correlation of the porosimetric information with functional information obtained by various techniques,
4) development of a procedure for estimating the molecular weight cut-off in UF and NF membranes and checking their validity in a wide range of commercial membranes.

All these stages, and its successful completion, should allow us to advance in what we consider a primary objective of this work and the research line supported in the SMAP group:

Contribute to the extension of LLDP technique applied to the structural characterization of synthetic membranes in the range of UF-NF and their possible standardization as reference technique in structural and functional studies of these membranes.

CHARACTERIZATION OF ULTRA AND NANOFILTRATION COMMERCIAL FILTERS BY LIQUID-LIQUID DISPLACEMENT POROSIMETRY

CHAPTER 1

1 OVERVIEW OF MEMBRANE SCIENCE AND TECHNOLOGY

1.1 INTRODUCTION

Membrane science and technology have seen the rationalization of production systems in the last decades. Their intrinsic characteristics of efficiency, operational simplicity and flexibility, relatively high selectivity and permeability for the transport of specific components, low energy requirements, good stability under a wide spectrum of operating conditions, environment compatibility, easy control and scale-up; have been confirmed in a large variety of applications and operations[1], both in liquid and gas phases and in a wide spectrum of operating parameters such as pH, temperature, pressure, etc. The possibility of using membrane systems as well as tools for a better design of chemical reactions is becoming attractive and realistic. For biological applications, synthetic membranes provide an ideal mechanical support due to their available surface area per unit volume.

Membranes and membrane processes were first introduced as an analytical tool in chemical and biomedical laboratories; they developed very rapidly into industrial products and methods with significant technical and commercial impact **[1]**. Today, membranes are used on a large scale to produce potable water from sea and brackish water, to clean industrial effluents, to recover valuable constituents, to concentrate, purify, or fractionate macromolecular mixtures in food and drug industries, as well as to separate gases and vapours in petrochemical processes. Membranes are also key components in energy conversion and storage systems, in chemical reactors, artificial organs, and in drug delivery devices. The membranes used in the various applications differ widely in their structure, in their function and the way in which they operate **[2]**, being particularly attractive tools for the separation of molecular mixtures.

1.2 MEMBRANE MARKET

Membrane filtration and separation technologies have undergone significant technological advancement in recent decades **[3]**. Such progress has revolutionized numerous industrial processes, biotechnology developments, as well as purification of urban water supply. Thanks to its ability to effectively separate undesirable constituents from any feedstream with consistent product quality, Membrane. Tech has evolved into a well-accepted method of filtration in many applications **[4]**, being most significative ones: from drinking water and wastewater treatment to seawater desalination; generation of high purity water for cooling powers and boiler feed too; separation of oil and chemicals from industrial waste-streams. Therefore, membrane filtration often plays an indispensable role, without which many of these products would not have existed.

The majority of membrane sales relate to water treatment and medical applications **[5],** both mainly considered as a principal tradeline. In the case of water treatment, for example, only for domestic use, total world demand has increased (see **Table1.1**). about 25% from 2006 to 2011.

1 As molecular separation, fractionation, concentration, purification, clarification, emulsification, crystallization, etc.

Table 1.1 Main membranes demand for domestic use in five years (US M$). Fredonian Goup **[6]**

Membrane Process	**2006**	**2011**
Microfiltration	980	1290
Reverse Osmosis	490	740
Ultrafiltration	420	630
Pervaporation	65	95
Other	155	185
Total Membrane Demand	2110	2940

Other studies report both higher and lower market size, **[7-12]**. In this way, membrane filtration is applicable to a broad range of highly specialized end user markets. The total world sales for membrane modules, are given as current year estimates and forecast for the period from 2006 to 2011 in **Table 1.2**.

Table 1.2 The World Market For Membrane Modules[2] (US$ Million)

Membrane Process	**2006**	**2007**	**2008**	**2009**	**2010**	**2011**
RO/NF	2222	2391	2571	2764	2936	3102
UF	1927	2090	2265	2443	2616	2779
MF	2928	3208	3517	3720	3939	4106
GS	679	758	846	935	1024	1102
Other Liquid Sep.	2605	2887	3200	3405	3598	3775
Total	10361	11334	12399	13267	14113	14864

The estimates *include:*

-All membranes media, whether organic polymer or inorganic.
-All the components of an element or module necessary to hold the medium in place and to house it ready for use.
-All replacement media or modules supplied for installation in existing systems.

The estimates *exclude:*

-Any equipment outside the membrane module design.
-Any or all prefilter for membrane systems.

The present market is focusing in Europe (33.8%), and American Continent (39.9%) followed by Asia (23.5%) and rest of the world (Australia and Africa: 2.8%); this means that almost three-quarters of membranes sales were in Europe and the American continent **[13]**. Main membrane processes (presented in **Fig. 1.1**) are:

2 The market value includes the sale to original equipment manufacturers and replacement parts, from point of sale to end user.

MicroFiltration (MF), this sector-sale is driven by two operation procedures, *dead-end or in-line filtration*, in which the entire fluid flow is forced through the membrane under pressure, and *cross-flow filtration* where the feed solution is circulated across the surface of the filter, producing two streams: a clean particle-free permeate and a concentrated retentate containing the particles. Nowadays, most products-market is moving towards *cross-flow* style of filtration at the expense of *dead-end filtration*. It is used MF for the removal of pathogens (bacteria and some viruses) from potable water as a main line of tertiary treatment of wastewaters or the polishing of fresh water with membrane reactors. MF is presently extending its range downwards in particle size, in order to deal with this form of treatment in a single process step. Additionally, the MF application has considerably expanded **[14],** due to the development of new biopharmaceuticals and new research sectors like genomics.

In the case of Reverse Osmosis and NanoFiltration (RO/NF), these processes has grown rapidly both around 39% from 2006 to present **[15]**; NF is essential in water solutions, and applications for non-aqueous solutions, NF membranes are prepared to work under strong chemical conditions, so they are known as "essentially solvent resistant membranes".

A good future is calling to NF process, as it will serve as an inexpensive pretreatment to current distillation techniques providing reduced overall costs and higher overall efficiency in the preparation of usable water. However, RO is still by far the largest of the two, and its market place is quite a mature one. There will be a continuing interest in RO processes for water desalination, especially in areas where water is already in short supply. This trend will be reinforced by rising of living standards. Chemical and pharmaceutical applications will continue to increase in number.

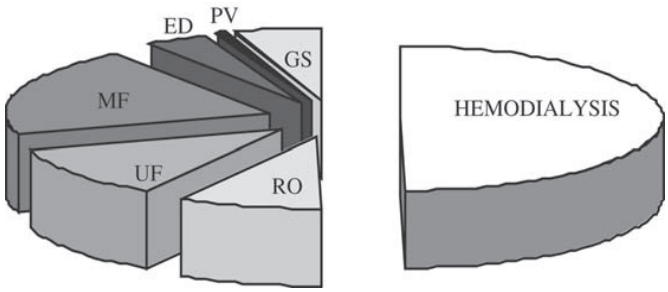

Figure 1.1: Membrane and module sale for different process applications. RO Reverse Osmosis (includes NF NanoFiltration), UF UltraFiltration, MF MicroFiltration, ED ElectroDyalisis, PV Pervaporation and GS GasSeparation.

Very closely following, UltraFiltration (UF) membrane market represents about one-fifth of the total market. UF membranes and modules brought about US$600 million in sales for domestic treatment in 2011 with an expected growing rate of 10% a year. This rate of increase is significantly below (or higher) that all membrane processes presented in

Fig. 1.1. In contrast to RO, the UF market **[16-17]** is shared by a large number of companies, but the leaders are Pall®, Amicon/Millipore® and Koch®. One of the largest industrial sectors for UF is still the recovery of electrocoating paints. UF membranes are also responsible for supplying pure water for the semiconductor industry. Growing demands of ultrahigh purity chemicals in this sector could also be supplied by UF with the availability of chemical-resistant membranes. Oil/water separation is now a large application for UF in industrial sectors such as metal cleaning and wool scouring, and is still growing with the implementation of new environmental legislation. The use of UF in the biotechnology industry is growing even faster than the sector itself.

The development of membrane reactors in Gas Separation (GS) is opening a number of new gas applications, from smaller applications ranging from dehydration of air and natural gas to organic vapor removal from air and Nitrogen streams. In this case, GS processes are growing rapidly from a small base, with a rate higher than 15% per year. This technology **[18]** is expanding rapidly and further growth is likely to continue for the next 10 years. Originally, the market for GS processes was close to US$1100 million, 6.2% in **Fig. 1.1**,but having much by far the highest growth rates of the membrane process segment.

Finally the "Other Liquid Separations Processes" category covers a range of membrane processes, operating by diffusion from the well-established, such as Dyalisis, Electro and Hemodialysis or ion exchange. In the case of Hemodialysis **[19],** is also a very important market, one million patients worldwide benefit from the process, each patient is dialysed approximately three times per week, with a dialyzer containing about $1m^2$ of membrane area. Economies of scale allow these devices to be produced for about US$15 each, and discarded after one or two uses, that implies, around 50% of the total market. Main applications use hollow fibres for waste recovery, food, pharmaceutical industries, analytical and medical applications, but also fuel cells, which are not yet fully commercialized. The total market volume excluding Hemodialysis in 2011 for the other liquid separations category is rising 6.8%.

Membrane field has advanced immensely **[20]**, and it continues advancing, having a special recognition as alternative to conventional applications in the industrial world, which is due to the fact they cover a wide range of applications.

In conclusion, we need them, for environmental and economic sustainability and primary devices. Still some problems remain that need attention, like membrane fouling and membrane chemical stability. Even though, the advantages are more than the inconveniences: economy, environment, versatility and easy to use, membranes are a leading choice for industrial treatment applications and should continue so many years.

1.3 FUNDAMENTALS OF MEMBRANES

1.3.1 Definition and Classification

*In all of the processes named in **Fig. 1.1** membrane behaves as a selective barrier that allows the passage of certain components and retains in the mixture others. In essence, a membrane is nothing more than a discrete, thin interface that moderates the permeation of chemical species in contact with it. Since it has not a definite meaning, we could consider it as "any region that acts as a barrier between two fluids, restricting or allowing the flow of one or more components, or both fluids through it".* **[21-22]**. *As this definition is somehow ambiguous, in the following paragraphs we will take into account different criteria to make a broad classification of membranes[3], covering most of their characteristics.*

Membranes can be classified according to different viewpoints **[23]**. The first clearest distinction which could be used for a possible classification is their nature, i.e. biological or synthetic membranes. Along this work we will focus only on synthetic membranes (those which are synthetically created and intended for separation purposes in laboratory or in industry). Moreover, there are sub-classifications for synthetic membranes such as surface chemistry, bulk structure, morphology (form, structure and specific structural features) production method or other parameters.

These have been fully analysed in the literature **[24-26]**, and next table (**Table 1.3)** summarizes, such classifications, focussing mainly on overview of material and structure. Basically this work is focused on UF and NF, especially on membranes that are polymeric, porous, and asymmetric.

Synthetic membrane filters were developed by Richard Adolf Zsigmondy, Nobel Prize winner chemist, at the University of Göttingen **[28]**, Germany, in 1927. They were first commercially by Sartorius® (now Sartorius-Stedim Biotech.) a few years later. They found immediate application in the field of microbiology and in particular in assessment of safe drinking water. In this sense, most important filters are microporous membranes (having microscopic pores). These are a thin porous film or hollow fiber having pores ranging from 0.01 to 10 μm, which are simplest of all the membranes in terms of principle of operation **[27].** They are primarily found as symmetric porous membranes, having a uniform structure across the section of membrane.
This characteristic is used in MF filters by trapping the particles deep inside the structure of the membrane, on the order of 0.01 to 10 μm in diameter, all particles larger than the largest pores are completely rejected by the membrane; but, for that reason, they are easily clogged.

---

3 Several precise and complete definitions of a membrane which cover all its aspect can be seen in several publications **[22-24].**

Instead asymmetric membranes are made up of a thin surface layer supported (0.2-0.5 mm), on a much narrow, porous substructure (1-10 μm around).

Table 1.3 Classification of synthetic membranes.

Overview	Classification	Main Features
Material	**Inorganic**	Mainly ceramics and metal, they form an special class of microporous membranes, used in UF and MF applications for which solvent resistance and thermal stability are required.
	Organic	Polymeric membranes prepared under different membrane formation conditions and having a wide application range. (MF, UF, RO/NF), so that different pore sizes are produced.
Structure	**Porous**	Presenting a pore size distribution, filtration works as a conventional filter or sieve.
	Dense	Nonporous, dense film through which permeants are transported by diffusion under the driving force of a pressure, concentration, or electrical potential gradient.
	Homogeneous	The composition of the membrane presents only one material.
	Heterogeneous	Different materials by a superposition of layers, make up the membrane by superposition of layers.
	Symmetric	Structural and morphological properties do not depend on filtration layer. Uniform structure.
	Asymmetric	The structure of the membrane changes across it. Active layer and support skin are found.
	Neutral	It is electrically neutral.
	Charged	It has electric fixed charges on the surface which can be positive or negatives ones.
	Hydrophobic	Membrane material repels water molecules.
	Hydrophilic	Water molecules are attracted to membrane material.

Asymmetric membranes **[28]** are produced either by wet phase inversion from single polymers **[29]** or as composite structures. Therefore the separation properties and permeation rates are determinated exclusively by the top layer or active one (see **Fig.1.3)**, while support layer functions as a mechanical support.

The advantages of the higher fluxes provided by asymmetric membranes, are so great that almost all commercial processes use such filters, due to excellent throughput and higher durability.

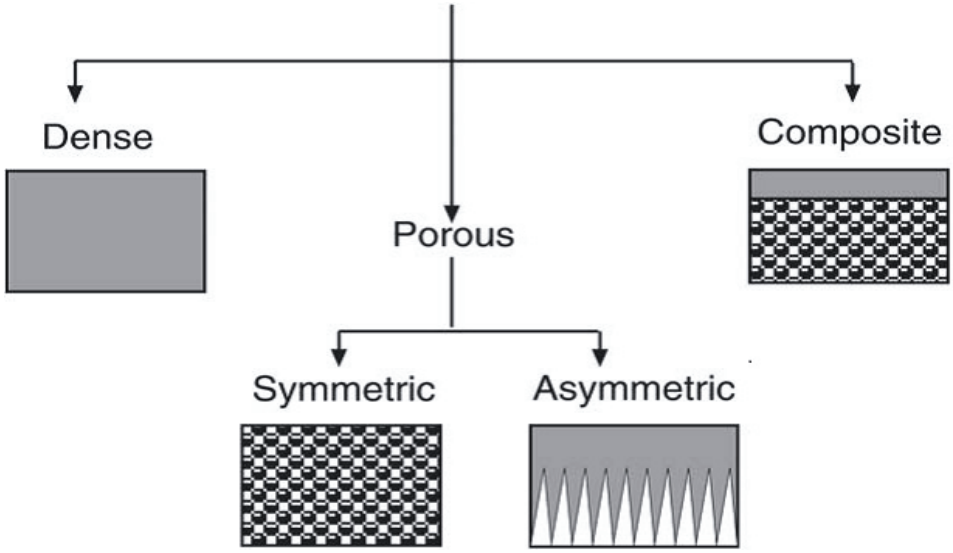

Figure 1.2: Membrane classification according to morphology.

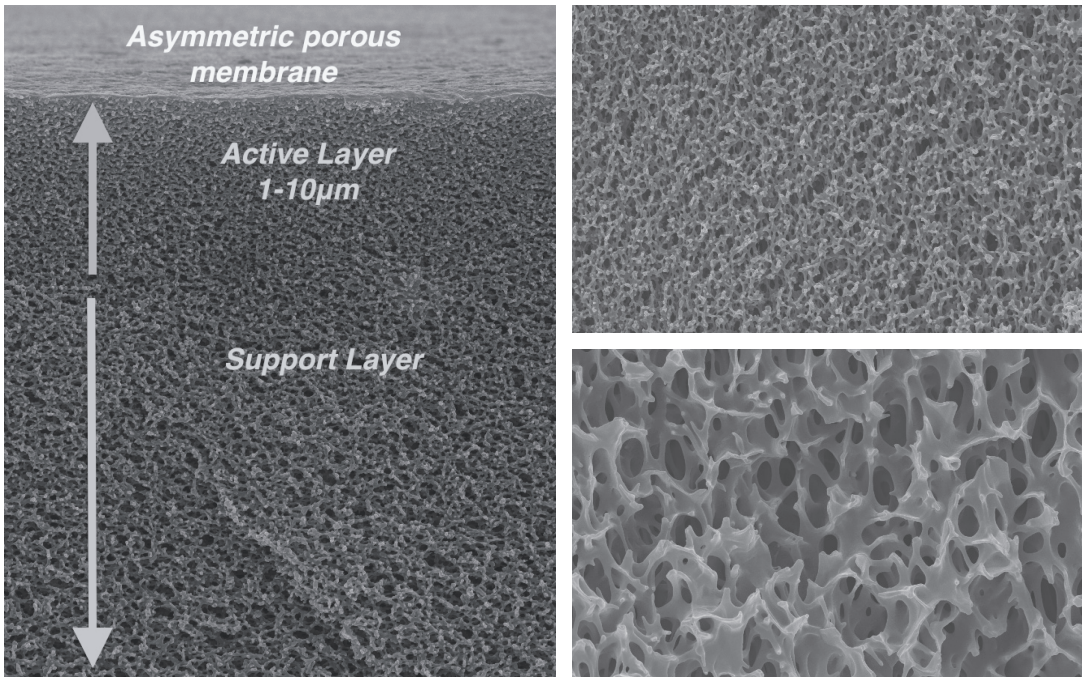

Figure 1.3: Membrane porosity of upper and lower parts of a membrane as imaged by SEM.

1.3.2 Membrane Module Design

The following section enumerates the principal module types, for industrial applications of membrane separation processes. Membranes are installed in suitable devices, and these should be designed to operate with large membranes surface areas.

The design requirements of a particular separation, and the mechanism of transport through the membrane, will dictate and frequently limit, material choice, thickness, pore size, etc. Therefore, these limitations must be accommodated into an appropriate configuration and membrane module design to withstand the imposed conditions of operation **[30-32]**.

Membrane modules are available in four different designs of membrane; *Spiral wound, Hollow fiber, Plate and framed and Tubular*, whose main characteristics are summarized in **Table 1.4**. In any case can be found many special modules for specific applications which are described **[29]** in the literature.

Next figure (see **Fig. 1.4**), indicates the existing relationship in membrane modules between the feed and permeate, all of them lead to complete mixing pattern between both the feed and permeate side of the membrane.
Flow pattern of membranes modules is usually related to the geometry and configuration, one of the most important points is if we apply *dead-end* filtration, where the feed stream is in plug flow, and the permeate flows in a normal direction away from membrane,

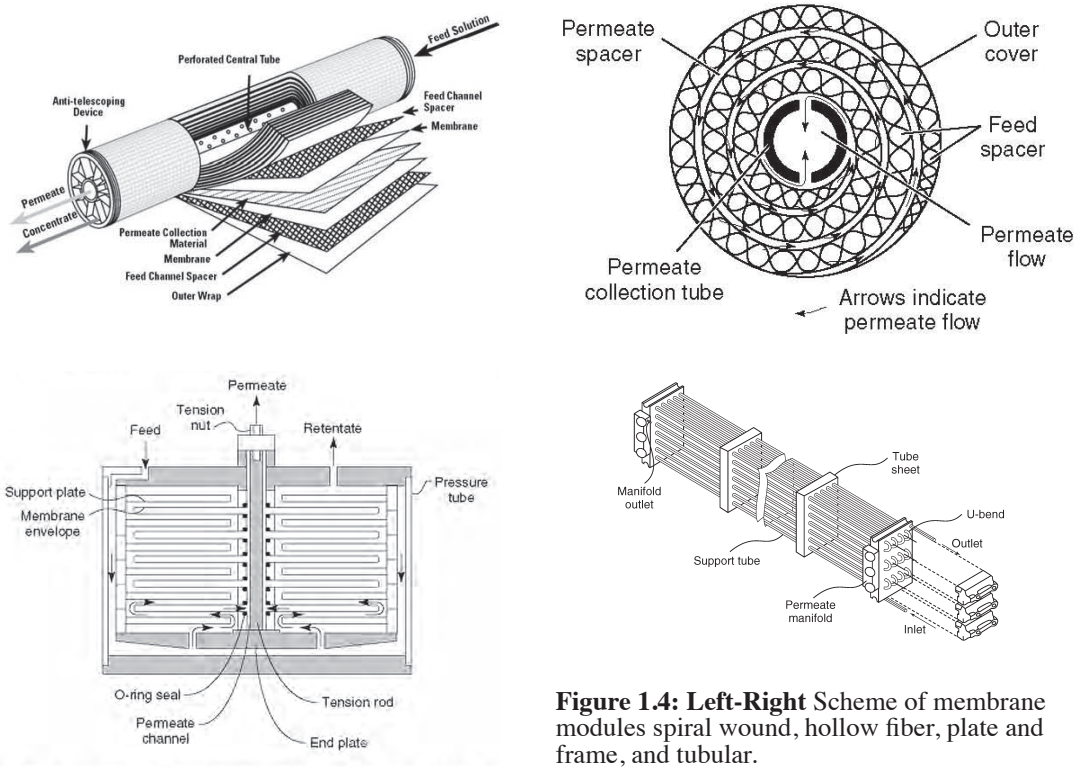

Figure 1.4: Left-Right Scheme of membrane modules spiral wound, hollow fiber, plate and frame, and tubular.

or *cross flow* filtration, then the feed or retentive side flows along and parallel to the upstream of the mebrane, but the permeate fluids to the downstream side of the membrane, (see **Fig. 1.5**, for a clear scheme of both operation ways). In the case of tubular and hollow fiber, modules are characterised by tangential flow, and spiral wound have axial-annular flow pattern. There are other flow patterns as *countercurrent flow*, **[33]** where, both the feed stream and the permeate stream are in plug flow "countercurrent" to each other.

Table 1.4 Main characteristics of membrane modules **[30-32].**

Characteristics	Plate and Frame	Spiral wound	Tubular	Hollow fiber
Resistance to mechanical damage	Good	Moderate	Very good	Good
Resistance to fouling	Good	Moderate	Very good	Poor
Packing density (m^2/m^3)	30 to 500	200 to 800	30 to 200	500 to 9000
Feed/Permeate	Forced across the surface / Flows after passing through membrane.	Pumped through all serial tubes connected / Flows normal to feed flow direction.	Flows through the tube / Passes through the wall of the tube into the module.	Flow out through the fibres / Flows out through the base of the fibre.
Manufacturing cost (US$/$m^2$)	50-200	5-100	50-200	50-200
Major applications	D, RO, PV, UF, MF	D, RO, GS, UF, MF	RO, UF	D, RO, GS, UF
Major advantages	High permeate side for pressure drop.	Membrane contamination is minimized by high feed.	Very compact packing density.	Tangential flow limit membrane fouling.

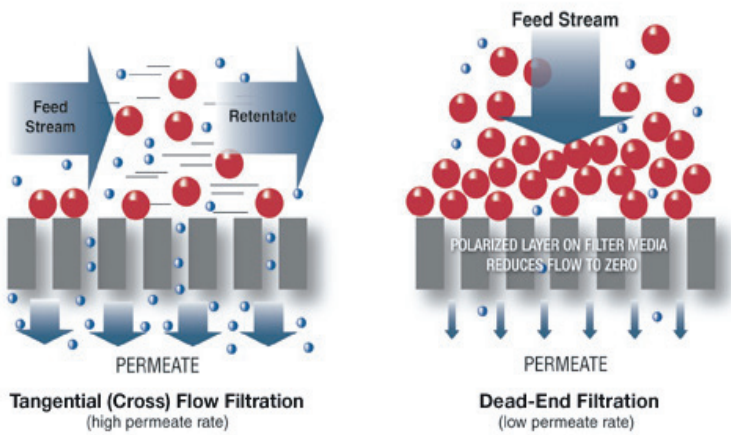

Figure 1.5: Schematic of Cross Flow (Tangential) and Dead-End Filtration.

1.3.3 Membrane Material

There are more than 100 different materials, which have been used for membrane making as we can find in a fast review of the patents and scientific literature in the field, **[34-38]**, and furthermore, more and more materials are being added every year. Thus we can ask ourselves, which are the key factors for the development of new materials applicable for membrane production?

If we come back to the above definition of synthetic membrane, we focussed in two key factors, flux and selectivity, whose optimization should lead to more efficient membrane materials **[39-40]**. In any case, and due to the very different nature of these separations, the types of membrane materials used, and the methods of fabrication for such membranes, differ quite significantly.

Membrane material science has produced a wide range of materials of different structure and with different ways of functioning. Traditionally these materials can be classified into three types **[41]**:

-*Organic* materials: including a vast number of polymers and elastomers, among which those based on cellulose had a significant role in the very beginning of Membrane. Tech.

-*Inorganic* materials: comprising many types of ceramic and metallic materials, and recently an increasing number of applications based on zeolites.

-*Mixed* or composite materials: normally membranes made of organic polymers which contain some inorganic material added or included during the synthesis process.

It is important to comment that a membrane material should ideally posses many of the following properties to be effective for separation **[42]**.

-*Appropriate chemical resistance*.
-*Mechanical stability.*
-*Thermal stability.*
-*High permeability.*

All these membrane properties are obviously relative and they must be tested for selected individual processes, but some of the more usual polymers, are being used as base material for membranes tested in this work, so we will briefly discuss in the following paragraphs a few polymeric and inorganic membranes widely used for membrane separation processes.

Cellulose and cellulose derivatives (C). Cellulose or regenerated cellulose is the most important natural polymer for membrane applications and processes, especially through development by Loeb and Sourirajan of the asymmetric membrane **[43]**. In the

early 1960's, Loeb and Sourirajan published a method for making asymmetric cellulose acetate membranes with relatively high water fluxes and salt rejection, thus making RO and NF separations both possible and practical as required for a viable desalination process. Cellulose has a very high structural regularity and intermolecular hydrogen bonding, which makes cellulose difficult to dissolve due to the highest concentration of α-cellulose. For membrane applications they are used as derivatives of cellulose, example Nitrate (Inorganic), Acetate, Triacetate (Organic) and mixed cellulose esters (Nitrocellulose) compounds. They are used for many laboratory applications including filters for sterilizing biological fluids, microbiology, contamination analysis and air monitoring.
Important advantages of Cellulose derivatives, are that they are available in a wide range of pore sizes from MF to RO, cast in sheets or as hollow fibers, suitable for aqueous and organic media, hydrophilic, mechanically stable and finally, they present, reasonably high porosity, providing superior flow rates, but rejecting low molecular weight contaminants poorly **[41].**
However, cellulose suffers from certain disadvantages also: narrow temperature range, low PH range and poor resistance to some alcohols[4], which may oxidize the cellulose membrane opening up the pores, and can be vulnerable to attack by bacteria and biological fouling.

Aromatic Polyamides (PA). Aromatic polyamide (AP, aramid) membranes were first developed by DuPont® in a hollow fiber configuration, but they can be found in sheet configuration too. Aramid membranes represent an important segment of a rapidly developing technology for the separation of components of aqueous solutions, gaseous mixtures and organic liquid mixtures. They are highly inching crystalline polymers with better thermal stability and higher resistance to solvents than do their aliphatic counterparts such as Nylon. By this way Polyamide membranes have better resistance to hydrolysis and biological attack than do cellulosic membranes. Aromatic Polyamides has been form for many years in the field of RO membranes. In this case, the polymer forms the active layer showing high salt rejection, high water permeability and high fouling tolerance, **[44].** Among their other applications, these membranes are used in waste-water treatment, desalination of sea water and dialysis.

Poly(Ether)Sulfone (PES). It is a heat-resistant, transparent, amber coloured, non-crystalline polymer having the molecular structure shown in **Fig. 1.6**. Properties of PES are: it remains in satisfactory condition after long-term continuous use without causing any dimensional change or physical deterioration; it has by far better high temperature properties than conventional polymers (it resists temperatures as high as 200ºC); it has wide pH tolerance (1 to 10), fairly good chemical liquids resistance and high degree of molecular immobility, rigidity or creep resistance. Thus this type of material is among the most used in Membrane Technology.
PS and PES membranes can be found in a wide range of pore sizes, ranging from 10 Å to 0.2 μm; then PES filters can be used in modules covering MF/UF/NF. These membranes[5]

4 Certain incompatibility was found to Isobutanol, used for LLDP analysis; as it will be commented in **Paper two**.
5 Most of the filters analysed in this study presented this polymer.

provide removal of fine particles, bacteria, viruses, and fungi; making it a versatile membrane for applications such as sample preparation, sterile filtration, Hemodialysis (H), waste water recovery, food and beverage processing, and Gas Separation (GS).
Regarding membrane configuration they are utilized in both flat sheet and hollow fibres in UF and MF processes. They are also used as porous supports, in thin film composite

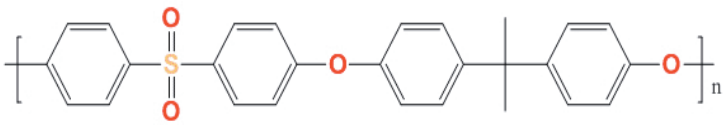

Figure 1.6: Polyethersulfone molecule.

membranes for RO desalination, offering extremely high flow rates at very low differential pressures when compared with Nylon or PolyPropylene (PP) media **[45-46]**.
The most serious disadvantage it posses, consists in the fact that they often present a powerful nonspecific adsorption capacity. This phenomenon, usually known as fouling, leads to a rapid deterioration of the membrane permeability.

PolyTetraFluoroEthylene (PTFE). Also known as Teflon®, the trade name given by Dupont®, may be visualized as Polyethylene with all its hydrogen atoms substituted by fluorine.
Among its advantages we can mention that is very stable to strong acids, alkalis and solvents, it permits to a very wide range of temperature, being also very hydrophobic. Other interesting application related with PTFE is the commercial membrane GoreTex® (see **Fig. 1.7).** This makes use of the high hydrophobicity of the membrane material so water (in liquid form) cannot pass through the membrane, while water vapour transport is allowed **[46]**. PTFE membranes find many uses in the treatment of organic feed solutions, vapours and gases.

PolyCarbonate (PC). It is a class of polyesters derived from carbonic acid and bisphenol-A. They are prepared in the form of thin dense films (approximately 10 microns thick) of high molecular weight, being used as the most common substrate for the preparation of microporous track etched membranes. In this fabrication method, they can be obtained porous MF membranes, with very narrow pore-size distribution (see **Fig. 1.8)** whose pore shape corresponds to extremely uniform cylindrical or slightly conic pores in a flat configuration. Due to these unique characteristics, these membranes have been used as model pores in fundamental studies of membrane transport phenomena **[47]**.
PC membranes having hydrophilic behaviour, are available in a range of pore sizes from 0.01μm to 12 μm, then mainly cover MF; they are resistant to most organic solvents, having an excellent chemical resistance, good thermal stability, non-hygroscopic and extremely weight stable.

PolyPropylene (PP). It is produced by the polymerization of propylene using well known Ziegler-Natta catalyst **[48].** It is usually available in the form of hollow fibres, but it is presented in flat disc filters too, being flexible, durable and virtually indestructible.
Significant properties are: hydrophobic, relatively inert, compatible with organic solvents,

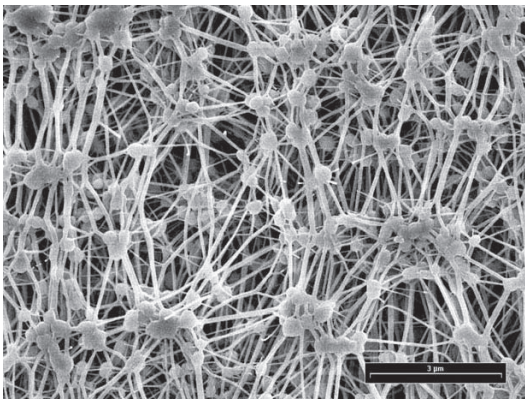

Figure 1.7: Gore Tex® membrane.

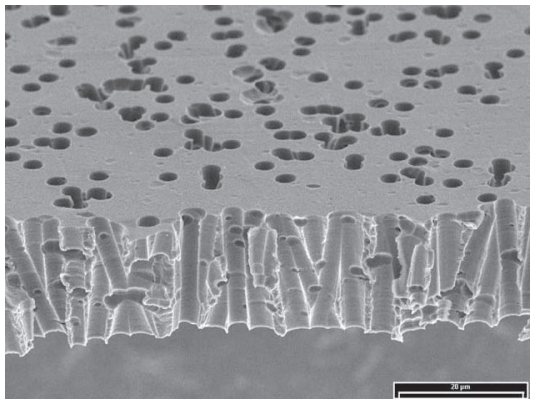

Figure 1.8: PolyCarbonate membrane.

making them highly suitable for High Performance Liquid Chromatography (HPLC), and can withstand moderately high temperatures.
Main applications includes their use as a separator in batteries, allowing ion migration across the membrane, oil mill and refinery industry, metallurgy industry food and pharmaceutical processes; these membranes usually have a mean pore size between 0.1μm and 20 μm.

PolyAcryloNitrile (PAN). It is another commercially available material based on free radical polymerization of AcryloNitrile (AN), **[49],** which has been widely applied in the preparation of separation membranes, due to its superior resistance to hydrolysis and oxidation. These membranes have received much attention in the fields of water treatment, PerVaporation (PV) and supports for other (bio-)macromolecules. Main application has been extensively UF, but it has been used as a support for NF and RO, **[51-52]**.

Inorganic membrane materials. The application of polymer membranes is generally limited to temperatures below about 200°C and to the separation of mixtures that are chemically inert. Most inorganic membrane, known as ceramics membranes, are materials having much better selectivity and permeability at high temperatures than polymeric membranes at low temperature. They are also much more resistant to chemical attack and to corrosive liquids and gases. The wide variety of materials that may be used in the fabrication of the inorganic membranes, covers from ceramic membranes to other inorganic compounds. The most common membranes are made of Al, Si. Ti, Zr[6] oxides or are established by adding some additional compounds present in minor concentration. Nowadays, inorganic materials compete successfully with polymers for commercial use.
Ceramic membranes are a type of inorganic materials such as alumina, titania, zirconia oxides or some glassy materials. They are available from several manufacturers in different shapes, mainly tubular and hexagonal, and with various channel diameters (see **Fig. 1.9**); they are manufactured by a number of methods, these include particle dispersion and slip casting, phase separation and leaching, anodic oxidation, thin film deposition, and so on **[50]**. These membranes offers sufficiently high permeability and selectivity for the

6 Some zirconia tubular membranes were studied during this work, as shown in **Paper four**.

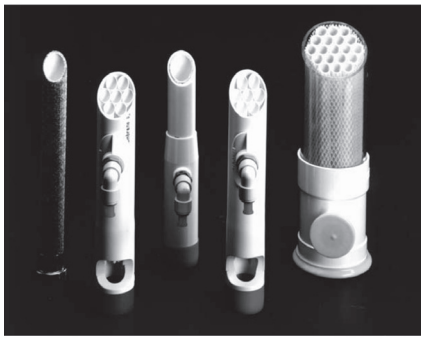

Figure 1.9: Typical tubular Ultrafiltration. The membrane is usually cast on a porous fibreglass or paper support, which is then nested inside a plastic or steel support tube.

targeted mixture and can be made into the membrane module for practical applications. They normally have an asymmetrical structure composed of at least two, but mostly three, different porosity levels. Indeed, before applying the active, microporous top layer, a mesoporous intermediate layer is often applied in order to reduce the surface roughness.

Main applications are: air separation by mixed oxygen ionic, electronic conducting ceramic and molecular sieve carbon membranes, hydrogen separation by metal, silica and zeolite, proton-conducting ceramic membranes, hydrocarbon separation by zeolite and silica membranes, and carbon dioxide separation by silica or zeolite membranes.

Other important materials **[50]** not summarized in previous paragraphs are also used as a membrane material, next table (**Table 1.5**) summarizes principal properties and applications of more common membrane materials.

Table 1.5 Some characteristics of main membrane process and materials used

Membrane type	Membrane structure	Preparation	Applications
Asymmetric CA, CN, PA, PS, PES, PAN.	Homogeneus or microporous "skin" on a microporous substructure.	Casting and precipitation.	UF, RO, MF, GS, PV
Composite CA, PA, PS, PI.	Homogeneous polymer film on a microporous substructure.	Deposition on microporous substructure.	RO, GS, PV
Homogenous S.	Homogeneous polymer film.	Extrusion.	GS
Ion exchange DVB, PTFE.	Homogenous or microporous co-polymer film, positively or negatively charged ions.	Immersion or ion exchange.	ED
Microporous: Sintered polymer PTFE, PE, PP.	0.1 to 20 μm pore diameter.	Moulding and sintering. Leaching.	Filtration (F)
Microporous: Ceramic, metal glass.	0.05 to 20 μm pore diameter. 10 to 100 μm pore diameter.	Moulding and sintering. Leaching.	GS, F (molecular mixtures)
Microporous: Sintered polymer PTFE, PE, PP.	0.1 to 5 μm diameter.	Stretching a partial crystalline film.	F (air, organic solvents)
Microporous: Track-etched PC, PEsT.	0.02 to 20 μm pore diameter.	Irradiation and acid leaching.	F (suspensions, sterile filtration)
Symmetric microporous phase inversion CA.	0.1 to 10 μm pore diameter.	Casting and precipitation.	Sterile filtration, water purification, dialysis

CA - Cellulose acetate. CN - Cellulose nitrate. CTA - Cellulose triacetate. DVB - Divinylbenzene. PA - Polyamide. PAN - Polyacrylonitrile. PC - Polycarbonate. PE - Polyethylene. PES - Polyethersulfon. PEsT - Polyester. PI - Polyimide. PP - Polypropylene. PS - Polysulfone. PTFE - Polytetrafluoroethylene. PVC - Polyvinylchloride. PVDF- Polyvinylidene fluoride. S - Silicon rubber.

ED - Electrodyalisis. F - Filtration. GS - Gas separation. MF - Microfiltration. PV - Pervaporation. RO - Reverse Osmosis. UF - Ultrafiltration.

1.4 MEMBRANE PROCESSES

In last previous pages, several types of membrane processes have been mentioned. In some more detail, they can be classified into several groups according to the driving force that causes the permeant flow across the membrane, such as:

-Pressure Difference
-Concentration Difference
-Temperature Difference
-Electrical Potential Difference

In the major part of membrane separation processes, the driving force is a pressure difference or a concentration difference across the membrane and it operates mainly by two basic processes: the first one is filtration, in which a fluid flows through pores in the membrane material that holds back those components of the feed that are above a certain size, being this size limit determined by average particle size in micrometers (or nanometers) or which is equivalent, by molecular weight; the second one is diffusion, in which components from the feed material pass through the non-porous membrane moving across the own membrane material, which holds back some or all the fluid.

1.4.1 Pressure Driven Membrane Processes

The Pressure driven processes are the technically and commercially most relevant membrane process. They work creating a pressure drop across the membrane which acts as driving force and whose magnitude depends on the size of particles to be separated/ retained. In operational terms, the processes involved are[7]:

-Reverse Osmosis (RO)
-NanoFiltration (NF)
-UltraFiltration (UF)
-MicroFiltration (MF)

1.4.2 Concentration Gradient Driven Processes

This term is often related to the concept of diffusion or the migration of a substance across the membrane due to a concentration gradient.
Then, if a concentration gradient of permeating molecules is established in both sides of the membrane, simple statistics laws show that a net transport of matter will occur from the high concentration to the low concentration region. This concept was first recognized, theoretically and experimentally, by Fick in 1855 **[53]**. Fick formulated his results as the equation now called Fick's law of diffusion.

$$J_i = -D_i \frac{\partial c_i}{\partial x} \qquad \textit{Eq 1}$$

7 These are listed in the order of descending operating pressure, or decreasing effectiveness in terms of the fineness of the separation achieved.

Where the proportionality factor D_i is called the diffusion coefficient (cm^2/s), being J_i the flux of component i ($g/cm^2 \cdot s$) and c_i the concentration of component i (gr/cm^3). Diffusion coefficient is a measure of the mobility of the individual molecules.

Diffusion is an inherently slow process. In practical diffusion-controlled separation processes, useful fluxes across the membrane are achieved by making the membranes very thin and creating large concentration gradients in the membrane. Most important process included in this section are:

-PerVaporation (PV)
-Gas Separation (GS)
-Vapour Permeation (VP)
-Dialysis (D)

1.4.3 Electrical Potential Driven Membrane Processes

In these processes, an electrical potential difference act as the driving force using the ability of charged ions or molecules to conduct an electrical current. If an electrical potential difference is applied to a salt solution, the positive ions (the cations) migrate to the negative electrode (the catode). If molecules are uncharged, there is not driving force but also polar molecules can lead to selective transport under electrical potential applied. This transport of ions across an ionic membrane is based on the Donnan exclusion mechanism, **[54],** but if now we considered an electrical potential difference and electrically charged membranes it can be used in various arrangements, such as:

-ElectroDialysis (ED)
-Membrane Electrolysis (ME)
-Bipolar Membrane (BM)
-Fuel Cells (FC)

In all cases the charged membrane constitutes a selective barrier where ions are either repelled or transported dependent on the ionic and membrane relative charge.

1.4.4 Temperature Gradient Driven Membrane Processes

Mainly emphasize on Thermo-osmosis or Thermo diffusion, which is a process where a porous or nonporous membrane separates two phases having a temperature gradient between them **[55]**. Then a volume flux exists from the warm side to the cold side until thermodynamics equilibrium is attained. Main temperature driven processes are:

-Thermo-Osmosis (TO)
-Membrane Distillation (MD)

Next table, **(Table 1.6)**, shows typical features that form the permeate and the retentate at both sides of a membrane used in some of the principal aforementioned processes.

Completing this section, there are other membrane processes such as facilitated or carry mediated membrane transport, liquid membrane separation, membrane contactors, membrane reactors, ect, in which membrane separation is combined with conventional processes. Finally the next "filtration chart" (see **Fig. 1.10**) illustrates the various particle sizes as well as the filtration methods **[56]** that can deal with each range of particle size and characterization methods.

Table 1.6 Classification of membrane processes attending to their driving force.

Driving Force	Membrane Processes	Permeate	Retentate	Type of membrane
Pressure Difference	Reverse Osmosis (10-100 bar)	Water, small polar solvents, salts	All solutes	Asymmetric skin type
	NanoFiltration (5-35 bar)	Monovalent ions, salts	Small molecules, divalent salts	Thin-film membranes
	UltraFiltration (1-10 bar)	Small molecules and water	Polymers, proteins, micelles, colloids particulates	Asymmetric microporous
	MicroFiltration (0.5-2 bar)	Dissolved solute and water	Suspended particles, water gases	Symmetric microporous
Concentration Difference	PerVaporation	Volatile small molecules and water	Low volatility species, less soluble in the membrane gases	Asymmetric homogenous polymer
	Gas/Vapour Separation	Gases, vapours mixtures	Smaller molecular sizes	Microporous polymer, ceramic and metal
	Dialysis	Small molecules, water, gases, vapours soluble in the extractant	Large molecules, water components of feed insoluble in extractant	Nonporous or microporous
Electrical Potential Difference	Electrodialysis	Ionized solutes and water	Non ionic solutes	Ion exchange membrane
	Membrane Electrolysis	Electrolyte solutes and water	Non electrolites solutes	Cation and anion exchange membrane
	Bipolar Membrane	Salt electrolytes		Cation and anion exchange sandwich
	Fuel Cells	Protons	Electrons	Proton exchange membrane
Temperature Difference	Thermo-Osmosis	Molecules,water, gases and vapours	Proteins, micelles, colloids particulates	Nonporous or microporous
	Membrane Distillation	Small molecules, water, gases, vapours	Molecules < 1 nm	Microporous

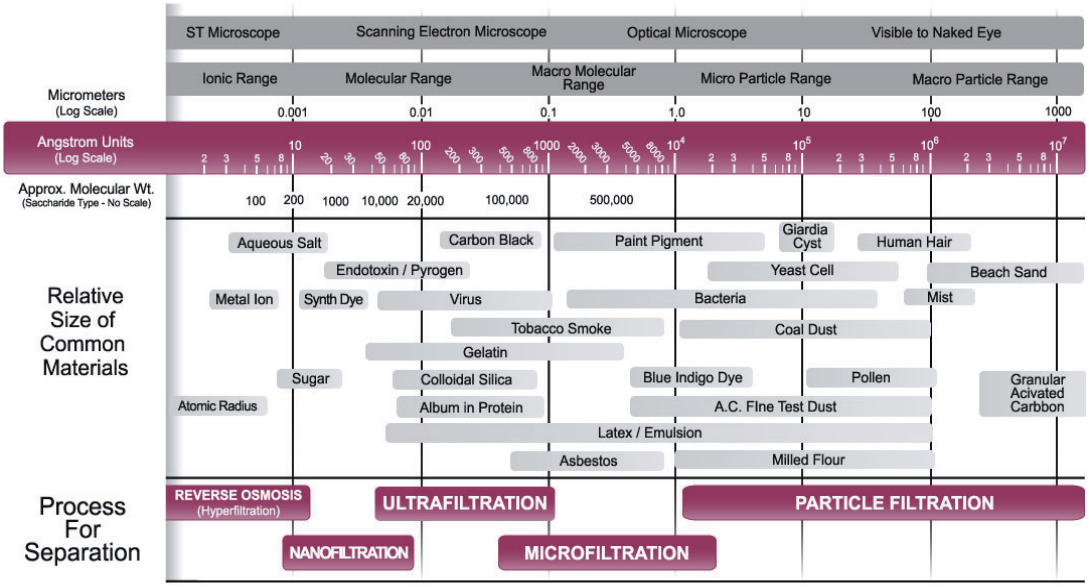

Figure 1.10: Filtration chart. It shows the pore size range of several filtration processes.

1.5 CHARACTERIZATION OF MEMBRANES

Characterization is a way of relating structural and morphological information coming from a particular class of membrane to the use it will have in a particular application. The term characterization refers to knowledge of the constitution, structure and functional behavior of the membrane **[56]**. This knowledge needs to be acquired by using appropriate methods, because the studied membranes are put into a large number of different uses even within a particular separation process, then a membrane will be characterized in terms of its pore size, Molecular Weight Cut-Off, porosity, thickness, symmetry, permeability, hydrophobicity and hydrophilicity, adsorption, crystallization, etc.

In other words, we can see that a complete characterization should include both the *functional* aspects of the problem and not less important, the *structural* ones. In a first view, *functional and structural* characterisation methods apply uniformly into two broad areas, porous media and non-porous media **[57]**.
In this sense *structural* characterization is essentially the determination of as much as possible from the following experimental parameters:

Pore Size. The pore size of a membrane gives an indication of the mean size of the pores present on a membrane. It is also correlated with the particle size that the membranes will be able to reject, so characterizing the membrane retention capabilities. The pore size of a membrane can range from 1000 to 0.0001 microns, covering the four main types of membranes, MicroFiltration (MF), UltraFiltration (UF), NanoFiltrations (NF) and Reverse Osmosis (RO). In UF, the pore size diameter quoted is usually an average value[8], but to confuse the issue, the value quoted in MF is usually defined in terms of the

8 UF, NF and RO membrane manufacturers frequently characterize their membranes using the "cutoff" concept rather than pore size.

largest particle able to penetrate the membrane. This nominal pore diameter can be 5 to 10 times smaller than the apparent pore diameter based on direct microscopic examination of the membrane. Membrane pores tend to be highly non-uniform, so then any assumption on shape and inner pore conformation is solely for the purpose of mathematical modelling and interpretation. However they can give accurate descriptions and quantitative analysis of how a membrane will behave in certain situations. *Pore size* is determined by bubble point analysis (only the biggest pore size), porosimetry (Gas-Liquid for MF or liquid-liquid for UF, while mercury porosimetry is usually intended for ceramic membranes), or microscopic analysis, with some other not so used methods also able to give information about pore sizes. However, the *pore size* measured gives not an absolute measure because the membrane pores are interconnected (net worked) instead of cylindrical through out capillaries.

Pore size distribution. It gives a quantitative description of the range of pore sizes present in the membrane sample. Obviously, any method giving a complete description of the whole pore size distribution, can be used to determinate the mean, maximum or minimum pore size present in the sample. It provides a more complete description of range of pores you will find in that membrane, but also this so exhaustive information makes more difficult to asses the particle sizes likely to be retained by the membrane.

Porosity (θ). The porosity is the pore volume divided by the volume of the raw material. If we note as: $V_m = V_t - V_e$, the solid volume material of the sample (being V_e is the empty volume or volume of the pores), whereas V_t is its geometrical or total volume, the porosity is given by the following equation.

$$\theta = 1 - \frac{V_m}{V_t} \qquad \textbf{Eq 2}$$

Porosity can be also given in terms of surface areas, supposed cylindrical shaped pores, since: $V_t = A_t \Delta x$, with Δx the thickness of the membrane or active layer. Surface porosity can be measured by analysing processed images obtained from microscopic analyses such as scanning electron microscopy (SEM), transmission electron microscopy (TEM), or atomic force microscopy (AFM).

Pore density: related with previous parameter, we can define the density of pores as the number of them present in the surface of the membrane, per unit of surface area.

Surface roughness. It could be defined as the deviation of the actual membrane surface topography from an ideal atomically smooth surface.

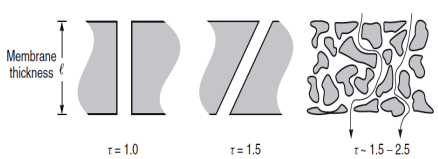

Figure 1.11 Typical tortuosity values for several membrane configurations.

Tortuosity (ψ). It reflects the length of the average pore compared to the membrane thickness (See **Fig. 1.11**). Simple cylindrical pores crossing the membrane normally to the surface have a unity value of tortuosity, that is, the average length of the

pore matches with the membrane thickness. Usually pores take a more meandering path through the membrane, so typical tortuosities are in the range [1.5, 2.5].

On the other hand, regarding the membrane/effluent coupling or *functional* parameters, then related with the membrane permeation (those specifically defined to characterize membrane as filter materials); the following are a brief summary of several commonly analysed parameters in a functional characterization.

Molecular Weight Cut-Off. The nominal molecular weight cutoff (MWCO) is a performance-related parameter, defined as the value of a given solute molecular weight for which the rejection is 90%, (see **Fig. 1.12**).This method is based on steric or size based rejection of solutes by a membrane **[58]**. Typically, a mixture of water soluble molecules and/or macromolecules is made and presented as the feed to the membrane. In the case of UF and MF, the macromolecule solution can be a mixture of proteins, or a polydisperse solution of a single hydrophilic polymer such as dextrans, polyethylene glycols or others. As the MWCO decreases, the mean pore diameter for the membranes has been found to decrease **[59]**. Really MWCO is only a rough indication of the membrane ability to remove a given compound given that molecular shape, polarity, and membrane-solute interaction strongly affect rejection **[60]**. Moreover, membrane surface characteristics (surface porosity and pore size distribution) may influence the apparent size of particles retained. There is currently no universally accepted industrial standardard for the determination of MWCO and values presented are hardly comparable amongst different manufacturers.

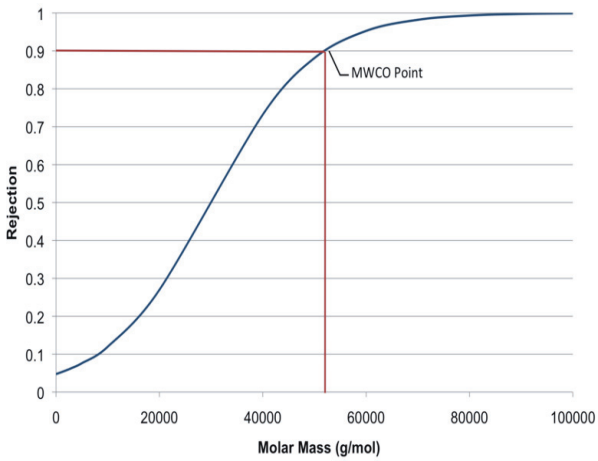

Figure 1.12: Solute rejection versus molecular weight.

Hydraulic Permeability. In 1856, Darcy observed that the rate of flow of water through a permeable layer of thickness Δx could be related to the driving pressure ΔP by the simple expression:

$$L_w = \frac{\triangle J_w}{\triangle P} \qquad \textit{Eq 3}$$

Last equation can be described in terms of hydrodynamic resistance for the filtration of solvent molecules (water), through the membrane, in this sense the permeate flux changes with the mean transmembrane pressure as:

$$J_w = \frac{\triangle V}{Adt} = \frac{\triangle P}{\eta_w R_m} \qquad \textit{Eq 4}$$

Where J_w *is* the water permeate flux, (m^3/s), calculated as the volume V flowing in time t through cross-section membrane area A, and measured at a single transmembrane pressure gradient ΔP, (N/m^2), L_w is the water permeability of the membrane, η_w is the viscosity of water, and R_m is the intrinsic membrane resistance[9] **[61]**. This resistance model is very commonly used to study membrane fouling, but if we consider a no fouling situation (clean membrane) with feed water completely free of any solutes, and assuming laminar flow through capillary tubes of nominal diameter, water permeability can be calculated from the distribution of pore densities N_d, by taking into account that flow of water should follow the Hagen-Poiseulle law:

$$L_{p,w} = \frac{\pi \sum_{j=1}^{n} N_d(j) d_p^4(j)}{128 \eta_w \psi \Delta x} \qquad \textbf{Eq 5}$$

Being, η_w the water viscosity (η_w=0.8937·10^{-3} Pa·s at 298 K), and ψ a tortuosity factor and Δx is a membrane thickness or capillary length m. It must be noted that the permeabilities are proportional to the fourth power **(Eq 5**) of the pore diameters (typically MF mean pore size is hundred times larger than the average UF pore and one thousand times larger than the nominal diameter of pores in RO membranes), larger than the nominal diameter of pores in RO membranes), so that permeability of MF membranes is higher than that of UF membranes, which is in turn much higher than that of RO membranes. These differences significantly impact the operating pressure and the way that these membranes are industrially used. Liquid permeability is usually the first measurement accomplished when a new membrane must be characterized.

The volume flow versus pressure is measured and the corresponding slope gives the permeability of the liquid used (normally water). Later, if all the pores are assumed to have the same known pore diameter, then permeability will be related to the porosity (θ) and the mean pore diameter (d_p) through the following law:

$$L_p(d_p) = \frac{\theta d_p^2}{32 \eta \psi \Delta x} \qquad \textbf{Eq 6}$$

Hydrophobicity and Hydrophilicity. Supposing a liquid drop deposited onto a solid surface, if the liquid is very strongly attracted to the solid surface (for example water on a strongly hydrophilic solid) the droplet will completely spread out on the solid surface and the contact angle will be close to 0°. Less strongly hydrophilic solids will have a contact angle up to 90°. On many highly hydrophilic surfaces, water droplets will exhibit contact angles of 0° to 30°[10]. A membrane being hydrophilic means that it has the tendency to allow liquid (mostly water and water solutions) to enter the pores, this condition reflects better wetting, better adhesiveness, and higher surface energy. If the solid surface is hydrophobic, the contact angle, (see **Fig. 1.13)** will be larger than 90, in fact highly hydrophobic surfaces have water contact angles as high as 150° or even nearly 180°. On these surfaces, water droplets simply rest on the surface, without actually wetting any significant extent

9 R_m can be determined from experimental data of pure water permeate flux, J_w under several ΔP.

10 The contact angle is commonly used in membrane material science to describe the relative hydrophobicity/hydrophilicity of a membrane surface.

and regarding the membrane behavior hydrophobicity, it implies there is a the tendency to resist liquid entering the pores. The higher fouling potential of hydrophobic membranes is due to the high binding affinity of proteins and humid substances. The contact angle, thus directly provides information on the interaction energy between the surface and the liquid.

Zeta potential. It is the name used to describe the electrokinetic potential in colloidal systems **[62].** Properly speaking the zeta potential is the electrical potential at the no slipping plane (it is a plane close to the solid surface where electrolytes are not mobile due to electrostatic attractions). The zeta potential describes the magnitude of the attraction and repulsion forces of particles and determines the potential stability of a colloidal system. If particles have a large negative or positive zeta potential, they will repel each other and there will be dispersion stability; however, if particles have low zeta potential values then there is no force to prevent the particles coming together and there will be dispersion instability.

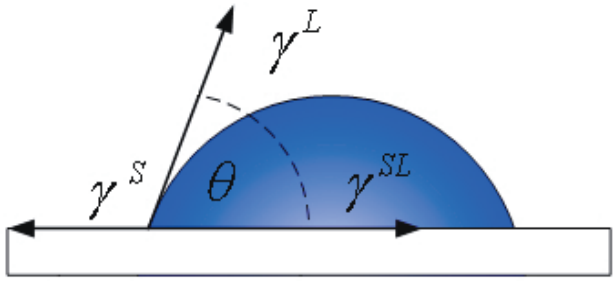

Figure 1.13: Contact angle (θ) can be evaluated from Young's equation. At equilibrium three interfacial tensions corresponding to solid/gas (γ^S), solid/liquid (γ^{SL}) , and liquid/gas (γ^L) interfaces are counterbalanced.

Microbial challenge test. This parameter is especially used in the case of membranes and devices focussed towards medical and pharmaceutical applications **[63]**. Micro-organism are often used as the particle challenge to filters and microfilters. Of course the microbial retention depends on the membrane pore size, so that the appropriate micro-organism must be selected. The perfomance of membranes in bacterial challenge test is often quantified by Log Reduction Value (LRV):

$$LRV = Log_{10}\left[\frac{c_f}{c_p}\right] \qquad \textbf{Eq 7}$$

where c_f and c_p are the concentration of particles or cells in the feed and permeate respectively. The reason of this logarithmic scale is the strong retention requirements that membranes used in pharmaceutical uses must accomplished, where retentions of 99 % are not enough to assure safe membrane usage the filter, **[64]**.

1.5.1 Characterization Methods

Several experimental techniques are used depending on the parameter or group of parameters required to determine characterization methods.
In following paragraphs, a brief description of the most important characterization methods will be introduced. Only those mostly used to obtain information on pore size and shape are included.

Bubble pressure breakthrough. This method, introduced by Bechhold, **[65]**, is based on the measurement of the pressure necessary to blow air through a liquid-filled porous membrane. Bubble point and related methods (commonly called fluid displacement techniques) use lower pressures than mercury porosimetry, being frequently used for estimation of mean pore size and pore size distributions of many commercial membranes. In the case of bubble point method it is used to obtain the maximum pore size present in a membrane sample, which makes it very useful for quality control in membrane manufacturing, being able to detect the presence of pinholes. This method have reached the status of recommended standard.

Mercury porosimetry. The method is based on the same principles as the bubble pressure method; but in this case mercury (a non-wetting fluid) is used to fill a dry membrane. The main drawback of this method is that membrane is distorted due to the very high pressure inside pores, that must be used to analyse small pores. Other important disadvantage is that the method results destructive for the membrane samples, given that some mercury remains always entrapped into the pores. Finally the technique is not able to discriminate active or open to flux pores, then ink-bottle ones are also included in the analysis.

Electron microscopy. This method uses several electronic microscopy devices for viewing of the top or cross sections of the membranes, such as SEM (Scanning Electron Microscopy), TEM (Transmission Electron Microscopy), STEM (Scanning Transmission Electron Microscopy), FESEM (Field Effect Scanning Electron Microscopy). Computerized image analysis of the corresponding micrographs is frequently used to obtain pore size distributions and porosities.

Atomic force microscopy. This technique similarly to electron microscopy allows the surface study of non-conducting materials, for example synthetic polymeric membranes down to the scale of manometers. It was developed by Binnig **[66]**, and its main advantage over the electron microscopy is that no previous preparation of the sample is needed. It presents good results in comparison with other characterization techniques. For conducting materials or those covered by a conducting layer, Tunnel Effect Microscopy can be used for analysing top views of the membrane down to molecular sizes.

Solute retention challenge. A filtration procedure is accomplished in which retentions are measured for solutes of various molecular weights, therefore various hydrodynamic molecular sizes. In that way and using appropriate retention models the molecular

weight cut-off of the membrane can be evaluated. Several solutes have been used to measure retention as proteins, dextrans or polyethyleneglycols. This method is more or less standardized, but has the disadvantage that is difficult to relate the retention values with the pore sizes. It is also strongly conditioned by the operational variables (cell design, solute concentration, recirculation speed and applied pressures) when the membranes are tested **[67]**,

Adsorption-Desorption methods. An analysis of pore size distribution can be also accomplished by gas adsorption/desorption devices. The technique is based on the Kelvin equation, and involves measuring the adsorption-desorption isotherms relating the vapour pressure of a liquid within a curved surface to the equilibrium vapour pressure of the same liquid in a plane surface. Its main advantages are that it determines pore sizes of a few Ångstroms.

Thermoporometry. This method suggested by Brunn, **[68]**, is based on the fact that the solidification point of the vapour condensed in the pores; is a function of the interface curvature; therefore, by using a differential scanning calorimeter (DSC), the phase transition can be easily monitored and the pore size distribution calculated.

Permporometry. It is a technique with similar characteristics to the adsorption-desorption method. This technique is based on the controlled blocking of pores by condensation of vapour, present as a component of a gas mixture, and the simultaneous measurement of the gas flux through the membrane. If the Kelvin equation is used, the pore size distribution is obtained. It is a useful technique especially to characterize UF/NF membranes.

Spectroscopic Methods. There are other techniques that can also be used to study the pore and determine its size, for example, NMR (Nuclear Magnetic Resonance), ESR (Electron Spin Resonance), IR (Infrared Spectroscopic) and RS (Raman Spectroscopy). In the case of NMR Measurements, **[69],** it has been demonstrated the determination of pore size in water-saturated membranes using (NMR), spin-lattice relaxation measurements.

This is not an exhaustive list, as there are some other characterization methods which giving important information they contribute to get a complete picture of the filter and its capabilities. Among those we can note the compatibility test, which allows membrane manufacturers to assure the chemical compatibility of their filters with the broad range of solutes present in a separation process. Also the presence of charges in the membrane, their density and distribution is an important parameter which can be determined from electrokinetic measurements. Usually streaming potential is measured to determine the zeta potential of the membranes but also filtration of ionic species or EFM (Electric Force Microscopy) can give an idea of such information. To resume the information presented in these pages, next table (**Table 1.7)** represents several experimental techniques, attending to the parameter studied. Finally we must remember that the interest of this work is placed on fluid penetration techniques, specially LLDP, whose range of pore size detection is presented in the next figure, (see **Fig. 1.14)**, along with that of other pore size determination techniques.

Table 1.7. Most useful and widespread characterization methods and parameters associated.

Techniques giving structural information		**Techniques giving functional information**	
Techniques	***Parameter***	***Techniques***	***Parameter***
· Bubble Point and related methods LLDP / GLDP	· Maximun Pore size and pore size distribution. · Porosity	·Solute rejection test	· Diffusion coefficient · MWCO · Microbial challenge test
· Mercury porosimetry (HGP)	· Pore size and size distribution · Porosity	·Permeability test	·Water permeability
· Microscopy (SEM, FESEM, TEM and AFM)	· Form and pore size structure · Surface roughness. · Surface Porosity · Tortuosity · Surface potential	·Electrical microscopy (AFM)	· Surface Potential
· Gas Adsorption and capillary condensation (GAD)	· Pore size distribution. · Porosity	·Electrokinetic processes	· Zeta potential · Charge distribution
· Thermoporometry (THP)	· Form and structure of the pore	·Electrical spectroscopy	· Surface Potential
· Permporometry (PMP)	·Pore size distribution ·Porosity		
· Spectroscopic methods (NMR,RM, ESR, and IR)	· Form and structure of the pore · Porosity		

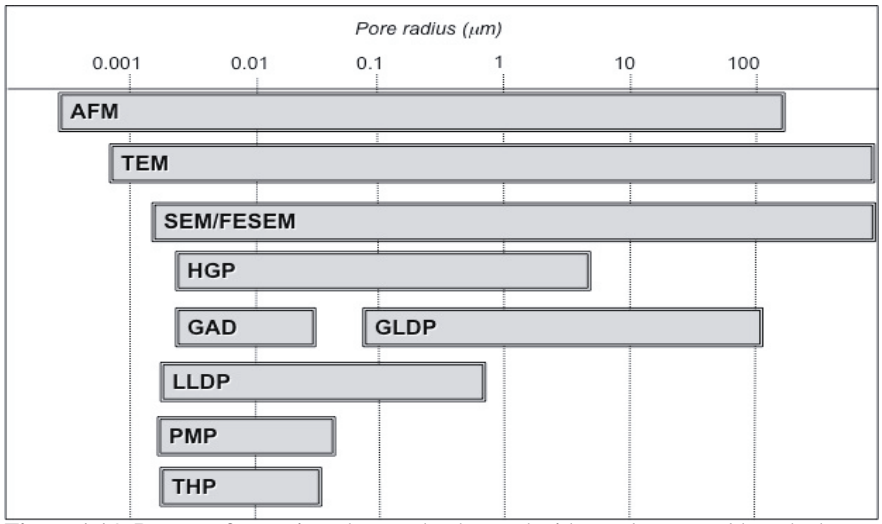

Figure 1.14: Ranges of pore sizes that can be detected with usual structural based characterization techniques.

1.5.2 Methods of liquid penetration

1.5.2.1 Fundamentals

It is well known that, when a liquid drop freely falls into a gas (for example water into air) or into another immiscible liquid phase, the drop tends to decrease its surface, due to a balance of interfacial forces, which results on acquiring a spherical shape. The mathematical description of this phenomenon brings us to the Young-Laplace equation (1805), **[70]**, which states that the pressure difference between the two phases, Δp, is directly proportional to the surface tension of the interface, γ, and inversely proportional to the drop radius R_d

$$\Delta p = \frac{2\gamma}{R_d} \qquad \textit{Eq 8}$$

Equation which refers to spherical drops but can be generalized to any surface shape.

$$\Delta p = \gamma\left(\frac{1}{R_1} + \frac{1}{R_2}\right) \qquad \textit{Eq 9}$$

Being R_1 , R_2, being the radii of curvature defining the surface. When $R_1 = R_2$, we arrive to simplified **Eq. 8** valid for for spherical surfaces. If now we suppose our liquid is forced to move inside a capillary tube, then the interface between that liquid and the other fluid (liquid or gas) filling the rest of the tube will adopt the shape of a meniscus. The shape of this meniscus, convex or concave, depends on the liquid-solid interaction and will be determined by the Young-Laplace equation. In the **Fig. 1.15**, we can see the radius of this meniscus, R_d , which is related to the radius of the capillary by $r=R_d \cos\theta$, being θ the contact angle between the liquid and the solid surface of the tube. Accordingly, the pressure required to expel the fluid from the capillary[11] is given by the Young-Laplace equation in the following form.

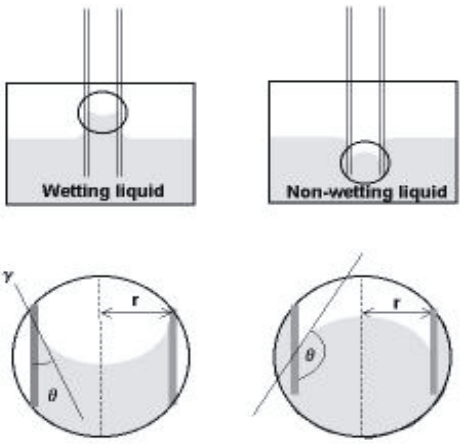

Figure 1.15: Capillary action of a wetting and non-wetting liquid relative to the walls of a capillary and its angle contact.

$$\Delta P = \frac{2\gamma}{r}\cos\theta \qquad \textit{Eq 10}$$

This equation is usually called *Washburn equation*, **[71].**

11Note that for non-wetting liquids, (i.e. for liquids having $\theta > 90^o$), this pressure, Δp is negative, which means we need to apply a positive pressure, $-\Delta p$, to intrude the liquid inside the capillary.

1.5.2.2 Bubble point method

This process is based on previous *Washburn equation***.** On the other hand, if the contact angle between liquid and capillary wall is zero, *cos θ=1,* we arrive to the usually called *Cantor equation***.** In 1908 Bechhold **[72]** was the first using Cantor's equation to size up pores measuring the necessary pressure to make air bubbles to blow through a membrane previously soaked of water. The method so developed has been used frequently to characterize membranes or filters and it is called bubble point. But this method is only useful for getting the maximum pore size among the pores present in the membrane pore size distribution. This maximum pore size corresponds to the minimal pressure necessary to see the first air bubbles arising from the membrane surface; for example for detecting a maximum pore size of 0.01μm the pressure becomes as big as 145 bar, if we are using the original air-water interphase. What we can do to diminish such applied pressures is to look for wetting liquids having sensibly lower surface tensions with typical membrane materials.

Several commercial devices have been developed that, based on this bubble point technique, are intended for evaluation of maximum pore size in membrane microfilters. Taking into account the typical surface tensions found for commonly used liquids, MF membranes need only some bars to detect their maximum pore size. Even tight UF membranes, presenting pores under 50 nm can be analysed using such bubble point devices for pressures under 10-15 bar, values which are reasonable. In market we can find some of such devices as *Sartocheck 4 (Sartorius), Flowstar XC (Palltronic), BpTester (PMI) or IntregrityTest II (Millipore)*, **[73].**

1.5.2.3 Fluid Displacement

The methods of bubble point and permeability can be combined to get the distribution of pore sizes, as proposed by Erbe, **[74]**. The successive increases of applied pressure allow estimating diameter for each pore class present in the distribution including the number of pores present in each one. The method has been improved along these years for both Gas-Liquid interphase, and more recently, Liquid-Liquid one, **[75]** permitting the evaluation of the size of pores corresponding to a wide range of porous materials.

Air Liquid Displacement

In the analysis of membrane filters using this technique, the membrane sample, previously wetted, is subjected to an increasing pressure, applied by a compressed clean and dry air source, at 313 K. As the pressure of air increases, it will reach a point where it can overcome the surface tension of the liquid in the largest pores and then it will start to push the liquid out. Increasing the pressure still further allows the air to flow through smaller pores, according to the *Washburn equation* (Cantor for perfectly wetting liquids).

When different pores of diverse sizes are opened the volume flow, J_v, of air increases accordingly until all the pores are emptied. By monitoring the applied pressure and the flow of gas through the sample when liquid is being expelled, a wet run is obtained. If the sample is then tested dry (without liquid in its pores), a dry run follows as show in **Fig. 1.16.** Comparison of both curves, using appropriate transport models, allows calculation of the contribution of each pore size to the total permeability along with the population of those **[76]**.

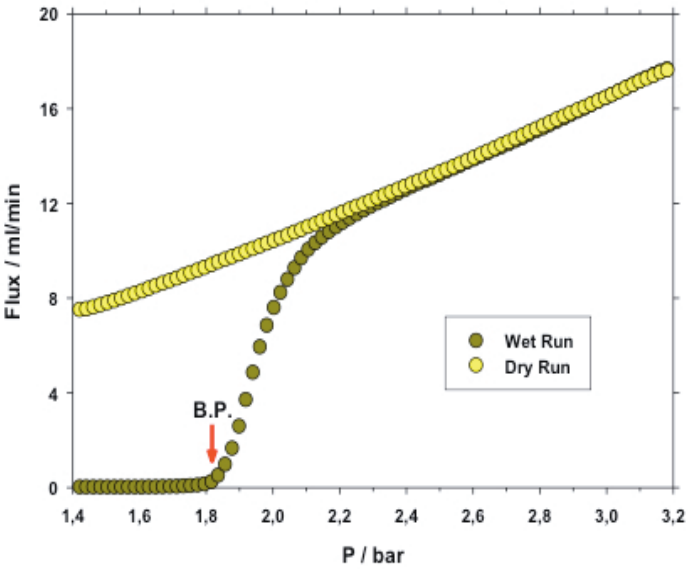

Figure 1.16: Typical wet–dry curves from the Coulter Porometer.

A Hagen-Poiseuille model for convective transport is normally used for accounting fluid transport inside capillary tubes. But gaseous fluids as the air used in this technique, also could be analysed using the Knudsen model for flow, and the pertinence of one or another model depends on the relative size of the mean free path of the gas molecules and the capillary diameter. Proper transitions between Knudsen and Poseuille models for analyzing GLDP results must be taken into account to get more precise results, **[77]**.

Finally, another source of error must be considered in the interpretation of porosimetric data. In both convective *(Hagen-Poseuille)* and diffusive *(Knudsen)* flow regimes, the model uses actual pore length to calculate pore contribution to total flow or permeabiltiy. This length is usually identified with the membrane thickness for symmetric membranes while for asymmetric ones, should correspond to the thickness of the active layer. Both cases suppose cylindrical pores normal to membrane surface with no tortuosity. But neither the actual thickness is easy to evaluate (especially for asymmetric membranes); nor the assumption of pore length equal to filter thickness without tortuosity can be as sured. In fact a recent work has improved data calculations by determining the tortuosity factor for each pore class in the distribution **[78]**.

Given that the contact angle depends on the liquid-membrane interaction, different liquids should be preferred for different membrane materials. In effect, liquids with low dielectric constant, hydrophobic liquids, should be selected when dealing with hydrophobic membranes, while high dielectric constant liquids should be preferred for hydrophilic materials. Nevertheless, the membrane material character could be unknown. In this case, a single liquid should be selected as a standard. Normally those exhibiting both radicals hydrophilic and hydrophobic; as for example, alcohols or halogen compounds, are useful.

Porometer manufacturers usually supply these liquids (*Porofil®, Fluorinert®, Porefil®, Porewick®, Galwick®* or similar combinations) which guarantee fast and complete wetting for almost all materials and present low surface tension, low vapor pressures and low reactivity, **[77]**. The usual organic liquids allow the analysis of pore sizes below 0.1 microns at applied pressure of about 10 bars.

Following the first commercial air-liquid porometer from Coulter, acquired time ago by Beckmann and now disappeared, more equipment have appeared over the years. Among those it can be commented that of PMI, one of the first in the market, which claims to lead down to almost nanometer range. Other companies manufacturing air-liquid porometers are Quantachrome or Porometer (a company originated at Benelux Scientific®).

Using such equipments, many groups continue evaluating pore size characteristics of membrane filters or comparing their results with those coming from different techniques, **[79]**. In literature the technique is sometimes named also as Capillary Flow Porometry, **[80]** or Liquid Extrusion Porometry, [**81]** but all refers to same procedure. Most equipments use a data smoothing algorithm which along the very steeply increase of pressure (typically more than 200 pressure steps are used in a complete analysis) lead to very soft almost Gaussian distributions. Also remarkable is the nice reproducibility of the method, which makes it very useful for characterizing not only membranes, but also many other porous materials. The upper range of application of the technique can be extended to pores up to 200 microns, allowing the application of the technique to sieving filters and also woven and non-woven textiles **[82].**

Liquid-Liquid Displacement

In this method, also proposed by Erbe, **[83, 84]** in 1933, and then refined by Grabar and Nikitine in 1936, **[85],** we will make use of the same principle of the gas-liquid porosimetry. But now the gas used to perform the porosimetric measurement is replaced by a liquid (so-called displacing liquid) which is not miscible with that (so-called wetting liquid) filling the membrane pores. The method is well described in the book of Kesting, **[86]**.

This method of operation can be done following the same procedure employed for GLDP, i.e. by gradually increasing the pressure of the displacing liquid and measuring the flow rate through the membrane pore as a function of the applied pressure, **[87, 88].** Also an alternative and more accurate route can be used, consisting on increasing stepwise the flow rate of the displacing liquid through a precise volumetric pump and measuring for each step the corresponding pressure, **[89, 90]**. In that case, syringe pump has proven to be very useful for such LLDP measurements as providing very stable fluxes without fluctuations and need to use any sort of dampening, **[90, 91].**

Table 1.8 List of different immiscible wetting liquid-displacing liquid pairs obtained from the phase demixing of two or three components mixture which can be selected for LLDP measures according to the membrane pore size.

Liquid Pair	Composition (v/v)	Interfacial tension γ (mN/m)	Temperature (ºC)	Ref.
Water/Isobutanol/ Methanol	25/15/7	0.35	18.7-24	**[85]**
Water/Isobutanol/ Methanol	4/5/1	0.80	20-23	**[85]**
Water/Isobutanol	1/1	2.2	18.7-21	**[85]**
Water/Isobutanol	1/1	2.0	25	**[97]**
Water/Pentanol	1/1	4.8	25	**[97]**
Water/Octanol	1/1	8.5	25	**[97]**

Liquids pairs with very low interfacial tension are very suitable for testing membranes having pore sizes in the nanometer range, since these pores can be invaded by the displacing liquid at very low pressures that do not alter the membrane structure. For example, according to Cantor equation, for Water/Isobutanol system ($\gamma = 1.7$ *mN/m*) and complete membrane wetting ($\theta = 0$), the wetting liquid which fills the pore with radius of 0.034 μm will be expelled out by the displacing liquid at a pressure of 1 bar, i.e. a value at which the membrane compaction that could represent an important source of error in LLDP measurements, **[92]**, is negligible. A great advantages of this method lies on the fact that the membrane is tested under wet state, i.e. in a condition very close to that occurring in largely important membrane separation processes, such as dialysis, Micro-Ultra-Nano-Filtration. The method is clearly sensitive to interactions between the membrane and the liquid pairs. Swelling phenomena during testing may deeply alter the permeation through the pore thus leading to unreliable results.

Various more or less automated devices have been developed in different research labs to perform the measurements but only a very limited number of commercial devices are available, **[93]**.

To summarize the advantages of LLDP, mostly common to GLDP, we can conclude that this technique:

* **It only accounts for pores open to flux.**
* **It test membranes in wet state, so closer to real operation way.**
* **Both techniques (GLDP and LLDP) cover most of the range of pore usually found in synthetic membranes, being LLDP able to analyse pores under the nanometer range, [94].**

The high potentiality of this technique in order to evaluate the active pores in the nanometer and subnanometer range makes convenient to establish a standard procedure. This, yet done for GLDP, **[95-97]**, is not still considered for LLDP, mainly by two con-

nected reasons:

* *LLDP procedure needs more careful sample preparation and analysis operation, which if not properly done, could easily lead to non reproducible or inconsistent results.*
* *Due to this previous reason, there not exist in market almost any commercial apparatus and possible users have not gained enough confidence on the quality of the method.*

1.6 CONCLUSIONS

The main purpose of this chapter as its title indicates, is to introduce briefly the membrane processes, including the diverse membrane processes with their more common applications, the filters they are used in those processes, and the functional and structural characteristics of those filters. In this sense, we have tried to include and briefly comment most of the usual characterization techniques, both structural and functional ones.

Finally we have devoted some more detail to introduce the techniques based on fluid displacement, as the origin and basis of the Liquid-liquid Displacement Porosimetry, whose improvement is the main scope of this thesis.

1.7 REFERENCES

[1] R.W. Baker, "Membrane Technology and Applications", Wiley and Sons, Chichester, (U.K) 2004.

[2] H. K. Lonsdale, The growth of Membrane Technology, J. Membrane Sci, 10 (1982) 81-181.

[3] S. Pereira, Viktor Nunes and Klaus. Peinemann, "Membrane. Tech in the Chemical Industry," Wiley-VCH, Weinheim (Germany) 2006.

[4] M. Mulder, "Basic Principles of Membrane Technology", Kluwer Academic Publishers, Amsterdam (The Netherlands) 1996.

[5] Y. Magara, S. Kunikane, M. Itoh, Advanced Membrane Technology for application to water treatment, Water Science and Technology, 37 (1998) 91–99.

[6] The Freedonia Group, Inc. World Membrane Separation Technologies, Industry Study with Forecasts for 2012, 468, Cleveland, OH (USA) 2012.

[7] Gobal Water Intellingence, Media Analytics Ltd. Global RO / NF Membrane Market Forecast to 2016 -CHART-, 10 (2009).

[8] K. Sutherland, "Profile of the International Membrane Industry - Market Prospects to 2008"-, Elsevier, Amsterdam (The Netherlands) (2003), 53–78.

[9] A.W. Crull, Who's on first. State of the market for RO, MF, UF. Filtration News, September-October 1997, 38.

[10] US water treatment market grows, Membrane. Tech, June 2003, 2.

[11] Medical membranes market set to grow, Membrane. Tech, November 2007, 6.

[12] Membrane technologies: Industry trends and applications, Membrane. Tech, June 1998, 11–12.

[13] B. Lesjean, E.H. Huisjes, Survey of the European MBR market: trends and perspectives, 231 Desalination, (2008), 71–81.

[14] S. Atkinson, Research studies predict strong growth for MBR markets, Membrane. Tech, February 2006, 8–10.

[15] European market for liquid separating membranes, Membrane. Tech, June 1998, 4.

[16] McIlvaine Corporation, RO, UF, MF, World Markets, Membrane. Tech, September 2005, 4**.**

[17] N. M. Wade, Technical and economic evaluations of distillation and reverse osmosis desalination processes, Desalination, 93 (1993) 343-363.

[18] H**.** Strathmann, L. Giorno, E. Drioli, "An Introduction to Membrane Science and Technology", Institute on Membrane Technology, CNR-ITM at University of Calabria, Rende (CS) (Italy) 2006.

[19] K**.** Sutherland, "Profile of the International Membrane Industry - Market Prospects to 2008"-, Elsevier, Amsterdam (The Netherlands) 2003, 45–51.

[20] D. Bhattacharyya, D. A. Butterfield, "New Insights into Membrane Science and Technology: Polymeric and Biofunctional Membranes", Elsevier, Amsterdam (The Netherlands) 2003.

[21] J.I. Calvo, "Caracterización de Membranas de Microfiltración. Aspectos estructurales y funcionales", PhD, Univ. of Valladolid, Valladolid (Spain) 1999.

[22] N. Lakshminarayana, "Equations of Membrane Biophysics", Academic Press, NY, (USA) 1984.

[23] M. Mulder, "Basic Principles of Membranes Technology", Kluwer Academic Publishers, Dordrecht (The Netherlands) 1991.

[24] V. Silva, "Theoretical Foundations and Modelling in NanoFiltration Membrane Systems", PhD, Univ. of Valladolid, Valladolid (Spain) 2010.

[25] J. A. I. Mengual, "Fundamentos de los Procesos de Transporte y Separación en Membranas", Univ. of Murcia, Murcia (Spain) 1989.

[26] L. P. Martínez "Caracterización Estructural y Superficial de Membranas Microporosas", PhD, Univ. of Valladolid, Valladolid (Spain) 1999.

[27] K. Scott, "Handbook of Industrial Membranes", First Edition, Elsevier Science Publishers, Amsterdam (The Netherlands) 1995.

[28] R.D. Noble, Stern S.A, "Membrane Separation Technology, principles and applications", Elsevier Science Publishers, Amsterdam (The Netherlands) 1995.

[29] C.A. Smolders, A.J. Reuvers, R.M. Boom, I.M. Wienk, Microstructures in phase inversion membranes. Part 1. Formation of macrovoids, J. Membrane Sci, 73 (1992) 259.

[30] K.Watanabe, H.Ohya, Membrane Experiments Series; Artificial Membranes. Membrane Society of Japan, (1993) 5–9.

[31] K. Scott, "Handbook of Industrial Membranes", First Edition, Elsevier Science Publishers, Amsterdam (The Netherlands) (1995).

[32] M. L. Crowder, C. H. Gooding, Spiral wound, hollow fiber membrane modules: A new approach to higher mass transfer efficiency, J. Membrane Sci, 137 (1997) 17–29.

[33] R.G. Gutman, "Crossflow Filtration", IOP Publishing Ltd, Philadelphia (USA) 1987.

[34] R. E. Kesting. "Synthetic Polymeric Membranes: A Structural Perspective", Wiley, Hoboken, NJ (USA) 1985, 237–261.

[35] K. Ebert, F. P. Cuperus, Non-aqueous applications of NF, A.I. Schäfer, A.G. Fane, T.D. Waite (Eds.), Nanofiltration – Principles and Applications, Elsevier, Oxford (2003), 521–536.

[36] Li N. N, Fane A.G, Winston Ho, W. S. and Matsuura T. "Advanced Membrane. Tech and applications", John Wiley and Sons, New Jersey (USA) 2008.

[37] Matsuura T, "Synthetic Membranes and Membrane Separation Processes", CRC Press, Florida (USA) 1994.

[38] I. Pinnau , B.D. Freeman, "Membrane formation and modification", American Chemical Society, Washington, D.C (USA) 2000.

[39] B.D. Freeman, I. Pinnau, "Division of Polymeric Materials: Science and Engineering", American Chemical Society, Washington, D.C (USA) 1999.

[40] K. P. Lee, T. C. Arnot, D. Mattia, A review of reverse osmosis membrane materials for desalination-Development to date and future potential-, J. Membrane Sci, 370 (2011) 1–22.

[41] R. W. Baker, "Membrane. Tech and Applications", J. Wiley and Sons, Chichester, (U.K) 2004.

[42] W.S.W. Ho and K.K. Sirkar, "Membrane Handbook", Van Nostrand Reinhold, New York, (USA) 1992**.**

[43] S. Loeb, S. Sourirajan, Seawater Demineralization by Means of a Semipermeable Membrane in Advances in Chemistry, ACS Series, (USA) 1963, 117-132.

[44] M. Trigo-López, P. Estévez, N. San-José, A. Gómez-Valdemoro, F. C. García, F. Serna, J.L. de la Peña, J. M. García Burgos, Recent Patents on Aromatic Polyamides, 2 (2009) 190-208.

[45] M. Charyan, "Ultrafiltration Handbook". Technomic Publishing Inc, Lancaster, (UK) 1986.

[46] G. Belfort, "Synthetic Membrane Processes: Fundamentals and water applications". Academic Press, New York (USA) 1984.

[47] A. Hernández, J.I. Calvo, P. Prádanos, F. Tejerina, Pore size distributions in microporous membranes. A critical analysis of the bubble point extended method, J. Membrane Sci, 112 (1996) 1-12.

[48] K. Scott, R. Hughes, "Fundamental of membrane: Industrial membrane separation technology", Springer, Glaswok (UK) 1996.

[49] G. Belfort, "Fundamentals and Water Applications". Synthetic membrane processes Academic Press, New York (USA) 1984.

[50] M.C. Porter, "Handbook of Separation Techniques for Chemical Engineers", McGraw-Hill, New York (USA) 1979.

[51] I.C. Kim, H.G. Yun, K.H. Lee, Preparation of asymmetric polyacrylonitrile membrane with small pore size by phase inversion and post-treatment process, J. Membrane Sci, 199 (2002) 75–84.

[52] Z.G. Wang, L.S. Wan, Z.K. Xu, Surface engineerings of polyacrylonitrile-based asymmetric membranes towards biomedical applications: An overview, J. Membrane Sci, 304 (2007) 8–23.

[53] K.W. Lawson, D.R. Lloyd, Review membrane distillation, J. Membrane Sci, 124 (1997) 1–25.

[54] S.P. Nunes, K.V. Peinemann, "Membrane. Tech in the Chemical Industry"; Wiley-VCH, Wemheim (Germany) 2001.

[55] S.S. Kulkami, E.W. Funk and N.N. Li, Membranes, in Membrane Handbook, W.S.W. Ho and K.K. Sirkar (Eds.), Van Nostrand Reinhold, New York (USA) 1992.

[56] S. Nakao, Determination of pore size and pore size distribution. Filtration membranes. J. Membrane Sci, 96 (1994) 131-165.

[57] F.P. Cuperus, "Characterization of Ultrafiltration Membranes", Ph.D. Thesis,Univ. of

Twente, Twente (The Netherlands) 1990.

[58] S.F.E. Boerlage, M. Kennedy, Z. Tarawneh, R. De Faber, J.C. Schippers, Development of the MFI-UF in constant flux filtration, Desalination, 161 (2004) 103–113.

[59] K.J. Kim, A.G. Fane, C.J.D. Fell, T. Suzuki, M.R Dickson, Quantitative microscopic study of surface characteristics of UF membranes, J. Membrane Sci, 54 (1990) 89-102.

[60] M. Mulder, "Basic Principles of Membrane. Tech", Kluwer, Dordrecht, (The Netherlands) 1991.

[61] B. Van der Bruggen, C. Vandecasteele, Distillation vs. membrane filtration: overview of process evolutions in seawater desalination, Desalination, 143 (2002) 207-218.

[62] R. Pastor, J.I. Calvo, P . Prádanos, A. Hernández, Surface charges and zeta potentials on polyethersulphone heteroporous membranes, J. Membrane Sci, 137 (1997) 109-119.

[63] R. Sahai, "Membrane Separations and Filtration", Encyclopedia of Separation Science, Oxford (UK.) 2000, 1717–1724.

[64] R. van Reis, A. Zydney, Membrane separations in biotechnology, Current Opinion in Biotechnology, 12 (2001) 208–211.

[65] H. Bechhold, The permeability of ultrafilters, Z. Phys. Chem, 64 (1908) 328-342.

[66] G.Binning, C.F. Quate, Ch. Gerber, Atomic force microscopy, Phys. Rev. Lett, 56 (1986) 930-933.

[67] J.I. Calvo, R. I. Peinador, P. Prádanos, L. Palacio, A. Bottino, G. Capannelli, A. Hernández, Liquid–liquid displacement porometry to estimate the molecular weight cut-off of ultrafiltration membranes, Desalination (2011) 174–181.

[68] M. Brun, A. Lallemand, J.F. Quinson, C.A Eyraud, A new method for simultaneous determination of the size and the shape of pores: Thermoporometry, Thermochimica, 21 (1997) 59-88.

[69] Jae-Deok Jeon, Soo Jung Kim, Seung-Yeop Kwak, ^{1}H nuclear magnetic resonance (NMR) cryoporometry as a tool to determine the pore size distribution of ultrafiltration membranes, J. Membrane Sci, (2008) 233–238.

[70] H. Bechhold, "The Permeability of Ultrafilters", Z. Phys. Chem, 64 (1908) 328-342.

[71] E.W. Washburn, "The Dynamics of Capillary Flow", Phys.Rev, 17 (1921) 273-283.

[72] H. Bechhold, M. Schlesinger, K. Silbereisen, L. Maier, W. Nurnberger, Pore diameters of ultrafilters, Kolloid Z, 55 (1931) 172-198.

[73] J.I. Calvo, Membrane characterization by porosimetric techniques, lesson presented at XXIV Summer School on Membranes, Genoa (Italy) 2007.

[74] F. Erbe, Blockierungsphënomene bei ultrafiltern, Kolloid Z, 59 (1932) 195-206.

[75] G. Capannelli, F. Vigo, S. Munari, Ultrafiltration membranes - characterization methods, J. Membrane Sci, 15 (1983) 289-313.

[76] J.I. Calvo, A. Hernandez, P. Pradanos, L. Martinez, W.R. Bowen, Pore size distributions in microporous membranes. Bulk characterization of tracketched filters by air porometry and mercury porosimetry, J. Colloid Inteface Sci, 176 (1995) 467–478.

[77] A. Hernández, J.I Calvo, P. Prádanos, F. Tejerina, Pore size distributions in microporous membranes. A critical analysis of the bubble point extended method, J. Membrane Sci, 112 (1996) 1-12.

[78] A. Shrestha, J. Pellegrino, S.M. Husson, S.R. Wickramasinghe, A modified porometry approach towards characterization of MF membranes, J. Membrane Sci, 421-422 (2012) 145–153.

[79] C.M. Gribble, G.P. Matthews, G.M. Laudone, A. Turner, C.J. Ridgway, J. Schoelkopf, P.A.C. Gane, Porometry, porosimetry, image analysis and void network modeling in the study of the pore-level properties of filters, Chem. Eng. Sci, 66 (2011) 3701–3709.

[80] D. Li, M.W. Frey, Y.L. Joo, Characterization of nanofibrous membranes with capillary flow porometry, J. Membrane Sci, 286 (2006) 104–114.

[81] S.S. Manickam, J.R. McCutcheon, Characterization of polymeric nonwovens using porosimetry, porometry and X-ray computed tomography, J. Membrane Sci, 407–408 (2012) 108–115.

[82] J.I. Calvo, A. Bottino, P. Prádanos, L. Palacio, A. Hernández, Membrane characterization: Porosity, in "Wiley Enciclopedia of Membrane Science and Technology", E.M.V. Hoek, V.V. Tarab ara and M. Peterca, (Eds.), Wiley and Sons, New York (USA), in press (2013).

[83] F. Erbe, Blockierungsphenomene bei ultrafiltem, Kolloid Z, 59 (1932) 32–44.

[84] F. Erbe, Die bestimmung der porenverteilung nach ihrer größe in filtern und ultrafiltern, Kolloid Z, 63 (1933) 277–285.

[85] P. Grabar, S. Nikitine, Sur le diamètre des pores des membranes en collodion utilisées en ultrafiltration, J. Chim. Phys, 33 (1936) 721–741.

[86] R.E. Kesting, "Synthetic Polymeric Membranes: A Structural Perspective", 2nd. Ed, Wiley and Sons, New York (USA) 1985.

[87] V. Hampl, K. Spurný, Analytical methods for determination of aerosols by means of membrane ultrafilters. Comparison of methods used for the determination of the mean radius and the pore distributions curve, Coll. Czec. Chem. Commun, 32 (1967) 4181–4189.

[88] L.Q. Wu, P. Huang, N. Xu, J. Shi, Effects of sol properties and calcination on the performance of titania tubular membranes, J. Membrane Sci, 173 (2000) 263–273.

[89] G. Capannelli, I. Becchi, A. Bottino, P. Moretti, S. Munari, Computer driven porosimeter for ultrafiltration membranes, in: K.K. Unger et al. (Eds.), Characterization of Porous Solids, Elsevier, Amsterdam (The Netherlands) (1988) 283-294.

[90] R.I. Peinador, J.I. Calvo, K. ToVinh, V. Thom, P. Pradanos, A. Hernandez, Liquid-liquid displacement porosimetry for the characterization of virus retentive membranes, J. Membrane Sci, 372 (2011) 366–372.

[91] J.I. Calvo, A. Bottino, G. Capannelli, A. Hernandez, Comparison of liquid–liquid displacement porosimetry and scanning electron microscopy image analysis to characterise ultrafiltration track-etched membranes, J. Membrane Sci, 239 (2004) 189–197.

[92] K. R. Morison, A comparison of liquid–liquid porosimetry equations for evaluation of pore size distribution, J. Membrane Sci, 325 (2008) 301–310.

[93] http://www.pmiapp.com/products/liquid-liquid-porometer.html. PMIAPP Europe 20 Dutch Mill Rd. Ithaca, NY (USA).

[94] J.M. Sanz, R. Peinador, J.I. Calvo, A. Hernández, A. Bottino, G. Capannelli, Characterization of UF membranes by liquid–liquid displacement porosimetry, Desalination, 245 (2009) 546–553.

[95] ASTM F316, Standard test method for pore size characteristics of membrane filters by bubble point and mean flow pore test, 2003.

[96] ASTM E1294, Standard test methods for pore size characteristics of membrane filters using automated liquid porosimeter, 1999.

[97] J. Fu, B. Li, Z. Wang, Estimation of fluid-fluid interfacial tensions of multicomponent mixtures, Chem. Eng. Sci, 41 (1986) 2673–2679.

CHAPTER 2

2 DEVELOPMENT AND OPTIMIZATION OF A LIQUID-LIQUID DISPLACEMENT POROMETER DEVICE

2.1 HISTORICAL

The fluid displacement techniques have been considered, for years, very promising solutions, due that are specially appropriate as being non-destructive, very fast and refer only to pores opened to flux, which are the only pores which really contribute to membrane permeation.

These advantages were recognised from the pioneering works of Erbe, improved later by Grabar and Nikitine **[85]**. Based on those pioneering works, different groups developed new devices **[98]**, or reviewed the existing results **[99]**.

After a reasonable success of the GLDP technique, especially when several commercial devices appeared in market, next natural step should have been to extend the technique to lower pore size membranes. As commented in previous chapter, the typical range of usual GLDP porometers goes down to 50 nm, which is enough for MF membranes or very open UF ones. But for analysing membranes having pores under 50 nm by using an air-liquid interface, too high pressures are needed.

At that point, Liquid–Liquid Displacement Porosimetry, LLDP, making use of a liquid–liquid interface inside the pores, solves the problem of the high pressure needed. This fact should have led to increasing interest in the use of this technique in UF membrane characterization.

Some authors as Capannelli et al. **[19]**, Gekas and Zhang **[100]** have used liquid porosimetry to characterize the pore size distribution of UF membranes. They were able to characterize the entire pore size distribution at pressures less than 8 bar. Other authors as Wienk et al. **[101]** pointed out some critical factors to be taken into account when using LLDP. Germic et al. **[102]** compared LLDP with other techniques as Permporometry or FESEM. Gijsbertsen-Abrahamse et al. **[103]** modelled the liquid interface inside the pores and concluded that there exists a systematic error on LLDP measurements when dealing with interconnected pores, as usually found in many polymeric or inorganic membranes. Other authors, McGuire, Morrison, et al **[104, 105]**, have tried to upgrade the algorithm of calculation in the distribution of sizes of pores, through a continuous distribution of the experimental data. To resume only few groups have continued regularly to publish on LLDP **[106, 109]**. Very recently a paper has been published on LLDP, but using an Isopropanol/Water interface instead the usual Isobutanol/Water one **[15]**. Finally DiLeo and Phillips **[16]** have proposed a liquid porosimetry technique *(CorrTest® TM)* in which data measured at a single intrusion pressure were used to effectively correlate dextran retention by UF membranes **[17]** and virus retention by viral retentive membranes **[18]**. In their work, they used polyethylene glycol, ammonium sulphate and water as porosimetric fluids.

Nevertheless not too much work has been done in LLDP in the last years due as seen to some difficulties in an appropriate design of the experimental protocol.

In order to summarise the present state of the matter, the usual important criticisms to the technique, give an idea of the problems that researchers found today when facing with LLDP; among those, difficulty of use and poor reproducibility of the results are quite common. In any case, the group of the University of Genoa, after a continuous work in LLDP over last 30 years, developed a more or less automated equipment to analyse UF membranes [**19**]**.** The SMAP group started to collaborate with the group of Genoa in 2000, and from then, always in close collaboration, both teams have updated and improved an automated Liquid-Liquid Porosimeter that features common aspects of the technique and provides accurate and reproducible results at pore radii as low a few manometers.

The aim of this thesis was to convert the data acquisition and elaboration software of this equipment to a LabVIEW® interface, as more powerful and commonly used in laboratories all around the world. Not less important, during this work, the setup characteristics and performance have been improved, and the application limits of the technique have been pushed up to the maximum possible.

In that way, we have developed and updated a fully automated and very precise equipment, that using LLDP, allows obtaining important information on the structure of UF membranes, including pore size distribution and porosity. Also this technique, as will be shown in **paper 4**, will serve to estimate the MWCO of UF membranes. The equipment so developed will be used along this thesis to characterize several commercial membranes and the information obtained will be compared with that arising from other characterization methods, to give complete information on the structure of the analysed filters. Always with the final objective of improving the LLDP technique and leading it to be considered as worthy to become the standard for UF membrane characterization of porosity related parameters

2.2 LLDP ANALYSIS FUNDAMENTALS

Following the previous comments about LLDP, now we are going to give a closer vision about this method of characterization. It must be remembered that the LLDP analysis is based on the fact that the pressure needs to be applied to a given liquid to displace another liquid from a capillary that is related with the surface tension between both immiscible liquids, and the radius of the capillary, following Cantor equation $\Delta p=2\gamma/r$ (supposed nil contact angle between liquid and capillary walls).

For a better understanding of the method we can consider, for the sake of simplicity, a very schematic membrane composed by 3 single pores, with respective radii: $r_1>r_2>r_3$. To displace the wetting liquid from the pore having radius r_1 it is needed to apply a pressure P_1 such that:

$$P_1 = \frac{2\gamma}{r_1} \qquad \textit{Eq 11}$$

At this pressure the flux of permeating liquid crossing the pore with radius r_1,will be J_1. The pore with radius $r_2<r_1$ will be permeated by the displacing liquid only if we apply a higher pressure: $P_2>P_1$; but increasing further the pressure, when it achieves a value, P_3 so that the permeating or displacing liquid will displace the wetting one from the pore having radius r_3, there will be flux coming from all 3 pores. Flux J_3 corresponding to pressure P_3 will be given by contribution of all the pores having radius equal or higher to r_3. Over P_3, any further pressure increased will determine a proportional increase of the flux across the membrane.

From experimental *Flux/Pressure* curve (see **Fig. 2.2)** and using Cantor equation we can obtain the permeability $L = J/P$ distribution of the pores *k-th* actually present in the membrane. While to obtain the distribution of the number of pores in the membrane N, per surface unit, having a given pore radius, r, for each *differential* pressure step, Δp_i. It is needed to use an adequate transport model If we assume laminar movement of the fluid through the pores, we can use the Hagen-Poiseuille[1] model to correlate volume flow J_v and applied pressure Δp_i following next equations.

$$J_v = \sum_{k=1}^{i} \frac{N_k \pi r_{pk}^4}{8\eta l} \Delta P_i \qquad N_k = \frac{\eta l J_k \Delta P_k}{2\pi\gamma^4} \qquad \textbf{Eq 12}$$

Where η is the dynamic viscosity of the displacing fluid, N_k represents the number of pores of radius r_k, i.e in the class *k-th* per unit membrane surface and l is the pore length, that in the event of the symmetric membranes is equal to thickness of the membrane. Nevertheless, in the case of asymmetric membranes it is necessary to calculate the width of the active layer (see **Fig. 1.3**), which differs from the support that gives consistency to the membrane. Equations **11 and 12** are the fundamental basis of LLDP. From these, they can be developed algorithms to analyse deeply the internal structure of the membranes.

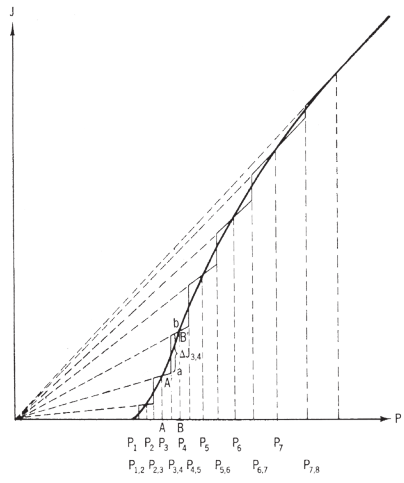

Figure 2.1: Graphical solution of the porosimetric curve from Erbe **[34]**.

The original graphical procedure to convert porosimetric data into pore calculations, as proposed by Erbe, **[74]**, and nicely presented in the book of Kesting, **[34]**, has been very often used for LLDP calculations. This procedure is summarily presented in **Fig. 2.1**. Other procedure comes from an apparently different algorithm, developed by Grabar and Nikitine, **[85]**. While this algorithm is based on a continuous experimental curve, it is fairly easy to adapt to discrete experimental results, so that it becomes very convenient for the purpose of programming and implementation in automated equipment, allowing automatic calculation of the resulting distributions.

1 Hagen-Poiseuille law in that previous simple form only holds for the convective flow through cylindrically shaped straight pores.

2.2.1 Grabar-Nikitine Algorithm

In the next paragraphs, we will give a resumed overview about the theoretical treatment that applied on experimental data of any porosimetric experience will allow to get the maximum information relevant for the purposes of membrane characterization.

The obtained experimental data consist in a raw of simple data pairs: flow of displacing liquid at each stage of analysis and resulting applied pressure across the membrane, resulting in a Flux vs. Pressure plot. On these experimental data pairs, we sill apply the calculation algorithm developed by Grabar and Nikitine to determine the number of pores open to flow in each increment, along with contribution of each step to overall permeability and other significant parameters. The algorithm makes use of the Hagen-Poiseuille model for convective flow through pores.

We will depart from the **Eq.12** connecting pressure, flow, number of pores and pore radius. Thus, fluid flow passing at the given pressure p, through the pores whose diameters are between *2r and 2(r + dr)* is:

$$Jdr = \frac{\pi p r^4}{8\eta l} n(r)\,dr \qquad \textit{Eq 13}$$

being η is the fluid viscosity, and l the thickness of the membrane. The overall flow that goes through the membrane at this pressure, is between $2r$ and $2r_{max}$.
By integration we obtain:

$$J = \frac{\pi p}{8\eta l} \int_{r}^{r_{\max}} r^4 n(r)\,dr \qquad \textit{Eq 14}$$

Differentiating this expression and substituting r by p according to Cantor, we get the number of pores for a given pressure increment:

$$n(r) = \frac{8\eta l P_{av}^{\,5}}{\pi (2\gamma)^5}\left[\frac{dj}{dp} - \frac{J_{av}}{P_{av}}\right] \qquad \textit{Eq 15}$$

Applying the definition of permeability, through the above expression, we obtain:

$$L(r) = \frac{\eta p}{\eta_1 2\gamma}\left[\frac{dj}{dp} - \frac{J_{av}}{P_{av}}\right] \qquad \textit{Eq 16}$$

The permeability is a function, among other things, of the relative viscosity of the pairs liquids used. Both differential pressure and flow are infinitesimal variables, and they match with the incremental values of pressure and flow in each experimental step of the analysis, while J_{av} and P_{av} correspond to the mean values of both variables in the corresponding step.
Next table summarizes the step to the discretization of the variables obtained from the experimental curve in the step i, $i+1=j$ (see **Fig. 2.2**).

$$dj \longrightarrow \Delta J = J_{i+1} - J_i \text{ and } J_{av} = \frac{J_i + J_{i+1}}{2}$$

$$dp \longrightarrow \Delta P = P_{i+1} - P_i \text{ and } P_{av} = \frac{P_i + P_{i+1}}{2}$$

$$dr \longrightarrow \Delta r = r_i - r_{i+1}$$

In terms of which **Eqs. 15** and **16** and continuous variables stands as follows:

$$n(r) \longrightarrow n_{ij} = \frac{8\eta l P_{ij}^5}{\pi(2\gamma)^5}\left[\frac{\Delta j}{\Delta p} - \frac{J_{ij}}{P_{ij}}\right] \qquad i = 1,2....k \qquad \textbf{Eq.17}$$

$$L(r) \longrightarrow \Delta L_{ij} = L_{i+1} - L_i = \frac{\eta p_{ij}}{\eta_1 2\gamma}\left[\frac{\Delta j}{\Delta p} - \frac{J_{ij}}{P_{ij}}\right] \qquad i = 1,2....k \qquad \textbf{Eq.18}$$

Remembering previous fundamentals, the effluent (flux-pressure) curve is obtained when consecutive pores of the membranes, between maximum value rmax and minimum value $r_{min} > 0$, are subsequently opened to flow of displacing liquid. The resulting curve presents a *S*-shaped aspect ending in a maximum slope (asymptotic permeability), which corresponds to the moment all the pores are opened to flow, so that the permeability becomes constant and no more pores can be opened.

It must be noted that above calculation of ΔL only stands for positive values, as negative ones means that yet opened pores are again closing or non contributing to total permeability. This fact will be used as a key point to automatic decision on ending analysis.

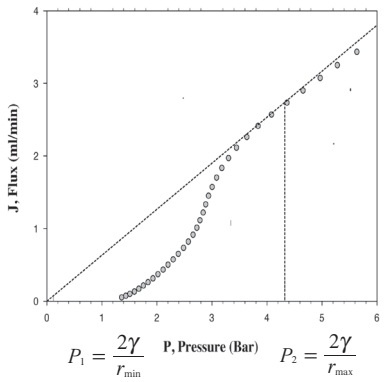

Figure 2.2: Effluent or porosimetric flux-pressure curve.

The previous equations, (**Eq.17-18**), when represented versus applied pressure (or better converting x-axis into pore sizes using Cantor equation) give us the pore number and permeability distributions of pore sizes. Other pore size distributions can be obtained easily from those.

For example, the total surface occupied by pores of a given range of radii can be obtained by multiplying the surface area of an individual pore of a given radius by the total number of such pore, hence.

$$A_{ij} = n_{ij}\pi r_{ij}^2 \qquad \textbf{Eq 19}$$

The total area A_t and the total number of pores N_t, can be obtained as follows.

$$A_t = \sum A_{ij} \qquad \textbf{Eq 20} \qquad\qquad N_t = \sum n_{ij} \qquad \textbf{Eq 21}$$

The curves of the pore size distribution obtained from the evaluation flux-pressure experimental curve, are reported in **Figs. 2.3.** In both figures we have presented the distribution of permeabilities and number versus pore size, i.e. the contribution (in percentage) of each pore size to the total permeability and number respectively.

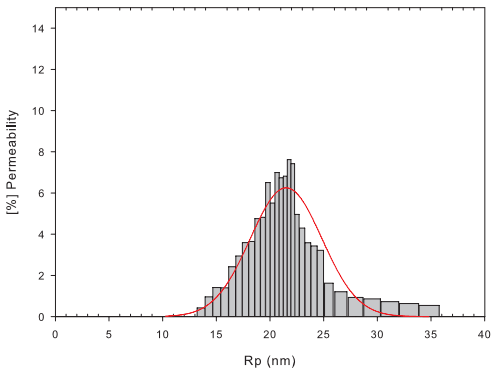

Figure 2.3a: Distribution of permeabilities vs pore size fitted to a Gaussian curve.

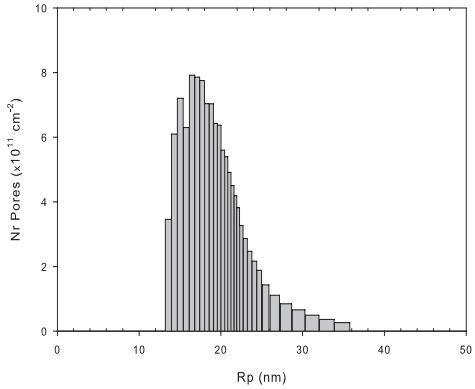

Figure 2.3b: Distribution of pore number vs pore size.

Finally all these distributions can be converted into cumulative ones, **(see Fig. 2.3c)**, using following calculation:

$$\zeta_{j,j+1}^{cum}(\%) = \sum_{i=0}^{j} \frac{z_{i,i+1}}{z_{tot}} 100 \qquad \textit{Eq 22}$$

Being ζ_i the cumulative value corresponding to distribution of z_i .

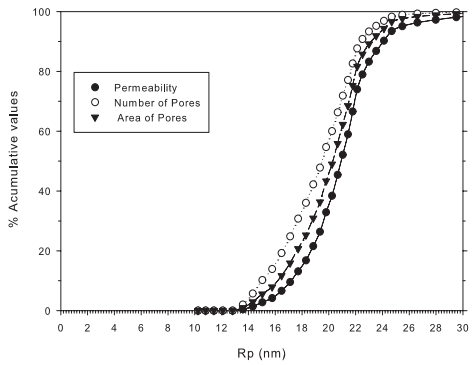

Figure 2.3c*:* Cumulative values of several distributions, vs pore size.

This mathematician algorithm allows to perform a reasonable data treatment based on experimental values, but of course, this is rather simplified not accounting for actual membrane conditions. For example the algorithm does not take into mind the contact angle θ (here supposed nil) or the existence of certain pore tortuosity ψ. McGuire **[104]**, assuming that pores are cylindrical capillaries parallel to each other, and using first order approximation in its numerical evaluation, tried to improve the algorithm.

Other authors as Morrison **[105]**, gave very similar numerical results adding extra variables, but these are often unknown so a better results is not necessary obtained.

As far as our experience has showed, this calculation, if being worthy of improvement, it is very appropriated for supplying easy-information about the structural and performance properties of the membranes, without losing any particular advantages inherent to a more complex evaluation.

2.3 AUTOMATED LLDP POROSIMETER

Once revised fundamentals and data conversion algorithm of LLDP, we will devote next section to a summarized description of the materials, devices and software implementation which composes our LLDP setup. Basically the porosimeter can be divided in two main constituent parts:

- *Experimental* device, including data acquisition software to control the porosimeter during the execution of the analysis.

- *Data analysis* software which allows to obtain all relevant information from the poremetric analysis.

Both parts will be commented in enough detail along the following sections

2.3.1 LLDP Setup

Departing from a visit of SMAP members to the University of Genoa, a LLDP porometer device based on the specifications of that running in Genoa was built up in Valladolid. This first equipment, initially run in manual operation up to be optimized and improved, was then automatized based on the VEE laboratory software, **[113]**. The resulting porometer showed to be very reliable and efficient and it was continuously tested in close collaboration with Genoa, who built up a new setup following our design. This is the basis of the actual porosimeter, which includes software controlled operation, data acquisition and data treatment, now with a new software developed during this thesis and running under LabVIEW® 8.5. The main components of the resulting setup and the features of the designed software will be detailed described afterwards.

Porosimeter set-up is composed by the following elements, (see **Figs. 2.3-4)**

a) *Syringe pump* (from ISCO®, mod. 500D, including pump controller. It has a capacity of 500 mL which is enough for most of the analysis. Only very permeable membranes need stop and refilling before ending the analysis. The pump is the most important element of the porosimeter (along with the most expensive), since it allows a very precise and steeply control of the flux implemented across the membrane cell.

Flow Range: 0. 001 to 204 ml/min ; *Flow Accuracy*: 0.5% of setpoint.

b) *Pressure transducer* (DFP®, from AEP, with digital display), connected to the output of the membrane cell membrane. The system can be used with two transducers exchangeable; whose only difference is the maximum operating pressure. For most analysis the max 50 bars transducer is used, but a max 25 bar one can also be connected instead.

Pressure Range: 0.1 to 50 bars; *Pressure Accuracy*: 0.001 Bar.

c) *Personal computer* (PC) connected through serial ports (RS-232C) to both pump and pressure transducer. This computer runs the LabVIEW® based software controlling Data Acquisition and Data Analysis.

d) *Thermostatic bath* to control the temperature of the bottles containing porosimetric liquids and the membrane cell.

e) *Measurement or membrane cell* for different membrane configurations: flat, tubular or hollow fibber. Nevertheless, only flat and tubular membrane cells were used in this thesis. This flat configuration cell was improved across the thesis to get optimized hydrodynamics and avoiding formation of air bubbles onto the membrane surface, which should result in false experimental data. The cell is adapted to 47 mm diameter membrane coupons, having an effective area of *17. 34 cm*^{2}.

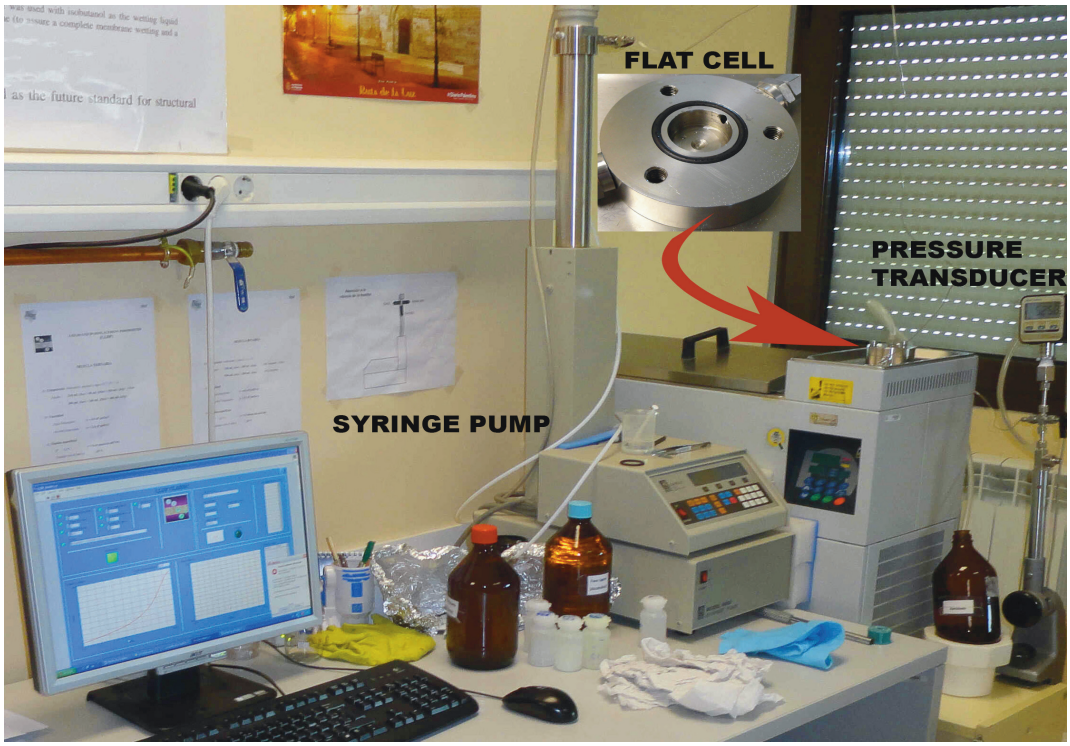

Figure 2.3: Experimental Set-up.

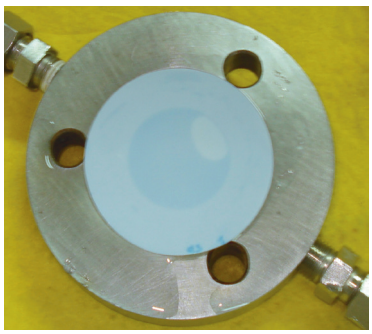

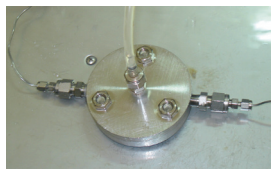

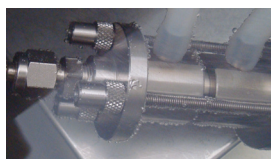

Figure 2.4: Tubular and flat membranes placed in their respective measurement cells.

2.3.2 Porosimetric Liquids Preparation

As it was shown in **Table 1.8,** several liquid pairs can be selected to perform porosimetric analysis. Those liquid pairs should be selected according the membrane porosity and the expected pore size range **[114].** For example, when analysing an UF membrane, having most of the pores in the range 1-2 nm to 0.05-0.1 μm, it should be used liquids with lowest possible surface tension, which corresponds to the Isobutanol/Methanol/Water mixture or the Isobutanol/Water one $\gamma = 0.35$ *dyne/cm* (Isobutanol/Methanol/Water) or *1.7 dyne/cm* (Isobutanol/Water) at 20ºC, respectively. Due to the high volatility of the methanol, the three components mixture changes strongly composition and properties being much less stable and needing to be prepared fresh every day. For that reason, most of the work presented in this thesis was done using the Isobutanol/Water mixture which has proved to be very stable (2/3 days and even more if needed) and allowing study of pores of 1 nm (radius) with an applied pressure of around 35 bars, which is very reasonable for UF membranes.

For the case of a MF membrane, where pore sizes can be from some hundreds of nm to several microns, it is needed to use liquid pairs with higher surface tension **[115, 116],** for example the Pentanol/Water mixture which presents a value of $\gamma = 4.8$ (Pentanol/Water) or Octanol/Water mixture having*: 8.5 dyne/cm (*Octanol/Water*)* at 20° C.

As shown in **Table 1.8**, all LLDP analysis liquids are obtained by phase separation from mixtures containing water and one or several alcohols **[112]**. Next we will comment a bit more about the different mixtures and the way of preparation:

1º) *Mixture consisting* of *Isobutanol* (2-methyl-l-propanol)*, Methanol and Water* in volumetric proportions {15:7:25 v/v}. In the phase separation of the mixture it is produced a light phase (about 30% by volume) rich in alcohol which has a viscosity at 20°C, η*=3.4 cP, where {1 cP = 1 mPa·s}* and a heavy phase mostly of water. The surface tension at 20°C between the two phases is γ*=0.35 dyne/cm*.

2º) *Mixture consisting* of *Isobutanol and Water* in proportion ratio {1:1 v/v}. The phase separation of the mixture produces a light phase (about 50% by volume) rich in Isobutanol which has a viscosity at 20°C: $\eta = 4.3$ *cP* and a heavy phase consisting mostly of water. The surface tension at 20°C between the two phases is $\gamma = 1.7$ *dyne/cm*.

3º) *Mixture consisting* of *n-Pentanol and water* in proportion ratio {1:1 v/v}. The phase separation of the mixture produces a light phase (about 50% by volume) rich in n-Pentanol which has a viscosity at 20°C, $\eta = 4.8$ *cP,* and a heavy phase consisting mostly of water. The surface tension at 20°C between the two phases is: $\gamma = 4.8$ *dyne/cm*.

4º) *Mixture consisting* of *n-Octanol and Water* in proportion ratio {1:1 v/v}. The phase separation of the mixture produces a light phase (about 50% by volume) rich in *n*-Octanol which has a viscosity at 20°C, η*= 11.1 cP*, and a heavy phase consisting mostly

of Water. The surface tension at 20°C between the two phases is $\gamma = 8.5$ *dyne/cm*.

LLDP analysis is usually performed at temperatures around 20-25°C, so it is convenient to prepare the liquid pairs at ambient temperature close to operation temperature. Also this temperature should be very convenient for liquid storage. In any case, LLDP liquids storage is not recommended for a long period, especially when working with the three components mixture (Isobutanol/Methanol/Water), due to the high volatility of the methanol compound, which could result in significant changes of composition. That storage is made in dark glass bottles correctly closed with screw caps.

The common procedure for LLDP liquids preparation is: Put into a separator funnel or Mariotte flask, water[2] and alcohol (should be at least 99% purity), in the proportions indicated in previous paragraph. The mixture must be gently shaken for at least 5 min, opening (every 30 seconds approximately) the funnel top to lead generated vapours to eliminate and after *lead* the mixture stand time enough to allow complete phase separation: alcoholic phase (upper) and aqueous phase (lower). Finally *check* both phases are totally separated and the interphase looks crisp and clean.

Note: Phase separation is completed in some hours (6-8 hours) for the Isobutanol-Methanol-Water mixtures and faster for the other cases. Nevertheless is preferably to lead the mixture stand overnight prior to proceed to phase transfer.

For each mixture Cantor equation **(Eq. 10**) stands as follows (always at 20ºC):

1º) $r_p\,(\mu m) = 0.007/P\,(bar)$, *for* $\gamma = 0.35$ *dyne/cm*.
2º) $r_p\,(\mu m) = 0.034/P\,(bar)$, *for* $\gamma = 1.7$ *dyne/cm*.
3º) $r_p\,(\mu m) = 0.096/P\,(bar)$, *for* $\gamma = 4.8$ *dyne/cm*.
4º) $r_p\,(\mu m) = 0.170/P\,(bar)$, *for* $\gamma = 8.5$ *dyne/cm*.

In that way, to analyse the pores of an hypothetical membrane having pores of 10 nm (0.01 μm) it is enough to apply 0.7 bar in case 1º, while 3.4 bar are needed in case 2º; and finally cases 3º and 4º lead to higher pressures needed: 9.6 and 17 bar, respectively.

On the contrary, if the membrane has pores of some microns, in cases **1º** and **2º,** those pores will be penetrated by permeating liquid at pressures very close to atmospheric one, then difficulting analysis of the pores. As a general rule we can say that mixture ***a)*** is preferably for NF, while mixture ***2º*** should be mostly applied for UF membranes, leading cases **3º** and **4º** for MF or very open UF membranes.

The permeating liquid is firstly aspired into the pump cylinder up to completely full it, and after then it can be sent a constant flow rate to the membrane cell. Flux and

2 Water should be bi-distilled and filtered (0.2 ppm) or Milli-Q (or equivalent) treated. Always use fresh water to prepare liquid mixtures.

pressure data are obtained increasing steeply the permeating liquid flux and measuring by means of the pressure transducer, the differential pressure drop across the membrane, corresponding to each flux value, being this procedure controlled by a PC. This software allows system preparation and data acquisition, management and analysis.

If we suspect that Isobutanol can be hazardous for the membrane material **[109]**, it is recommended to wet the membrane with water phase, it prevents a collapse structure risk after drying, so use alcoholic phase only for pumping. Working in such a way, the alcohol still damages the porous structure but it does after opening pores, so after finishing the analysis, which otherwise could not be done. The permeating LLDP liquids obtained from mixtures of Water and Isobutanol (or n-Pentanol or n-Octanol) can be reused for porosimetric analysis (of course after some hours of rest, if not the mixture will remain too turbid and results will be not proper).

While in the case of mixtures of Isobutanol, Methanol and Water it is not recommended to reuse the permeating liquid, due to the high volatility of the Methanol. For this reason the permeating liquid once passed through the membrane cell, must be conducted to another reservoir intended to discard it taking care to avoid pouring into the thermostatic bath or sink.

To wet the flat or tubular membranes is enough to maintain them in contact with the LLDP impregnation liquid during 15-30 minutes or for at least 2 hours if they are dry. Obviously these times are purely indicative and may vary depending on the materials and porous membranes. Our experience shows that this wetting process (critical to obtain reliable results) is strongly enhanced if the wetting is done under vacuum. For this purpose the membrane sample is introduced into a *Petri box* containing the wetting liquid and both are inserted into a desiccator connected to a vacuum tube. The tube is connected to tap water, creating a vacuum close to 150 mm Hg (depending on the tightness of the system) in terms of which 30-40 minutes of wetting are enough to ensure a complete sample soaking. If the membrane is wet or moist with a preservative substance (as for example glycerine) is necessary, before introducing it into the LLDP liquid, to remove the substance. This can be accomplished (unless the manufacturer suggests otherwise) simply putting the membrane in a bath with running water for at least 30 minutes. In the case of hollow fibber membranes, impregnation must be completed after the fibber was being located in the membrane cell.

2.3.3 LLDP Analysis

Following the previous proceedings, in the case of flat membrane (bathed in the liquid impregnation LLDP inside a *Petri box*)) it is placed on the measurement cell (where is also housed the rubber *O-ring*), ensuring that:

· *Membrane sample* dimensions are sufficient to cover the *O-ring*.

· *The selective membrane* layer (see **Fig. 1.3)** is in contact with the bottom of the cell (see **Fig. 2.4),** where they are housed entrance and exit conduits of the LLDP permeating liquid.

· *The drainage* of permeate material placed at the top of the cell is always bathed with the LLDP impregnation liquid.

After we are advised to be sure that all the system is ready to perform the analysis (the measurement cell must be closed and screwed with the membrane yet bathed inside, and all connections, valves and elements should be ready for operation), the pump starts the purge of the system process, applying a flux constant of 5 mL/min. This purge process will allow filling all the system with porosimetric liquid also avoiding bubbles inside the tubing. Completing this now we are ready to start the measurement process itself, it being one of the most critical steps in LLDP, as a well executed analysis surely will conduct to reliable results.

Once sample is correctly placed in the membrane cell and all the system is properly filled with pushing liquid and pressurized, we can start the automated analysis, which is launched by executing the software running under LabVIEW 8.5 ® (**[118]**, from National Instruments®). This software will conduct the data acquisition procedure under our supervision from appropriate dialogue boxes and graphical interfaces. From the moment the program is launched to the end of the analysis, all steps including data acquisition and data treatment will be executed automatically by the software.

When LLDP.exe (the executable program), has been launched, it will take control of the pump and pressure transducer. First, after a welcome screen (see **Fig. 2.5**), program will lead us to the main input screen (showed in **Fig. 2.6**) where we can input analysis parameters.

Figure 2.5: LLDP welcome screen

A good selection of these parameters will be critical to assure a good analysis, but there is not any rule which guarantees optimized selection. Only experience and previously knowledge about the sample to be analysed will help us to make correct decisions.

In any case, all important parameters will be commented with along with their influence on data acquisition step, to get a better testing of our membranes. These parameters are:

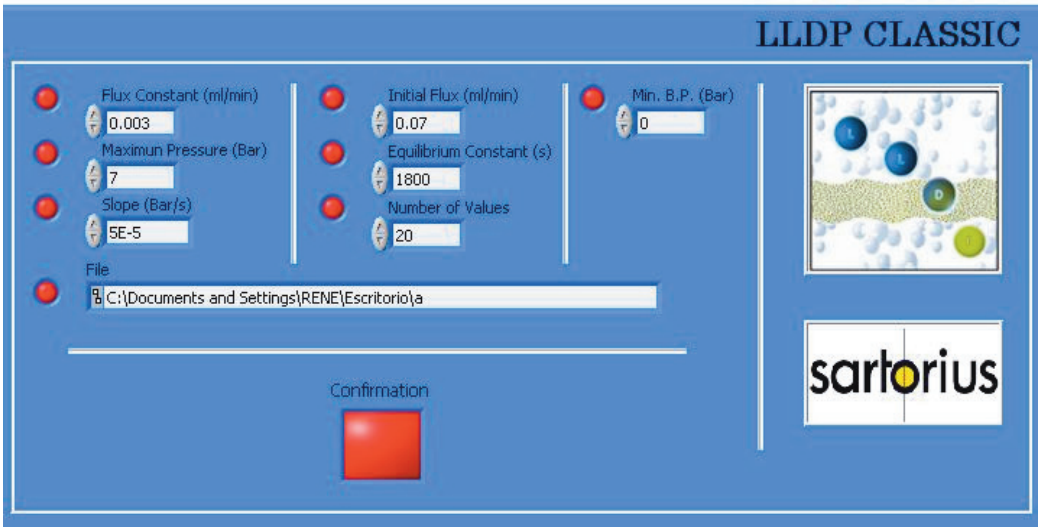

Figure 2.6: Parameter input screen.

Flux Constant (mL/min): This constant controls the flux increment intervals, and its values must be in the range 0.001 to 0.1 ml/min. After the initial flux which is also an input parameter, following values of flux will be implemented according next equation;

$$F = F_0 + \alpha i^2 \qquad \textbf{Eq 22}$$

Maximum Pressure (bar): The maximum pressure parameter stops the program execution when applied pressures overcome the settled value. This parameter serves to avoid pressure values dangerous for the system but also to stop experience once all the pores are opened. So we must be sure that the value settled for this parameter is big enough to cover whole pore size distribution.

Slope (bar/s): It is needed to assure the system is close enough to the equilibrium, which means to discriminate if system is still evolving or on the contrary has achieved an equilibrium value of pressure for the given value of flux implemented to the pump. The way of doing that is from time evolution of the pressure versus time. When these successive values of pressure collected by the system are stable enough we can obtain a representative value of pressure from the mean of several pressure readings from the manometer. The pressure line is plotted with last 10 readings of pressure and their corresponding times, so that: $P = mt+P_0$. We can say that system evolution has finished (or system has achieve equilibrium) when $m=0$. Of course, this requirement will not be exactly fulfilled any time (due to experimental errors), so we can decide how small is enough to be sure we can conclude we are in equilibrium. The value of m for this dialog box must be compressed in the range: 0.00001 to 0.01 bar/s.

Initial flux: J_0 (mL/min): An initial value of flux is imposed to the system to start analysis; this value must be compressed in the range: 0.001 to 10 mL/min.

Equilibrium Constant: τ(s) : This parameter will be settled for measurement *i-th* according to following equation:

$$t = \frac{i}{\tau^2} \qquad \textbf{Eq 23}$$

which gives the minimum time between measurement i and start of data acquisition for measurement *i+1*. As we can see, this time strongly decrease after the first measurement. This equilibrium time parameter is intended to assure the system formed by wetting liquid, membrane and permeating liquid has effectively reached the corresponding equilibrium, for a given pressure-flux conditions. In that sense, τ is especially important for the first data point, while once assured this first point is correctly obtained, the rest of them do not need big equilibrium times. The value of τ must be compressed in the range: 20 to 5000.

Number of Values: Corresponds to the minimum data pairs acquired (equilibrium flux-pressure pairs) before which experience cannot be automatically finished. The value of this parameter must be in the range: 10 to 1000.

Minimum Bubble Point (bar): This parameter not present in earlier versions of software, serves to avoids collecting data pairs considered useful when real equilibrium has not been yet achieved. As commented previously, this fact results of critical importance at the beginning of the experience, when pressure increases so slowly that the corresponding slope of the pressure-time evolution line is very
small even not corresponding to real equilibrium. To avoid that error is needed to use previous knowledge about our samples to decide which pressure are not possible to be considered as real BP. For example, if we know from previous experiences that the normal BP for a given piece of membrane is placed around 1 bar, we can select 0.5 bars for the Min. BP parameter. In that way we are sure that data pairs corresponding to pressure values under 0.5 bar will be ignored and software automatically will increase implemented fluxes up to have stables pressure values closer to the actual Bubble Point. Default value for this parameter is zero, in that case all data pairs are acquired once slope conditions are fulfilled.

Note: Supposed we have introduced by mistake or misunderstanding a value for one of the parameters not applicable (excessive or too small), the system automatically sets this value to the closer acceptable one.

When all parameter values have been introduced or default values have been confirmed (one by one, or all together using the Confirmation button), we can effectively start the analysis process. Behind this point initial parameters cannot be changed.

A good selection of these parameters is important for a successful analysis, as commented for some of them; this selection is frequently based on previous test runs which allow optimizing the parameter values. This tentative runs are quite normal for a given membrane analysis. Usually several pieces or coupons are to be analyzed and the resulting outputs of these pieces (let say 5 as general rule) will be pro-mediated. Then

the first piece of membrane can serve as tentative test to optimize acquisition parameters while rest of them will lead to fully reliable results. Of course, experience and know how will help strongly in diminishing the number of tentative tests.

Once parameters have been confirmed and measurement has started (after pressing the corresponding Start button), the acquisition program will start placing us in a measurement screen (shown in **Fig. 2.7**). This screen plots in left side at real time a pressure-versus time graph. It serves to give us an idea of the time evolution of the pressure (for each settled flux value), and this plot must approach to a horizontal straight line before

We can assume equilibrium has been reached. When this equilibrium condition has been fulfilled (see slope parameter), the corresponding values of settled flux and mean pressure are acquired as a correct data pair and plotted in the right side graph, at the same time this new data pairs is saved to the corresponding file. Those values of equilibrium pressure-imposed flux not considered as valid (under minimum Bubble Point) are not plotted here. The right side table displays that acquired and plotted values, i.e. Flux versus Pressure. And finally the permeability obtained as the ratio of those data pairs acquired is presented in the table placed on right side of the top box (not shown here). In such a way we have a complete picture of the measurement evolution, following the time evolution

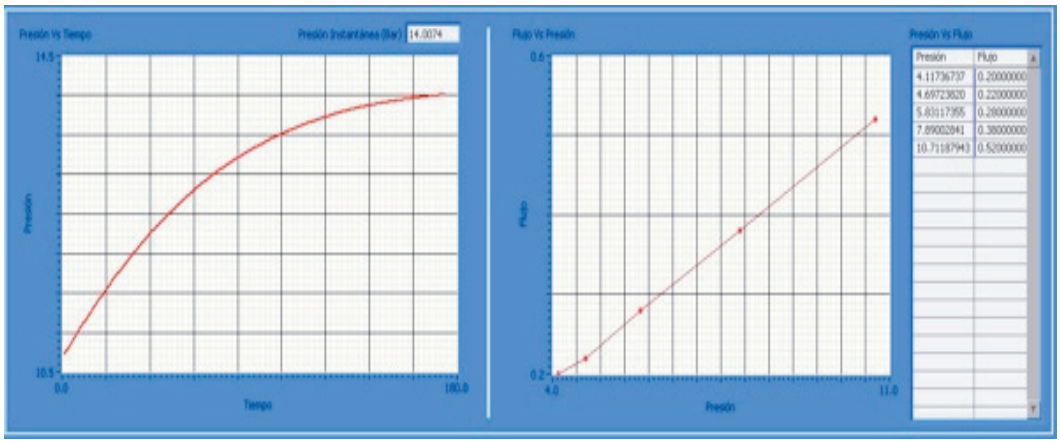

Figure 2.7: Output values screen Pressure and Flux.

of pressure (left side plot) and the aspect of the final porosimetric run (right side plot).

Also the permeability table is important to have an idea when experience should be close to end. The analysis should conclude when all the pores are opened to permeating liquid. According to *Hagen-Poiseuille* model, this means a constant value of permeability will be obtained (as no more opened pores can increase the total permeability); so when this parameter starts to increase slowly, we can guess the experiment is close to finish. A rule implemented in the program makes it to stop when five consecutive data pairs lead to decreasing permeability, $L_{i+1}<L_i$, *with* $i=1,..,5$.

This is the normal way of stopping the analysis, but for security purposes, some other causes to stop analysis have been implemented:

The applied pressure, measured by manometer, is higher than the maximum pressure parameter settled by operator at the beginning of the experience. In any case, if pressure is higher than 50 bar (security valve limit), the program is automatically stopped .

Seven consecutive equilibrium pressure values are decreasing. This could be due to several different reasons: membrane sample breaking, not adequate wetting of the sample, or not proper cell closing, etc; all of them conducting to stop the analysis and leading operator the decision about re-launch or analyzing a new membrane coupon.

* *Finally* a stop button is placed in the measurement screen so operator can stop analysis when it decides, without waiting for achieving all stop conditions.

At this moment, we have finished the data acquisition step and we are ready for data elaboration.

2.3.4 Data Analysis and Treatment

Once program analysis has been finished, several data files will be generated. Supposed we have finished the experience in a normal way (constancy of several consecutive permeability values) or even if the experience has stopped before ending by any of the reasons previously described, all valid data pairs are continuously saved so the resulting files can be used as input in the data treatment software. This additional software, named GRABAR.exe has been now integrated into the main routine (LLDP.exe), so it will be automatically launched just after finishing a normally ended experience. In the case of an alternative finishing, the Data Treatment software needs to be launched by operator using the corresponding icon. Next step will be to introducing several parameters that will be necessary to convert porosimetric data into several pore size distributions and other relevant complementary information:

Surface tension (dyne/cm): This is the main parameter relating, through the Cantor equation, the pressure applied to open the pores and the pore radius of such pores. The value for this parameter depends on the pair of liquids used, as shown in **Table 1.7**. Slight changes in this parameter can be obtained controlling the temperature at which analysis has been done. As a general rule, decreasing the temperature leads to decreasing surface tension.

Cell radius (m): What we need to know here is the effective membrane area, necessary to convert the flux-pressure data into permeability values. For the case of flat membranes, the value of this parameter corresponds to that of the Viton® *O-ring* which controls the effective membrane area. While for other membrane configurations it must be appropriately estimated according to the sample effective length and diameter.

Membrane Thickness (µm): This parameter corresponds to the pore length, and it is necessary to convert permeabilities into corresponding number of pores assuming Hagen-Poiseuille convective flow through cylindrical shaped pores. In most of the cases, this value is not known and/or it is difficult to estimate, even using cross-sectional images of our membranes. For asymmetric membranes, this value should be that of the skin layer, normally around some microns. While for symmetric membranes, thickness should be that of the whole filter, which is normally in the range of some cents of microns. Finally it must be commented that for tortuous pores, the membrane thickness should be corrected using a tortuosity factor resulting in increasing thickness.

Viscosity (cP): The corresponding value for the permeating liquid will be introduced. It is important to take into account which of the liquids in the pair will be used for pushing the other, as the viscosity of both phases (aqueous or alcoholic) is clearly different.

Only the first two parameters of those here considered, surface tension and cell radius (or more properly effective membrane area), are needed to convert applied pressures into pore sizes to be opened. So using only those, we can get a permeability distribution as the contribution of each successively opened class of pores, to the total permeability. The other two are related with the convective flow model, which using Hagen-Poiseuille equation, serves to know how many pores in each class are needed to give such permeability. These parameters are used to obtain the pore number, pore area or pore volume distributions, where a geometric modelling of the pores (cylindrical straightforward pores) is necessary.

Once we have introduced these parameters, *GRABAR-NIKITINE* Algorithm makes the calculations and saves the resulting information in a <input>.treatment.xls (Excel file), while most significant values resulting from the analysis are presented on screen, (see **Fig. 2.8**). Now the different columns of the .xls output file are commented:

-Pressure (bar): Experimental values of equilibrium pressure for each implemented flux.

-Flux (mL/min): Values of flux implemented to the pump leading to valid equilibrium points.

-Permeability (%): Contribution in percentage of a given pore radius interval to the total permeability of the membrane.

-Mean Radius (m): Mean radius of that interval according Cantor equation.

-Cumulative Volume (%), Cumulative Permeability (%), Cumulative Number (%), Cumulative Area (%): These four columns show the results of the calculation of volume, permeability, number and area distributions presented in a cumulative way from

0 % (minimum pore) to 100 %, which corresponds to the biggest pore present in the distribution, (maximum pore size). Those columns and some other (not commented here) serve us to plot the pore size distributions for the analysed membrane, (see **Figs. 2.3**).

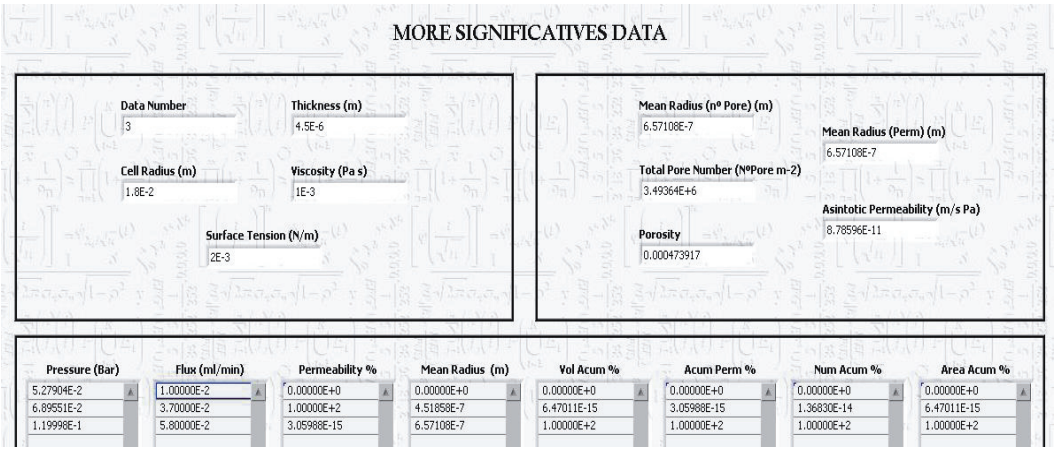

Figure 2.8: Screen capture of Grabar Algorithm showing the input parameters and the main resulting information.

From these, the most important ones are:

- *Cumulative Permeability* (%): It gives information directly obtained from experimental data. To obtain this distribution we don't need to assume any transport model or pore geometry so this distribution should be the most reliable one.

- *Cumulative Number (%)*: It is obtained from previous one assuming convective flow through cylindrically shaped pores. Consequently results are indirect and so, not so reliable.

The ***Cumulative distributions*** are very useful to estimate the actual MWCO (**Chapter 4** will focus in this functional parameter). Based on the gyration radius of a dextran macromolecule and using an empirical correlation **[117]**, the weight of dextran is matched with the size of 90% biggest pores identifying from (see **Fig. 2.3c)** the cumulative number distribution plot for a given sample **[118, 119].**
Finally, as shown at the top right of the **Figure 2.8**, (**GRABAR)**, gives some representative values of the whole information obtained from our membranes. These values are:

Mean Radius (Number): This value gives an idea of the mean pore size (radius) *weighting* the radius of each pore class by the number of them.

$$< r_n >= \frac{\sum_i n_i r_i}{\sum_i n_i} \qquad \textit{Eq 24}$$

Mean Radius (Permeability): Similarly to the previous value, in this case the permeability contribution for each class of pores *weights* it:

$$< r_l >= \frac{\sum_i L_i r_i}{\sum_i L_i} \qquad \textit{Eq 25}$$

Total Pore Number (Pores/m²): The summation of the whole values of the pore number distribution divided by the total sample area leads this value, which can be found as pore density in membrane manufacturer's leaflets. This value is calculated as:

$$N = \sum_{k=i}^{n} \Delta r_k \frac{8\eta l p_k^5}{\pi (2\gamma)^5} \left[\frac{\Delta j_k}{\Delta p_k} - \frac{J_{av_k}}{P_{av_k}} \right] \qquad \textit{Eq 26}$$
$$for\ i = 1, 2.....k$$

Asymptotic Permeability: Gives an approximate value of the total permeability of the membrane for the permeating liquid, and corresponds to the slope of the porosimetric experience, once all the pores haven been emptied by the wetting liquid.

Porosity: Express the total porosity of the membrane (%), evaluated as the summation of the percentage area distribution. So it is really a surface porosity.

Continuous pore size distributions for microporous membranes can be determined from liquid permeation data using the mathematical treatment developed in this chapter. Following the theoretical outline offered by the bubble-point method, a fully automated system (Liquid-Liquid-porometer) has been designed for this purpose (see **Fig. 2.3-4**).

2.4 CONCLUSIONS

Along this chapter we have showed the main features of LLDP technique. It has been also described the LLDP device designed at SMAP, whose main elements and automatized procedure of operation has been thoroughly commented.

From the resulting liquid porometry experiences, continuous pore size distributions for microporous membranes can be determined using a mathematical treatment, also described in this chapter.

Once we were convinced that the resulting device and the implemented software runs proper and accurately, it was used for characterizing a range of membrane having pore sizes from UF to NF and made from a variety of materials. The results of these characterizations have been published in several well reputed international journals, also parts of them have been presented in several international congresses, as follows:

1.- J.M. Sanz, R. Peinador, J.I. Calvo, A. Bottino and G. Capannelli.
Characterization of UF Membranes by Liquid-liquid Displacement Porometry.
Engineering with Membranes 2008, Vale do Lobo, Algarve (Portugal), 25-28 de mayo de 2008, Universidad de Oviedo, Universidad Nova de Lisboa and EMS.

2.- J.I. Calvo, A. Bottino, G. Capannelli, A. Hernández, R.I. Peinador and R. Firpo.
Pore size distribution and MWCO estimations of polymeric membranes by liquid-liquid displacement porosimetry.
Euromembrane 2009, Montpellier (Francia), 6-10 de septiembre de 2009, ENSCM, Université Montpellier 2 and EMS.

3.- Aldo Bottino, José Ignacio Calvo, René I. Peinador, Gustavo Capannelli and Antonio Hernández.
Structural characterization of UF membranes: LLDP vs. FESEM image analysis.
ICOM (Int. Conf. on Membranes and Membrane Processes) 2011, Amsterdam (The Netherlands), 23-29 de julio de 2011.

In the next pages, full text of resulting papers arising from this thesis will be presented, ending with a summary of main conclusions of the work done.

2.5 REFERENCES

[98] W. Kujawski, P. Adamczak, A. Narebska, A fully automated system for the determination of pore size distribution in microfiltration and ultrafiltration membranes, Sci. & Technol, 24 (1989) 495–506.

[99] S. Munari, A. Bottino, P. Moretti, G. Capannelli, I. Becchi, Permoporometric study on ultrafiltration membranes, J. Membrane Sci, 41 (1989) 69–86.

[100] V. Gekas and W. Zhang, Membrane characterization using porosimetry and contact angle measurements: A comparison with experimental UF results, Process Biochem, 24 (1989) 159-166.

[101] I.M. Wienk, B. Folkers, T. van den Boomgaard, C.A. Smolders, Critical factors in the determination of the pore size distribution of ultrafiltration membranes using the liquid displacement method, Sci. Technol, 29 (1994) 1433–1440.

[102] L. Germic, K. Ebert, R.H.B. Bouma, Z. Borneman, M.H.V. Mulder, H. Strathmann, Characterization of polyacrylonitrile ultrafiltration membranes, J. Membrane Sci, 132 (1997) 131–145.

[103] A.J. Gijsbertsen-Abrahamse, R.M. Boom, A. van der Padt, Why liquid displacement methods are sometimes wrong in estimating the pore-size distribution, J.AIchE, 50 (2004) 1364–1371.

[104] K.S. McGuire, K.W. Lawson, D.R. Lloyd, Pore size distribution determination from liquid permeation through microporous membranes, J. Membrane Sci, 99 (1995) 127–137.

[105] K. R. Morison, A comparison of liquid–liquid porosimetry equations for evaluation of pore size distribution, J. Membrane Sci, 325 (2008) 301–310.

[106] J. M. Sanz, D. Jardines, A.Bottino, G. Capannelli, A. Hernández, J.I. Calvo, Liquid–liquid porometry for an accurate membrane characterization, Desalination, 200 (2006) 195–197.

[107] J.I. Calvo, A. Bottino, G. Capannelli, A. Hernández, Pore size distribution of ceramic UF membranes by liquid–liquid displacement porosimetry, J. Membrane Sci, 310 (2008) 531–538.

[108] M.C. Almecija, J.E. Zapata, A. Martinez-Ferez, A. Guadix, A. Hernandez, J.I. Calvo, Analysis of cleaning protocols in ceramic membranes by liquid-liquid displacement porosimetry, Desalination, 245 (2009) 541–545.

[109] R.I. Peinador, J.I. Calvo, P. Pradanos, L. Palacio, A. Hernandez, Characterization of polymeric UF membranes by liquid-liquid displacement porosimetry, J. Membrane Sci, 348 (2010) 238–244.

[110] A. Shrestha, J. Pellegrino, S. M. Husson, S. R. Wickramasinghe, A modified porometry approach towards characterization of MF membranes, J. Membrane Sci, 421-422 (2012) 145–153.

[111] M. W. Phillips, A. J. DiLeo, A Validatible Porosimetric Technique for verifying the integrity of virus-retentive membranes. Biologicals, 24 (1996) 243–253.

[112] J.I. Calvo, R.I. Peinador, P. Prádanos, L. Palacio, A. Bottino, G. Capannelli, A. Hernández, Liquid–liquid displacement porometry to estimate the molecular weight cut-off of ultrafiltration membranes, Desalination, 268 (2011) 174–181.

[113] R.I. Peinador, J.I. Calvo, K. ToVinh, V. Thom, A. Hernández, Liquid–liquid displacement to characterize retention of virus membranes, J. Membrane Sci, 372 (2010) 366-372.

[114] J.M. Sanz, J.I. Calvo, P. Prádanos, A. Hernández and F. Tejerina "UF Membrane Characterization by liquid-liquid porometry", presented at Euromembrane 2004, Hamburg (Germany) 2004.

[115] J.I. Calvo, A. Bottino, G. Capannelli, A. Hernández, Comparison of liquid–liquid displacement porosimetry and scanning electron microscopy image analysis to characterise ultrafiltration track-etched membranes, J. Membrane Sci, 239 (2004) 189-197.

[116] M. C. García-Payo, M. A. Izquierdo-Gil, and C. Fernández-Pineda, Wetting study of hydrophobic membranes via liquid entry pressure measurements with aqueous alcohol solutions. J. Colloid Inteface Sci, 230 (2000) 420–431.

[117] L.P. Cheng, H.V. Lin, L.W. Chen, T.H. Young, Solute rejection of dextran by EVAL membranes with asymmetric and particulate morphologies. Polymer, 39 (1998) 2135–2142.

[118] J.S. Schultz, R. Valentina, C.Y. Choi, Reflection coefficients of homopore membranes: the effect of molecular size and configuration, J. Gen. Physiol, 73 (1979) 49–60.

[119] J.I. Calvo, R.I Peinador, P. Prádanos, L. Palacio, A. Bottino, G. Capannelli, A. Hernández. Liquid–liquid displacement porometry to estimate the molecular weight cut-off of ultrafiltration membranes. Desalination, 268 (2011)174–181.

LIST OF PUBLICATIONS

Paper one

J.M. Sanz, R. Peinador, J.I. Calvo, A. Hernández, A. Bottino, G. Capannelli. **Characterization of UF membranes by liquid–liquid displacement porosimetry,** *Desalination 245 (2009) 546–553*.

Reprinted with permission from Elsevier B.V.

Available online at www.sciencedirect.com
ScienceDirect
Desalination 245 (2009) 546–553
DESALINATION
www.elsevier.com/locate/desal

Characterization of UF membranes by liquid–liquid displacement porosimetry

J.M. Sanz,[a,b] R. Peinador,[a,b] J.I. Calvo,[a,b,*] A. Hernández,[a,b] A. Bottino,[c] G. Capannelli[c]

[a]*Departamento de Física Aplicada, Facultad de Ciencias, Universidad de Valladolid, 47071 – Valladolid, Spain, Real de Burgos, s/n, 47071–Valladolid (Spain*
Tel. +34 983423758, email: jicalvo@termo.uva.es
[b]*Real de Burgos, s/n, 47071 Valladolid, Spain*
cDipartimento di Chimica e Chimica Industriale, Universitá di Genova, Via Dodecaneso 31, 16141 Genova, Italy

Received 30 June 2008; revised 11 January 2009; accepted 09 February 2009

Abstract

Several UF membranes with fairly different structure have been characterized by using a liquid–liquid displacement porometer, which has been developed under a close collaboration of our laboratories. Three polysulfone membranes from Millipore and three polycarbonate membranes from Nuclepore–Whatman were studied. The results of pore size distributions showed nice reproducibility and accuracy. The technique is also able to accurately evaluate membrane porosity for membranes with simple cylindrical pore-like structure. In addition the possibility to estimate MWCO, by LLDP results, makes the technique very useful for process selection. Finally SEM pictures of the Millipore membranes show that usual porosimetric liquids do not alter membrane structure.

Keywords: Ultrafiltration; Membrane characterization; Polymeric membranes; Pore size distributions; Liquid–liquid displacement porosimetry

1. Introduction

Membrane-based separation technologies have found a widespread use in biotechnological, pharmaceutical or food industries. Size exclusion based processes as Microfiltration (MF), Ultrafiltration (UF) or Nanofiltration (NF) offer a range of separations able to recover, concentrate or purify valuable solvents in all these fields.

In this frame, membrane characterization is an invaluable tool for both membrane users and manufacturers, helping both to make appropriated decisions on which membrane to be chosen for a given separation process. Several characterization methods can be considered depending on the membrane characteristics and the relevant

*Corresponding author.

Presented at the conference Engineering with Membranes 2008; Membrane Processes: Development, Monitoring and Modelling – From the Nano to the Macro Scale – (EWM 2008), May 25–28, 2008, Vale do Lobo, Algarve, Portugal.

0011-9164/09/$– See front matter
doi: 10.1016/j.desal.2009.02.019

parameters for each application. Techniques such as electron microscopy, mercury porosimetry, or gas–liquid displacement porometry have been frequently used to analyse the structural characteristics of the membranes. Alternatively, solute retention tests, chemical and mechanical stability tests and permeability measurements, among others, were considered when the main interest focuses on membranes actual performance.

In recent years, there has been strong interest paid to those techniques able to characterize UF and NF membranes, in a manner which most resembles the membrane's use in several industries. UF membranes are usually characterized by their molecular weight cut-off value (MWCO), as measured under variable and not always clearly stated conditions.

The fluid displacement techniques are especially appropriate as they are non-destructive, very fast and refer only to pores opened to flux, which are the only pores which really contribute to permeation. These advantages were recognized from the pioneering works of Bechold et al. [1] and Erbe [2], later improved by Grabar and Nikitine [3]. Based on those early works, several groups developed different devices working in a more or less automated manner.

Nevertheless, nowadays, there not exist commercial equipments useful for UF or NF membranes. Based on previous experience of some of the authors [4,5], we have developed a fully automated and very precise equipment, that allows obtaining important structural information of UF membranes, and which has been used to characterise flat polymeric [6], or tubular ceramic membranes [7], with accurate results at pore radii as low as a few nanometers, or even under nanometer [8].

In this paper, our aim is to show how the liquid–liquid displacement technique is able to give important and reliable information about membrane properties with good reproducibility. Also SEM images of the membranes have been used to show that an appropriate choice of working liquids can avoid chemical and structural modifications on the analysed membrane material.

2. Materials and methods

2.1 Membranes

Three polysulfone membranes from Millipore and three polycarbonate track-etched membranes from Nuclepore–Whatman were considered in this study. The polysulfone membranes present MWCO values of 300 (M300), 30 (M030) and 10 (M010) kDa, respectively. While for polycarbonate membranes, they are usually labeled by their pore size instead of MWCO. These pore sizes are more likely to be correlated with track-etching process parameters, as beam particle density or etching time. Those selected in this work have nominal mean pore diameters of 15 (N15), 30 (N30) and 50 (N50) nm, respectively. Track-etched membranes are frequently used as test filters as their structure closely resembles that of cylindrical straight pores.

Several samples of each membrane, in the form of 47 mm diameter disks, were soaked in wetting phase for 1 h with vacuum to help a better membrane wetting. Then they were placed in the LLDP device, where a syringe pump allowed stepwise increase of the displacing liquid flux in order to progressively displace wetting liquid from the membrane wetted pores.

2.2 LLDP

The porosimeter used in this work consists in an automated device developed in close collaboration between our groups. The main features of the system are shown in Fig. 1 as it has been described elsewhere [1]. Also that work describes the way to prepare the wetting-displacing fluid pairs. In our case we chose an isobutanol–water pair using isobutanol for wetting and water to displace it.

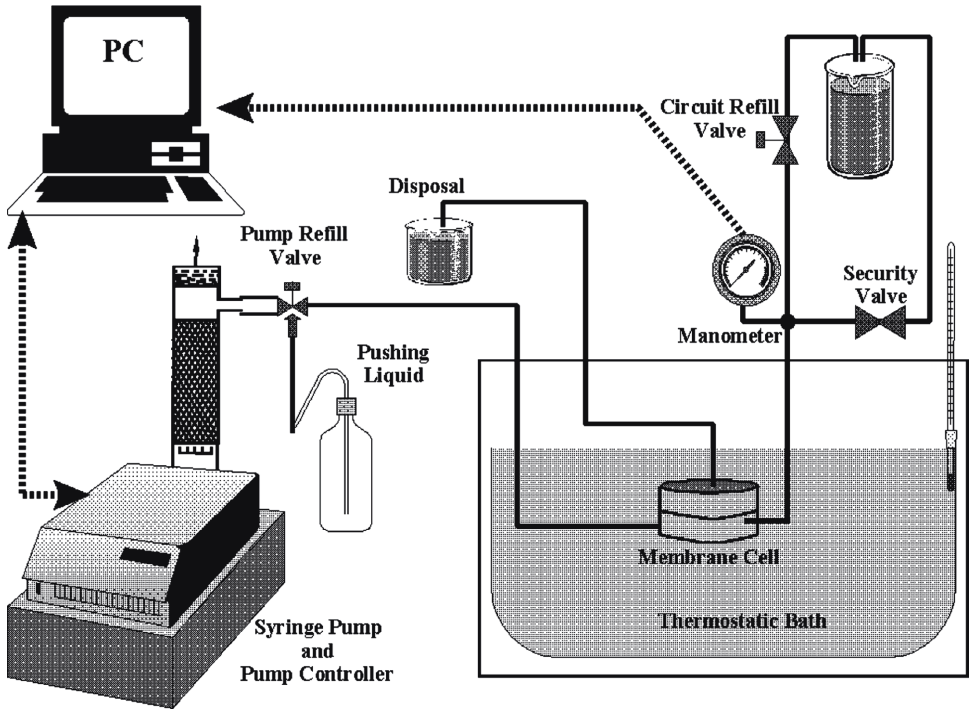

Fig. 1. Scheme of the LLDP porosimeter.

The pressure drop, P, corresponding to the flux of the displacing water through a given pore of radius, r_p, is given by Cantor equation:

$$P = \frac{2\gamma}{r_p}$$

being γ the surface tension of the water–isobutanol–membrane interface.

Assuming that the pores are cylindrical, the Hagen–Poiseuille equation can be used to correlate the volumetric flow, Q, and the number of pores, n, having a given pore radius, r. For each pressure step, p_i, the corresponding volume flow measured is correlated with the number of pores thus opened by: where η is the dynamic viscosity of the displacing fluid and l is the pore length, which roughly corresponds to the membrane thickness in the case of symmetric membranes, while for asymmetric one, it should be evaluated as active layer thickness.

$$Q_i = \sum_{k=1}^{i} \frac{n_k \pi r_k^4 P_i}{8\eta l}$$

By increasing the pressure stepwise, corresponding pore radius and flow values, represented as the permeability of the membrane (flow/pressure ratio), are obtained. Therefore by measuring the equilibrium pressure drop corresponding to each increment of water flux a pore size distribution of the membrane can be evaluated.

2.3 Scanning electron microscopy

Clean and LLDP used samples of Millipore membranes were imaged with a Stereoscan 440 (from Leo) SEM equipment, at accelerating voltages of 10 and 20 kV. Membrane samples were fixed to a SEM spin stub with a conductive adhesive and then coated with a thin layer of gold by

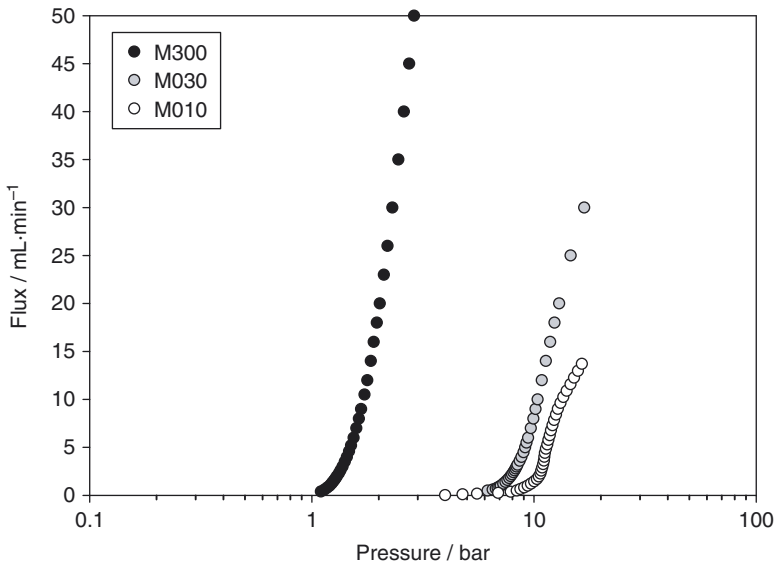

Fig. 2. Several examples of porosimetric runs for the different Millipore analysed membranes.

using a sputtering device (Agar, PS3). Then images were taken from bottom view (support) and cross sections of membrane, being these later obtained by fracturing the membrane at liquid nitrogen temperature.

3. Results and discussion

The raw results showing the behavior of the water flux as a function of the pressure drop for an example of the three Millipore membranes are shown in Fig. 2. Logarithmic x-axis has been used to allow comparison of quite different samples. It can be seen that bubble points are placed in a wide range corresponding to large molecular weight cut-off (MWCO) differences. Also should be noted that after the corresponding bubble point, the rest of data points lead to a sharp increase on flux thus corresponding to a fast pore opening.

From the result on previous figure, application of Cantor equation allowed to obtain the corresponding pore size distributions shown in Fig. 3, where the contribution of each pore size to the total permeability can be easily observed. All the distributions are quite narrow as expected from sharp increases in the previous figure.

Similarly and using the model of Hagen–Poiseuille for the water transport through the pores, Fig. 2 can be converted into the pore

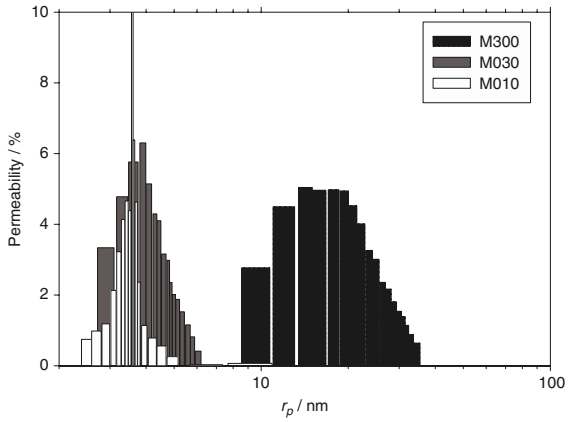

Fig. 3. Differential permeability distribution of pore size for the different Millipore analysed membranes. The histogram shows the contribution of each pore size class to the total permeability.

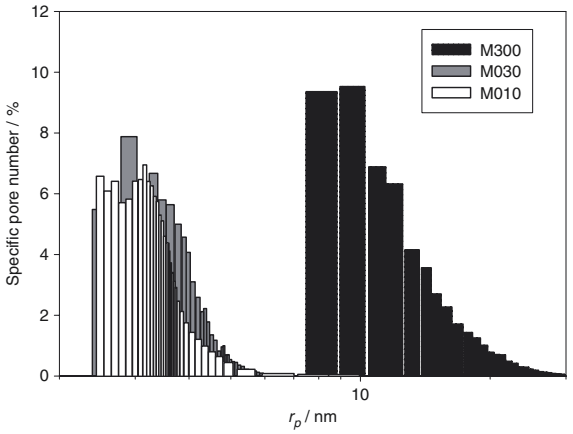

Fig. 4. Differential pore number distribution for the different Millipore analysed membranes. The contribution of each pore size class to the total pore number has been obtained using a convective transport model through the pores.

number vs. pore size distribution, shown in Fig. 4. The main difference with permeability distribution is that pore number is usually shifted to the left (lower pores) according with the fourth power dependence of the flow, or permeability, on the pore radius.

In a similar manner, Figs. 5–7 show the corresponding raw results along with permeability and pore number distributions for the three Nuclepore–Whatman membranes analysed. From Fig. 5 it can be seen that flux vs. pressure curve does not increase so sharply as found with Millipore ones. This fact can be attributed to lower porosity of the track-etched membranes, [1].

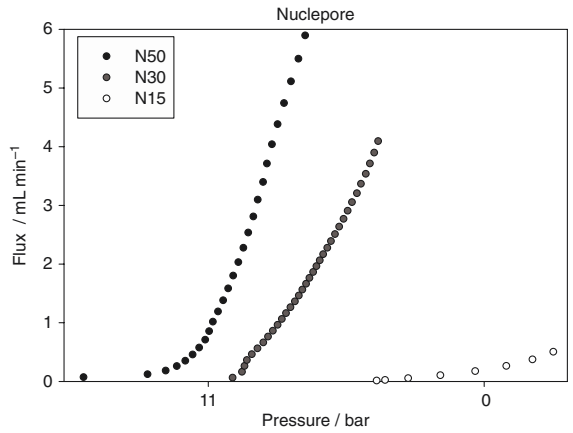

Fig. 5. Several examples of porosimetric runs for the different Nuclepore analysed membranes.

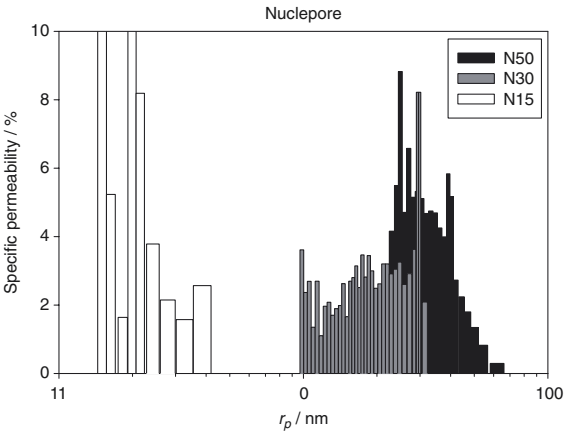

Fig. 6. Differential permeability distribution of pore size for the different Nuclepore analysed membranes. The histogram shows the contribution of each pore size class to the total permeability.

Summarizing the results of LLDP, Table 1 reports the values of mean pore size obtained from the two pore size distributions shown in

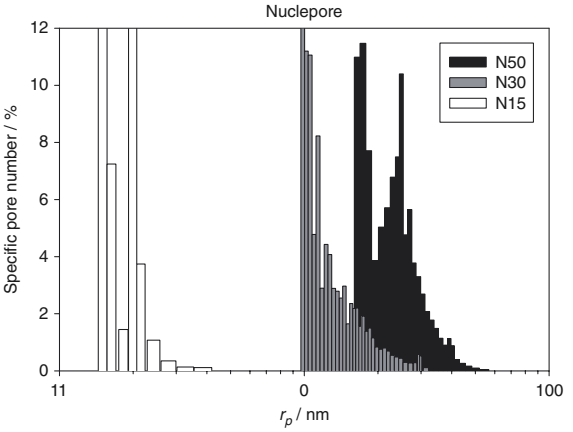

Fig. 7. Differential pore number distribution for the different Nuclepore analysed membranes. The contribution of each pore size class to the total pore number has been obtained using a convective transport model through the pores.

Table 1
Results from LLDP along with estimations of MWCO for all Millipore membranes

Membrane	Nominal MWCO (kDa)	Estimated MWCO (kDa)	r_{pn} (nm)	r_{pp} (nm)	Porosity (%)
M300	300	513	11.5	20.6	58
M030	30	31	3.7	4.1	78
M010	10	20	3.5	3.6	44

Note: r_{pn} evaluated from pore number vs. pore size distribution. r_{pp} evaluated from pore permeability vs. pore size distribution.

Figs. 3 and 4. These distributions for the different Millipore membranes, allow obtaining a mean value of pore size along with the membrane porosity, and finally an estimation of the MWCO, based on the gyration radius of the dextran macromolecule. For such estimation, the gyration radius for a given molecular weight of dextran is matched with the size of 90% biggest pores, using an empirical correlation [9]. It is worthy noting the fair agreement between such MWCO estimations and the values given by manufacturer. This fact reinforces the utility of the technique as a primary selection key during the fabrication process.

Also Table 2 shows similar results for Nuclepore–Whatman membranes. For these membranes MWCO has not been estimated as these track-etched membranes have so big pores compared with usual UF membranes that any calculation will be affected by great errors. Instead of, resulting LLDP values are compared with nominal ones. For such comparison remember that nominal pore size stands for mean pore diameter while Table 2 presents the mean values of the pore radius. Finally, the calculation of the porosity is based on a convective flow model for the water transport inside the pores, so using the membrane thickness as pore length, absolute pore numbers, porosities and surface pore densities can be easily estimated. This assumption, quite erroneous for normal asymmetric membranes, is easily comprehensible for track-etched ones, where pores are assumed to cross straightly all the membrane. The agreement on nominal and LLDP values of pore size and pore density is excellent, except for the smallest membrane, N15. This fact can be attributed to overestimation of the contribution of smallest pores at pressures as high as 10 bar, where slight fluctuations on permeability lead to estimation of a big number of very small pores. Also values of porosity obtained from LLDP are very small as usually found in track-etched membranes, where bigger porosities normally lead to undesirably high fraction of double pores.

To assure that porosimetric liquids do not affect the membrane structure, so giving false results, we have compared SEM pictures from

Table 2
Results from LLDP for all Nuclepore membranes

Membrane	Nominal mean pore Size (nm)	Porosity (%)	r_{pn} (nm)	r_{pp} (nm)	Nominal pore density (pores/m^{2}H10^{12})	LLDP Pore density (pores/m^{2}H10^{12})
N15	15	6.3	1.78	2.93		395
N30	30	2.1	13.0	18.3	6.0	7.35
N50	50	1.8	25.9	32.0		7.88

Note: r_{pn} evaluated from pore number vs. pore size distribution. r_{pp} evaluated from pore permeability vs. pore size distribution.

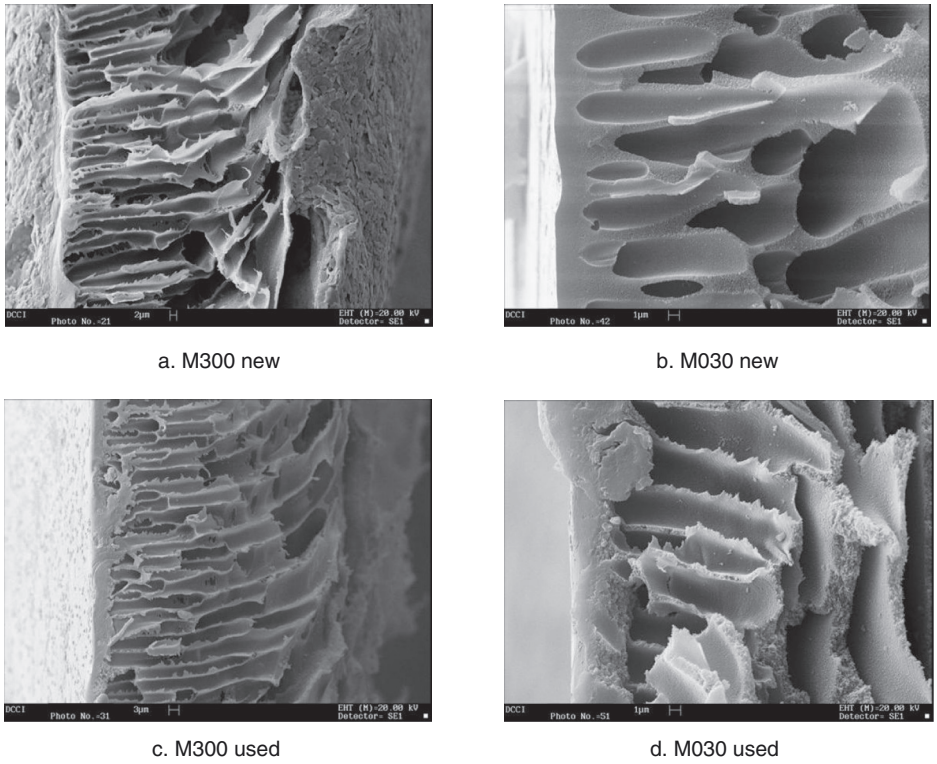

a. M300 new

b. M030 new

c. M300 used

d. M030 used

Fig. 8. Cross-section SEM images from several samples of Millipore membranes (M300 and M030), before and after LLDP analysis.

our membranes clean and after LLDP analysis. Top-view of the membrane active layer were not imaged, as SEM had not enough resolution to discriminate individual pores. Bottom view pictures (not reported here) of M300 and M030 membranes did not reveal any difference between new and LLDP tested samples. Cross sections micrographs of same membranes are shown in Fig. 8. It can be seen how there is not substantial change in the membrane structure after LLDP analysis neither for big pores (M300) or small ones (M030).

4. Conclusions

The LLDP has shown accuracy and reproducibility on the characterization of several commercial polysulfone and polycarbonate membranes. The experiments have been performed with nice velocity, giving a complete picture of the membrane structure in some hours. For cylindrical shaped pores, the use of appropriate transport models allow to accurately obtain porosity and pore densities, while for not so regular structures (as those usually found in casting polymeric membranes) the technique can be easily used to estimate MWCO, a key parameter for membrane manufacturers without the necessity to perform complicate and time consuming retention experiments.

Acknowledgement

Spanish authors want to acknowledge Junta de Castilla y Leon for financial support of this work through project: “VA112A06”.

References

[1] H. Bechold, M. Schlesinger and K. Silbereisen, Pore diameters of ultrafilters, Kolloid Z., 55 (1931) 172.
[2] F. Erbe, The determination of pore distribution according to sizes in filters and ultrafilters, Kolloid Z., 63 (1933) 277.
[3] P. Grabar and S. Nikitine, Sur le diamètre des pores des membranes en collodion utilisées en ultrafiltration, J. Chim. Phys., 33 (1936) 721–741.
[4] G. Capannelli, F. Vigo and S. Munari, Ultrafiltration membranes characterization methods, J. Membr. Sci., 15 (1983) 289.
[5] S. Munari, A. Bottino, G. Capannelli and P. Moretti, Membrane morphology and transport properties, Desalination, 53 (1985) 11–23.
[6] J.I. Calvo, A. Bottino, G. Capannelli, A. Hernández, Comparison of liquid–liquid displacement porosimetry and scanning electron microscopy image analysis to characterise ultrafiltration track-etched membranes, J. Membr. Sci., 239 (2004) 189.
[7] J.I. Calvo, A. Bottino, G. Capannelli and A. Hernández, Pore size distribution of ceramic UF membranes by liquid–liquid displacement porosimetry, J. Membr. Sci., 310 (2008) 531.
[8] J.A. Otero, O. Mazarrasa, J. Villasante, V. Silva, P. Prádanos, J.I. Calvo and A. Hernández, Three independent ways to obtain information on pore size distribution of Nanofiltration membranes, J. Membr. Sci., 309 (2008) 17.
[9] L.-P. Cheng, H.-Y. Lin, L.-W. Chen and T.-H. Young, Solute rejection of dextran by EVAL membranes with asymmetric and particulate morphologies, Polymer, 39 (1998) 2135.

Paper two

René Israel Peinador, José Ignacio Calvo, Pedro Prádanos, Laura Palacio, Antonio Hernández.
Characterisation of polymeric UF membranes by liquid–liquid displacement Porosimetry, *Journal of Membrane Science, 348 (2010) 238–244*.

Reprinted with permission from Elsevier B.V.

Journal of Membrane Science 348 (2010) 238–244

Contents lists available at ScienceDirect

Journal of Membrane Science

journal homepage: www.elsevier.com/locate/memsci

Characterisation of polymeric UF membranes by liquid–liquid displacement porosimetry

René Israel Peinador, José Ignacio Calvo*, Pedro Prádanos, Laura Palacio, Antonio Hernández

Departamento de Termodinámica y Física Aplicada, Facultad Ciencias, Universidad de Valladolid, 47071 Valladolid, Spain

ARTICLE INFO

Article history:
Received 31 July 2009
Received in revised form 3 November 2009
Accepted 5 November 2009
Available online 13 November 2009

Keywords:
Membrane
Ultrafiltration
Pore size distribution
Porosity
Liquid–liquid porosimetry

ABSTRACT

Two series of commercial polymeric (regenerated cellulose and polyethersulfone) membranes made by Millipore® have been characterized, obtaining their pore size distribution by liquid–liquid displacement porosimetry (LLDP). A fully automated porosimeter designed by us has been used in the determination of pore size distributions. Results show a good accuracy and reproducibility of LLDP measurements.

Binary and ternary liquid mixtures have been used to wet and penetrate into the membrane pores when performing LLDP leading to quite similar results when an effective surface tension is assigned for the ternary mixture. The use of different liquid mixtures and soaking conditions allowed to assure a proper wetting of the membrane pores without damaging the membrane structure during the analysis.

1. Introduction

Membrane based separation technologies have found a widespread use in biotechnological, pharmaceutical and food industries or to treat other industrial effluents. In the case of Ultrafiltration, UF membranes have been widely applied in separation technologies such as virus removal, low concentration effluents treatment or water purification [1–3].

UF membranes are usually classified and selected for applications according to their actual molecular weight cut-off (MWCO), which can be defined as the molecular weight of a given solute that exhibits a rejection coefficient greater or equal to 90%. Of course such MWCO definition is only valid for a given solute molecule and under the measurement conditions used to perform the retention experiments. This makes complicated to compare cut-off results obtained by different labs or by using different solutes and thus to be sure that a given membrane is going to be appropriate for a given application.

Typically the pore geometry for UF membranes can be envisaged as a three-dimensional network of interconnected voids and channels having a non-uniform size and shape. Also important in UF membranes is the existence of a thin (usually 1 μm in thickness or lower) skin layer on the filtration surface. The existence of such skin layer is responsible for the separation properties of the filter and also gives, due to its low thickness, a high hydraulic permeability while the more open/porous sublayer (around 100 μm in thickness) provides good mechanical support. Additional mechanical strength is sometimes provided by casting the membrane on a spun-bonded polyethylene or polypropylene backing [4]. Usually the support does not play any role in the membrane performance, the size and distribution of the pores actually present in the skin layer being the only important factor for the separation properties. Thus, a proper knowledge of the size distribution of such pores (PSD) is of great interest to estimate the sort of particles these filters should retain.

Several complimentary methods have been employed to determine the PSD of porous membranes, including the microscopic observation methods (SEM or AFM) [5,6], the bubble pressure method [7], usually known as gas–liquid displacement method, the mercury intrusion porosimetry [7,8], the permporometry [9], the gas adsorption–desorption method [6–10], and the differential scanning calorimetry (DSC) thermoporometric methods [11,12]. New methods of membrane characterization have been proposed based in other techniques as nuclear magnetic resonance [13].

All these methods together cover a broad range in applicability, sensitivity, and information they give. However, some of them present specific disadvantages such as irreversible damage of the samples or high time consumption, which strongly limited their general application. Additionally, some of them, as occurs with mercury intrusion or gas adsorption–desorption techniques, need to assume additional features on the shape and structure of the

* Corresponding author. Tel.: +34 983423758; fax: +34 983423136.
E-mail address: jicalvo@termo.uva.es (J.I. Calvo).

0376-7388/$ – see front matter © 2009 Elsevier B.V. All rights reserved.
doi:10.1016/j.memsci.2009.11.008

pores in order to obtain porometric information, which makes the interpretation of their results more difficult and less reliable. Others as DSC thermoporometry are limited in the range of detectable pore sizes. Finally, thermoporometry, gas adsorption–desorption and mercury porosimetry and all the microscopic techniques are unable to distinguish between pores contributing to the actual flow (active pores) and other pores/voids that do not control permeation. Only bubble point based techniques along permporometry and solute retention test are designed to get information on such active pores.

Among the usual membrane structure characterization techniques, those based on the bubble point test have gained increasing interest. In the case of MF membranes, there exist commercial devices that are able to obtain accurate PSD in a quite short time and using small areas of membrane sample. Some examples are the Coulter Porometer II™ which is no more manufactured, Capillary Flow Porometer™ from PMI or Porometer 4™ from Benelux Scientific. Unfortunately, this is not the case for UF or NF membranes, since the use of a gas–liquid interface for so small pores, lead to extremely high pressures that should distort the membrane structure and give wrong results [14]. On the other side, liquid–liquid displacement porometry (LLDP), which makes use of a liquid–liquid interface inside the pores, solves the problem of the high pressure needed. This fact should have lead to increasing interest on the use of this technique in UF membrane characterization. Nevertheless not too much work has been done in LLDP in the last years due to some difficulties in an appropriate design of the experimental protocol.

Germic et al. [15], discussed and compared features of several methods of membrane characterization, comparing specially LLDP with permporometry, as two active pores detecting methods. They pointed out the possible problems of swelling/drying effect due to the adsorption of isobutanol inside the membrane material matrix and also the limitations of the capillary pore model to analyse complex pore geometries as those usually found in ultrafiltration, where filters are normally considered a network of connected pores. Gijsbertsen-Abrahamse et al. [16], modelled the liquid interface inside the pores and concluded that there exists a systematic error in LLDP measurements when dealing with interconnected pores, as usually found in many polymeric or inorganic membranes. Shah et al. [17], used isopropanol and a water–isopropanol mixture as porosimetric liquids so getting a very low surface tension, 0.4 mN/m, which leads to very low pressure to be applied. Nevertheless they were not able to analyse some of the filters they studied (specifically the Biomax™ ones that we study here). Moreover, porosimetric data were fitted to an assumed Gaussian distribution to simplify the process of subsequent calculations. Chakrabarty et al. [18,19], used a ternary mixture to characterize polysulfone membranes made by phase inversion method and having different PEG's as polymeric additives. Morison [20], studied the different algorithms to be used in the conversion of liquid–liquid porosimetry data into pore size distributions. Some papers [21,22], deal with liquid porometry only as an extension of the well known gas–liquid porometry.

Most of the work made on LLDP has been done by the group of Genoa [23–25], with more recent contributions by the group of the Nanjing University [26,27]. In recent years some of the authors have collaborated with the group of Genoa, to develop a fully automated and very precise equipment, that using LLDP, allows obtaining important information on the structure of UF membranes, including pore size distribution and porosity [28,29,14,30–32]. This equipment will be used in this work to characterize commercial polymeric membranes and the information obtained will be compared with that arising from other characterization methods, to give an idea of the accuracy of the technique.

2. Experimental

2.1. Membranes and chemicals

Several UF membranes were used in our analysis. They consist in a series of three Ultracel™ membranes with different nominal retentions (MWCO = 5, 10, and 30 kDa; they will be named PL5, PL10 and PL30) and a series of three Biomax™ membranes (MWCO = 5, 10, and 30 kDa; here named PB5, PB10 and PB30). All these membranes were obtained from Millipore Corp. (Bedford, MA, USA), in the form of flat disks having a diameter of 47 mm. Membrane samples were rinsed with water (under no TMP applied) for 1 hr to clean them from glycerol, used by the manufacturers for storage. Then membrane samples were dried and immersed into the LLDP wetting phase for half an hour under vacuum (150 mmHg) at room temperature to assure complete membrane soaking.

Ultracel™ membranes are made from regenerated cellulose, cast onto a microporous polyethylene substrate which creates a uniform, robust structure, with high integrity and a very good resistance to back pressure. They provide very low protein binding and low fouling during use, according to manufacturer. Biomax™ membranes are composed of polyethersulfone and are resistant to harsh chemicals used in cleaning, biological decontamination, and sanitization. The polyethersulfone Biomax™ membranes have been modified to reduce non-specific protein binding compared to conventional polyethersulfone membranes. Due to their different material and manufacturing process, both membrane families offer different capabilities, being Ultracel™ more intended for maximum recovery while Biomax™ membranes offer maximum flow characteristics.

Several liquid mixtures can be used to perform LLDP measurements. Among them a simple one, which is very easy to prepare and very stable, is composed by a 1:1 (w/w) mixture of water/isobutanol. Several experiments were done using a ternary mixture, composed of 15:7:25 isobutanol/methanol/water. This mixture offers a lower surface tension, but it is also more instable, in such a way that it is necessary to perform the measurements fastly enough to avoid changes in surface tension properties. Due to this fact, the ternary mixture is only preferred when other possibilities are not useful. All alcohols were of reagent grade and were used as received without further purification. The mixtures were prepared by pouring proper amounts of milli-Q grade water and alcohol into a separator funnel and shaking it vigorously. The mixtures were then allowed to stand overnight. The separated alcohol-rich phase was drained off and used as the wetting liquid and the aqueous-rich phase was used as the displacing liquid. But these roles could be interchanged if needed.

2.2. Liquid–liquid displacement porosimetry

The porosimeter used in the analysis consists in an automated device developed in the University of Valladolid [14]. A detailed description of the equipment and the experimental procedure can be seen elsewhere [14]. The main feature of the equipment is the use of a precise syringe pump ISCO-250D, allowing accurate and very stable fluxes without fluctuations in such a way that no dampening is needed. A scheme of the set-up is depicted in Fig. 1. The experimental procedure allows the correlation of the applied pressure and the corresponding pore radius opened at this applied pressure using the Cantor equation, provided that the contact angle between the liquid–liquid interface and the membrane material could be assumed to be zero,

$$p = \frac{2\gamma}{r} \quad (1)$$

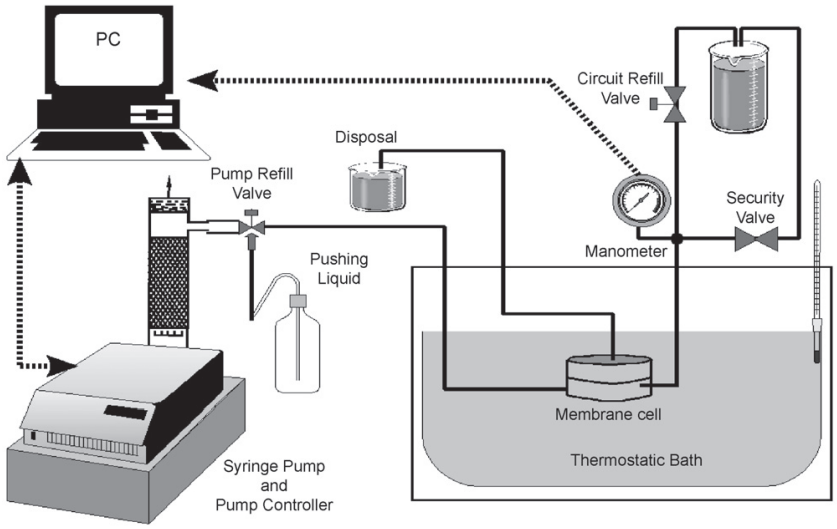

Fig. 1. Scheme of the experimental device.

where p is the applied pressure, γ the interfacial tension and r is the equivalent pore radius.

If the pores were assumed cylindrical, the Hagen–Poiseuille equation could be used to correlate the volumetric flow, Q, and the number of pores, n, having a given pore radius, r. For each pressure step, p_i, the corresponding volume flow measured, Q_i, can be correlated in such a way with the number of pores that were opened in all the previous steps by:

$$Q_i = \sum_{k=1}^{i} \frac{n_k \pi r_k^4 p_i}{8\eta l} \tag{2}$$

where (is the dynamic viscosity of the displacing fluid and l is the pore length, which roughly corresponds to the membrane thickness in the case of symmetric membranes, while for asymmetric ones, it should be correspond to that of the active layer thickness. n_k and r_k are, respectively, the number of pores and the radius of the pores opened up to the kth step ($k = 1, \ldots, i$).

From pore numbers as obtained applying Eq. (2), we can calculate the total membrane porosity as the summation of the areas of those pores divided by the total area of exposed membrane:

$$\theta = \frac{1}{A_m} \sum_{i=1}^{m} \pi r_i^2 \tag{3}$$

The application of the Hagen–Poiseuille assumes that the pores are cylindrical, which is not the case for ultrafiltration membranes. Thus as long as possible, we will try to use directly obtained data to evaluate the pore size distribution, without using any transport model for the liquid flow inside the pores. By increasing the flux stepwise, applied pressures at equilibrium and corresponding pore radius values are obtained. From flow and pressure values, the permeability or permeance of the membrane (flow/pressure ratio), is obtained. Considering the final permeability as that of the whole membrane for the displacing liquid (so, once all the pores emptied from wetting liquid) we can calculate the contribution to that permeability of each pressure-flow step (permeability distribution). If later we assume a Hagen–Poiseuille model for the liquid transport inside the pores, we can obtain the number of pores needed to get such permeability (pore number distribution), When this is done it is only to give a rough idea on the number of pores required to give the measured flow for each pore radius in the distribution.

Temperature was controlled by a thermostatic bath to keep it at 25 °C (±0.1 °C) for the binary mixture experiments, while ternary experiences were done at 15 °C (±0.1 °C), in order to minimize the consequences of its instability.

3. Results and discussion

3.1. Biomax™ membranes

The raw results, i.e. the porosimetric (flux-pressure at 20 °C) curves for three runs and one of the Biomax samples (PB30) are shown in Fig. 2. The three tests shown exemplify the many runs performed on fresh disks of the same membrane, using the binary mixture (with the alcoholic phase as wetting liquid and the aqueous one as displacing fluid). The tests showed always fairly good reproducibility as can be seen in Fig. 2, where the extreme runs are

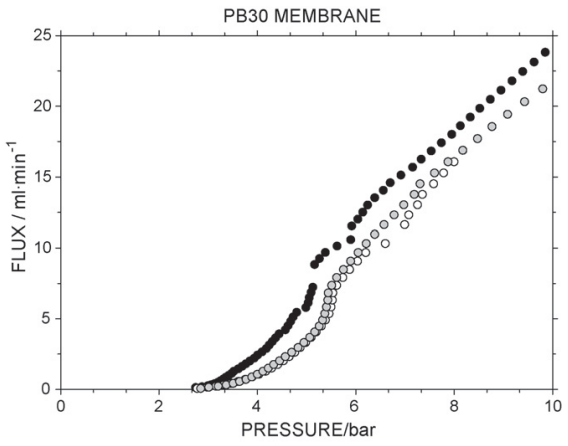

Fig. 2. Porosimetric curves (flux vs. pressure) for several runs with a PB30 membrane using alcoholic phase as wetting liquid and aqueous phase as displacing one.

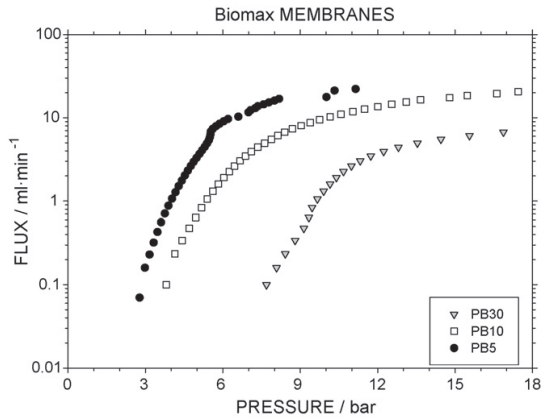

Fig. 3. Comparison of porosimetric curves for different Biomax™ membranes, using alcoholic phase as wetting liquid and aqueous phase as displacing one.

presented. This was true especially after the first one, which was used to select the appropriate flow range and increment steps. It is worth noting that final permeability (i.e. the final slope in a flux versus pressure plot as those shown in Fig. 2) does not pass exactly through the origin, as expected. This fact, yet still not very significant could be related with a slight underestimation of the actual pressure that appears when dealing with membranes having interconnected pores as proposed by Gijsbertsen-Abrahamse et al. [16]. Fig. 3 shows the porosimetric runs for all the Biomax membranes studied, using logarithmic y-axis to include in the same figure quite different final permeabilities. As expected bubble points are bigger as MWCO decreases.

The corresponding curves of the pore size distribution obtained from the usual algorithm [23], for different runs are reported for PB30 membrane and shown in Fig. 4 (only three runs are shown to avoid data overlapping). It can be observed that all runs gave a sharp distribution centred at very close mean pore values (around 7–8 nm). Figure shows the distribution of permeabilities versus pore size; i.e. the contribution (in percentage) of each pore size to the total permeability. This is done so, as mentioned, to avoid giving model depending distributions as should be the case if pore number distributions were shown. These curves for each Biomax

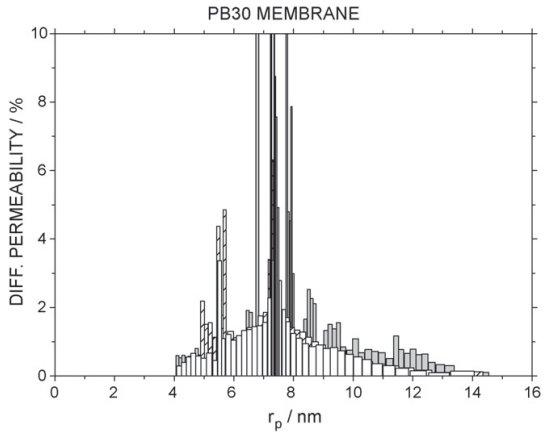

Fig. 4. Differential permeability distribution for several runs of a PB30 membrane using alcoholic phase as wetting liquid and aqueous phase as displacing one.

Table 1
Average pore sizes for Ultracel™ and Biomax™ membranes from ref. [13], obtained using NMR.

Membrane	Mean pore size (nm)	
Ultracel™	PL30	6.1
	PL10	4.9
	PL5	2.8
Biomax™	PB30	7.6
	PB10	5.9
	PB5	4.4

membrane and run, have been used to obtain the average values of the pore size which are presented in Table 2 (named as $r_{m,f}$). It is worthy noting the nice accordance between our results and that of Jeon et al., obtained from Nuclear Magnetic Resonance [13], and summarized in Table 1, for easier comparison. Also in Table 2 are presented the mean pore sizes, $r_{m,n}$, obtained from raw data after applying the Grabar–Nikitine algotihm [33].

For all Biomax membranes, porosimetric distributions along with Hagen–Poiseuille model for the transport through the pores, was used to get the overall porosities of the samples, also presented in Table 2. The corresponding porosities are similar for all the samples, and have been evaluated by using a value of 10 μm for the thickness of the membrane active layer. Since we have not information about the actual value, we used one close to that used for Ultracel™. Of course, a better determination of such active layer thickness should also help to get more reliable values of the porosity.

3.2. *Ultracel™ membranes*

When analysing Ultracel™ membranes, some troubles were initially found. A primary test was performed by using the isobutanol rich phase as the wetting liquid and the water rich phase as the displacing one, as was previously done for the Biomax™ membranes. This was done so because the alcohol rich phase normally wets better the polymeric structures due to the strong wettability of alcohols with many polymers [28]. Following such procedure, the apparatus was not able to record any point in the porosimetric curve. Once the membrane cell was opened, we found that the membrane sample had been strongly affected by the isobutanol phase, leading to a breaking of the continuous interphase between the active layer and the support, which now appeared as totally detached. The resulting destroyed membrane can be seen in Fig. 5, where it can be observed how the isobutanol affects the transition region between the skin layer and the porous support, just disconnecting both parts of the membrane. Since isobutanol is compatible with cellulose and polyethylene, we think the most probable reason for this behaviour is that isobutanol produces some swelling at the interfacial junction between both layers (support and skin) so decreasing the adhesion of them (perhaps due to differential expansion of both layers), which eventually separate from each other, without significant damage in any of the layers themselves. The support itself did not suffer any disturbance, as can also be seen in this figure and the cellulose layer apparently has only a certain wrinkling due to the very small thickness (we measured such thickness once detached from support using an electro-magnetic coating

Table 2
Overall porosity and mean pore radius obtained from direct flow data and from transport model estimation, for Biomax™ membranes.

Membrane	Porosity (%)	$r_{m,n}$ (nm) (number)	$r_{m,f}$ (nm) (flux)
PB30	53.3 ± 3.5	6.45 ± 0.16	7.44 ± 0.41
PB10	66.0 ± 4.0	3.76 ± 0.28	5.20 ± 0.10
PB5	35.8 ± 3.6	3.56 ± 0.04	3.88 ± 0.09

Fig. 5. Picture of an Ultracel™ membrane after porosimetric analysis, using alcoholic phase as wetting liquid and aqueous phase as displacing one.

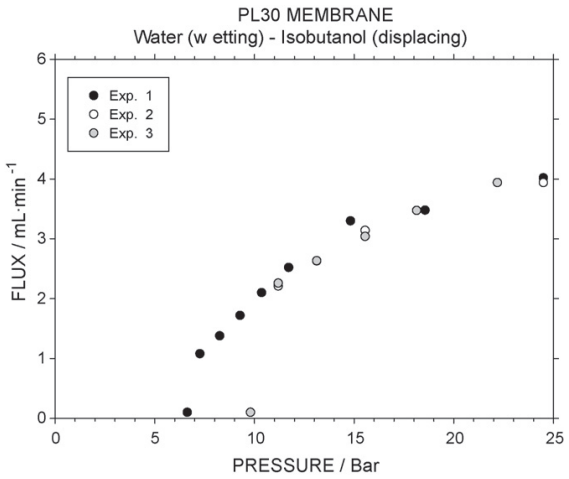

Fig. 6. Porosimetric curves (flux vs. pressure) for several runs with a PL30 membrane using aqueous phase as wetting liquid and alcoholic phase as displacing one.

thickness device. The resulting value of $9.3 \pm 1.0\,\mu m$, will be used in the transport model calculations for Ultracel™ membranes).

Two alternative methods could be used to avoid this problem, and both were tried by us:

(a) The role of both the wetting and pushing solutions can be interchanged, by using the aqueous phase to wet the filter prior to its analysis, while the alcoholic phase (mostly isobutanol) can be used to open the water filled pores by pushing the wetting solution out. Such operation procedure reduces strongly the interaction time of isobutanol with the pore structure, and so it could be expected that the analysis should be performed before isobutanol had damaged the membrane structure. Also the high hydrophilicity of the cellulose should help to get better wetting using the aqueous phase.

(b) Another possibility is to perform the porosimetric analysis, by using a different pair of wetting and pushing liquids. The ternary mixture (15:7:25 isobutanol/methanol/water), seems to be very appropriate as it gives a lower surface tension and the presence of methanol surely should minimize the membrane damage, giving more reliability to the porometric results. Working at 15 °C, we have demonstrated [31], that surface tension is reduced from $\gamma = 2$ mN/m, for the isobutanol/water mixture and 25 °C, to a value of $\gamma = 0.43$ mN/m.

As mentioned, both approaches were used in the analysis of Ultracel™ membranes and their resulting outputs will be conveniently compared and discussed.

3.2.1. Change of wetting liquid

Fig. 6 shows the results of the porosimetric curves corresponding to the PL30 membrane. As can be seen, curves have much less significant points that those of the polyethersulphone membranes (see Fig. 2 for comparison). Also it is observed a sharp and fast flux increase, once the bubble point pressure was overcame. This fact is probably due to the effect of the entrance of isobutanol into the biggest pores of the membrane. While the applied pressure does not reach the bubble point, the alcohol do not significantly affect the skin-support interface, since it only acts substantially on the membrane surface. But once these biggest pores became opened to isobutanol, the liquid enters easily inside the pores and its damaging action is accelerated. In a short time, pores are degraded and structure strongly changed (mostly making pores much bigger), and then the liquid can flow more easily. This means that we get increasing fluxes without the need of a significant pressure increase. Finally, when all pores (or at least most of them) have been occupied by isobutanol, membrane continues its degradation and eventually the experience ends abruptly. The data acquisition software detects several consecutive points of decreasing pressure and it ends the experience, since, of course, a decrease in permeability makes no sense in a porosimetric analysis apart from the occasional fluctuations within the error range.

Nevertheless, even with such imperfect experiences, we have been able to get important information concerning the mean pore size of the membranes. Fig. 7 shows the permeability distributions for the PL30 membrane, as obtained from the porosimetric runs of Fig. 6. The distributions obtained are extremely narrow, with scarcely two or three values of pore size corresponding to the most frequent ones. The following points in the porosimetric curve do not contribute to the permeability distribution, as they correspond to decreasing permeabilities that are rejected automatically by the calculation algorithm.

Thus obtained results for the mean pore size, both from permeability distributions and from number ones (the latest obtained

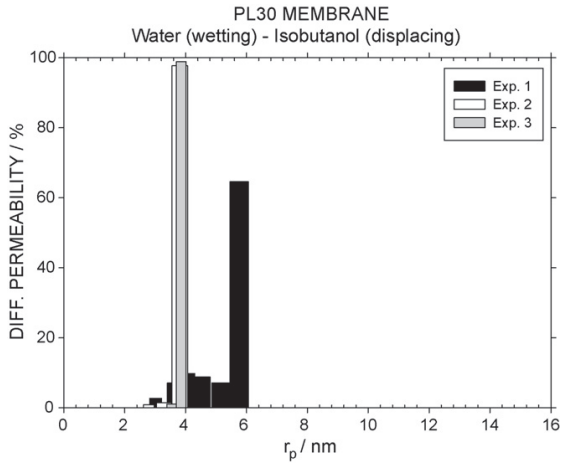

Fig. 7. Differential permeability distribution for several runs of a PL30 membrane using aqueous phase as wetting liquid and alcoholic phase as displacing one.

Table 3
Mean pore radius obtained from direct flow data and from transport model estimation, for Ultracel™ membranes.

Membrane	$r_{m,n}$ (nm) (number)	$r_{m,f}$ (nm) (flux)
PL30	4.03 ± 0.34	4.30 ± 0.80
PL10	2.16 ± 0.14	2.21 ± 0.12
PL5	2.07 ± 0.33	2.07 ± 0.34

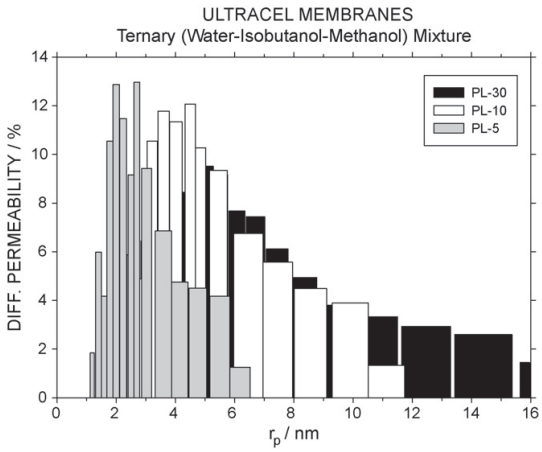

Fig. 8. Differential permeability distribution for different Ultracel™ membranes using ternary mixture (alcoholic phase as wetting liquid and aqueous phase as displacing one).

from the previous one, by using a Hagen–Poseuille model for the transport inside cylindrically shaped through pores), for all Ultracel™ membranes, are shown in Table 3. Again it is worthy noting the good agreement of our results with mean pores obtained from NMR characterization [13].

We think that the somehow surprising agreement of the mean pore sizes with those given by Jeon et al. is related with the action of isobutanol on the support adhesion. Since this liquid affects to the support–skin interface, we can suppose that in these experiments what we have clearly and reliably determined is the bubble point of mostly the active layer. In our experiments the bubble point (usually found at the end of the distribution curve) now matches the most frequent pore size found in the active layer.

3.2.2. Change of liquid mixture

An example of the results obtained using the ternary mixture are presented in Fig. 8 for all three PL membranes, in terms of the permeability distribution. From these distributions, the values of the usual parameters presented in Table 4 have been obtained. It can be seen that now the distributions are more regular, with much more data points than when the water–isobutanol mixture was used. This means that now, as predicted, the effects of isobutanol in the ternary mixture are substantially retarded in such a way that the experiments can be completely performed before the membrane structure was damaged. Anyway it should be noted that

Table 4
Mean pore radius obtained from direct flow data and from transport model estimation, for Ultracel™ membranes, for experiments using the ternary mixture.

Membrane	$r_{m,n}$ (nm) (number)	$r_{m,f}$ (nm) (flux)
PL30	3.85 ± 0.45	6.16 ± 0.83
PL10	3.15 ± 0.63	4.86 ± 0.43
PL5	1.55 ± 0.37	2.70 ± 0.32

NMR measurements do not analyse only active pores but total ones, so differences in resulting values are to be expected.

4. Conclusions

Two series of polymeric flat membranes have been analysed using a precise, accurate and fast automated LLDP device. The results are very interesting, with a nice agreement between different runs, and also very good agreement was found for experiences performed using different liquid mixtures. A fair agreement with other authors data [13], have been obtained. The NMR porosimetry is of courde a much more laborious and indirect method. Note that, as mentioned, the NMR porosimetry refers to all the pores or voids present within the membranes including those not opened to flux. The fair agreement should mean that similar pore size distributions are present within both open and closed pores.

The liquid–liquid displacement porometry is a technique which offers not only accurate characterization of ultrafilters, but enough flexibility to get reliable results in difficult conditions. Here the Biomax™ filters have been analyzed using the LLDP technique and water–isobutanol mixture. As mentioned, previous attempts to use an isopropanol–water system [17], were unsuccesful. The possibility to choose among different liquid mixtures, and also to select the role that both liquids play in the porosimetric analysis offers a great advantage and allows analysing many different filters made of different material and so presenting diverse degrees of hydrophicility/hydrophobicity, The technique allows also measuring membrane modules in different geometries, including flat, tubular or hollow fibbers. It is probably (along with perhaps permporometry) the only technique nowadays able to give fast and accurate information on active pores in UF membranes.

Anyway, the LLDP technique should benefit from more work of research, mainly in the determination of the relevant properties of the usual liquid mixtures (e.g. surface tension or contact angle). Specially interesting should be to dedicate more effort to the properties of interesting ternary mixtures, that allowing to analyse smaller pores are also less volatile and not so prone to have important changes in composition along the experience duration. Finally a very interesting goal should be to effectively correlate structural information on pore sizes with retention characteristics of the analysed filters, so allowing prediction of performance characteristics of the filters from structural characterisation.

Finally we can conclude that the LLDP technique can be considered nowadays an accurate technique able to give the complete PSD information in very reasonable times (1–1 1/2 h for most of the experiences).

Acknowledgements

Authors would like to acknowledge the support of this work through projects: CTQ2006-01685 and MAT2008-00619 from Ministerio de Educación y Ciencia (Plan Nacional de I + D + i) and GR18 from the Castilla and León Regional Government.

Nomenclature

A_m	total area of the membrane exposed to the flow
m	total number of points in the porosimetric experience (dimensionless)
n	number of pores having a given pore radius, r (dimensionless)
n_k	number of pores opened in step k (k = 1, ..., i) (dimensionless)

l	pore length (m)
p	applied pressure (Pa)
p_i	pressure corresponding to the ith step of analysis (Pa)
Q	volumetric flow (m^3/s)
Q_i	volumetric flow corresponding to the ith step of analysis (m^3/s)
r	equivalent pore radius (m)
r_k	pore radius of the pores opened in step k ($k = 1, \ldots, i$) (m)
$r_{m,f}$	mean pore radius from permeability distribution (m)
$r_{m,n}$	mean pore radius from pore number distribution, as obtained from permeability one after applying Hagen–Poiseuille transport model (m)
r_p	pore radius (m)

Greek letters

γ	interfacial tension of the liquids pair and the membrane surface (mN/m)
η	dynamic viscosity of the displacing fluid (Pa s)
θ	membrane porosity (dimensionless).

References

[1] C. Cabassud, C. Anselme, J.L. Bersillon, P. Aptel, Ultrafiltration as a non-polluting alternative to traditional clarification in water treatment, Filter. Sep. 28 (1991) 94.
[2] W.S. Ho, K.K. Sirkar, Membrane Handbook, Van Nostrand Reinhold, New York, USA, 1992.
[3] K. Scott, Handbook of Industrial Membranes, Elsevier Adv. Technol., Oxford, UK, 1995.
[4] M.C. Porter, Handbook of Industrial Membrane Technology, Noyes Publications, NJ, USA, 1989.
[5] T.-S. Ching, J.-J. Qin, A. Huan, K.-C. Toh, Visualization of the effect of die shear rate on the outer surface mophoklogy of ultrafiltation membranes by AFM, J. Membr. Sci. 196 (2002) 251–266.
[6] P. Prádanos, Mª.L. Rodríguez, J.I. Calvo, A. Hernández, F. Tejerina, J.A. de Saja, Structural characterization of an UF membrane by gas adsorption–desorption and AFM measurements, J. Membr. Sci. 117 (1996) 291–302.
[7] J.I. Calvo, A. Hernández, P. Prádanos, L. Martínez, W.R. Bowen, Pore size distributions in microporous membranes. II. Bulk characterization of track-etched filters by air porometry and mercury porosimetry, J. Colloid Interface Sci. 176 (1995) 467–478.
[8] C. Alié, R. Pirard, J.-P. Pirard, Mercury porosimetry applied to porous silica materials: successive buckling and intrusion mechanisms, Colloid Surf. A: Physicochem. Eng. Aspects 187–188 (2001) 367–374.
[9] P. Schneider, P. Uchytil, Liquid expulsion permporometry for characterization of porous membranes, J. Membr. Sci. 95 (1994) 29–38.
[10] J.I. Calvo, P. Prádanos, A. Hernández, W.R. Bowen, N. Hilal, R.W. Lovitt, P.M. Willians, Bulk and surface characterization of composite UF membranes. Atomic force microscopy, gas adsorption–desorption and liquid displacement techniques, J. Membr. Sci. 128 (1997) 7–21.
[11] K. Ishikiriyama, M. Todoki, T. Kobayashi, H. Tanzawa, Pore size distribution measurements of poly(methyl methacrylate) hydrogel membranes for artificial kidneys using differential scanning calorimetry, J. Colloid Interface Sci. 173 (1995) 419–442.
[12] J.N. Hay, P.R. Laity, Observations of water migration during thermoporometry studies of cellulose films, Polymer 41 (2000) 6171–6180.
[13] J.-D. Jeon, S.J. Kim, S.-Y. Kwak, ^{1}H nuclear magnetic resonance (NMR) cryoporometry as a tool to determine the pore size distribution of ultrafiltration membranes, J. Membr. Sci. 309 (2008) 233–238.
[14] J.I. Calvo, A. Bottino, G. Capannelli, A. Hernández, Comparison of liquid–liquid displacement porosimetry and scanning electron microscopy image analysis to characterise ultrafiltration track-etched membranes, J. Membr. Sci. 239 (2004) 189–197.
[15] L. Germic, K. Ebert, R.H.B. Bouma, Z. Borneman, M.H.V. Mulder, H. Strathmann, Characterization of polyacrylonitrile ultrafiltration membranes, J. Membr. Sci. 132 (1997) 131–145.
[16] A.J. Gijsbertsen-Abrahamse, R.M. Boom, A. van der Padt, Why liquid displacement methods are sometimes wrong in estimating the pore-size distribution, AICHE J. 50 (7) (2004) 1364–1371.
[17] T.N. Shah, H.C. Foley, A.L. Zidney, Development and characterization of nanoporous carbon membranes for protein ultrafiltration, J. Membr. Sci. 295 (2007) 40–49.
[18] B. Chakrabarty, A.K. Ghoshal, M.K. Purkait, Effect of molecular weight of PEG on membrane morphology and transport properties, J. Membr. Sci. 309 (2008) 209–221.
[19] B. Chakrabarty, A.K. Ghoshal, M.K. Purkait, Preparation, characterization and performance studies of polysulfone membranes using PVP as an additive, J. Membr. Sci. 315 (2008) 36–47.
[20] K.R. Morison, A comparison of liquid–liquid porosimetry equations for evaluation of pore size distribution, J. Membr. Sci. 325 (2008) 301–310.
[21] W. Piatkiewicz, S. Rosinski, D. Lewinska, J. Bukowski, W. Judycki, Determination of pore size distribution in hollow fibre membranes, J. Membr. Sci. 153 (1999) 91–102.
[22] R. Ghosh, Novel membranes for simulating biological barrier transport, J. Membr. Sci. 192 (2001) 145–154.
[23] G. Capannelli, F. Vigo, S. Munari, Ultrafiltration membranes—characterization methods, J. Membr. Sci. 15 (1983) 289–313.
[24] S. Munari, A. Bottino, G. Capannelli, P. Moretti, Membrane morphology and transport properties, Desalination 53 (1985) 11–23.
[25] A. Bottino, G. Capannelli, A. Grosso, O. Monticelli, M. Nicchia, Porosimetric characterization of inorganic membranes, Sep. Sci. Technol. 29 (8) (1994) 985–999.
[26] L.-Q. Wu, P. Huang, N. Xu, J. Shi, Effects of sol properties and calcination on the performance of titania tubular membranes, J. Membr. Sci. 173 (2000) 263–273.
[27] X. Ju, P. Huang, N. Xu, J. Shi, Studies on the preparation of mesoporous titania membrane by the reversed micelle method, J. Membr. Sci. 202 (2002) 63–71.
[28] A. Bottino, J.I. Calvo, P. Prádanos, G. Capannelli, A. Hernández, Characterisation of UF membranes by liquid–liquid displacement porometry and scanning force microscopy, in: Proceedings of Prague Macromolecules Microsymposia, Prague, Czeck Republic, July 16–19, 2001.
[29] J.M. Sanz, J.I. Calvo, P. Prádanos, A. Hernández, F. Tejerina, UF Membrane Characterization by Liquid–liquid Porometry, Euromembrane'2004 (Book of Abstracts), TUHH-GKSS, Hamburg, Germany, 2004.
[30] J.M. Sanz, D. Jardines, A. Bottino, G. Capannelli, A. Hernández, J.I. Calvo, Liquid–liquid porometry for an accurate membrane characterization, Desalination 200 (2006) 195–197.
[31] J.A. Otero, O. Mazarrasa, J. Villasante, V. Silva, P. Prádanos, J.I. Calvo, A. Hernández, Three independent ways to obtain information on pore size distribution of nanofiltration membranes, J. Membr. Sci. 309 (2008) 17–27.
[32] J.I. Calvo, A. Bottino, G. Capannelli, A. Hernández, Pore size distribution of ceramic UF membranes by liquid–liquid displacement porosimetry, J. Membr. Sci. 310 (2008) 531–538.
[33] P. Grabar, S. Nikitine, Sur le Diamètre des Pores des Membranes en Collodion utiliseés en Ultrafiltration, J. Chim. Phys. 33 (1936) 721–741.

Paper three

René Israel Peinador, José Ignacio Calvo, Khuong ToVinh, Volkmar Thom, Pedro Prádanos, Antonio Hernández.
Liquid–liquid displacement porosimetry for the characterization of virus retentive membranes, *Journal of Membrane Science, 372 (2011) 366–372*.

Reprinted with permission from Elsevier B.V.

Journal of Membrane Science 372 (2011) 366–372

Contents lists available at ScienceDirect

Journal of Membrane Science

journal homepage: www.elsevier.com/locate/memsci

Liquid–liquid displacement porosimetry for the characterization of virus retentive membranes

René Israel Peinador[a], José Ignacio Calvo[a,*], Khuong ToVinh[b], Volkmar Thom[b], Pedro Prádanos[a], Antonio Hernández[a]

[a] SMAP (UA-UVA-CSIC), Departamento de Física Aplicada, Facultad Ciencias, Universidad de Valladolid, Real de Burgos, s/n, 47071 Valladolid, Spain
[b] Sartorius-Stedim Biotech GmbH, Membrane R&D Biotechnology, August Spindler-Str. 11, 37079 Göttingen, Germany

ARTICLE INFO

Article history:
Received 17 September 2010
Received in revised form 14 February 2011
Accepted 16 February 2011
Available online 22 February 2011

Keywords:
Virus retentive membrane
Dextran retention
Phage retention
Pore size distribution
Liquid–Liquid porosimetry

ABSTRACT

Parvovirus retentive membranes made from polyethersulfone (PES) have been characterized by different techniques including dextran and phage retention. Results have been correlated with the pore size distributions of such membranes as obtained by liquid–liquid displacement porosimetry (LLDP).

The results of LLDP concerning pore size distributions are proved to be consistent with those obtained by image analysis of SEM transversal sections and refer to the narrower pore section. Moreover, the maximum pore size determined by LLDP fairly correlates with the measured retention capabilities of the membranes. LLDP results suggest that the technique can be an accurate method for the determination of pore size characteristics of virus retentive membranes. This technique can be simplified to be even faster and straightforward by detecting only the maximum pore size of the membrane.

1. Introduction

Mammalian cell cultures used in the production of monoclonal antibodies and therapeutic recombinant proteins are vulnerable to contamination by viruses. Plasma-derived pharmaceuticals can also be potentially infected by viral pathogens [1]. Due to these vulnerabilities, biopharmaceutical manufacturing procedures need robust and efficient purification steps to prevent microbiological contamination of the products [2]. Chlorination has been in the past a very popular technique for quality control of treated water in terms of viral/microbiological safety. Nevertheless, chlorination can give rise to undesired by-products and an adequate control of dosage is difficult, especially in small scale plants [3]. Finally, most viruses are more resistant to chlorine than bacteria. Another possibility relies in size exclusion filtration using virus retentive membrane filters that are used mainly in downstream-processing of pharmaceutical solutions. Virus retentive membranes have severe requirements, as they must remove more than 99.9% of virus particles while passing almost the entire protein product in the feed stream [4]. The difference in size between a parvovirus and an antibody is relatively small, making size-based virus clearance a challenging technology.

Several degrees of virus removal have been reported for UF and even MF membranes [5–8], or membrane adsorbers [9]. Viruses could be expected to be completely retained by tight UF membranes (with molecular weight cut-offs of 10–100 kDa), according to the molecular weight of the viruses [10]. Nevertheless, it has been reported, that small viruses have penetrated membranes theoretically included in the NF range [3], while log reduction values (see Eq. (1) below) in the 6–7 range can be obtained with pre-treatment through MF membranes [11,12].

The manufacturers of virus retentive membranes classify the virus clearance filters into two broad categories based on the removal needs of the biotechnological industry – filters that are capable of removing 50 nm or larger viruses (retroviruses) and filters that can remove both small (~20 nm parvoviruses) and large viruses.

Virus retentive membranes typically exhibit a pore size gradient, where the pore size increases from the skin layer progressing towards a large pore microfiltration layer. The skin provides the selectivity needed to exclude viruses, while the thicker support layer provides mechanical support for the membrane. Obviously, the advantage of a thin retentive membrane skin consists in a large overall flux. The overall LRV of a membrane could be increased simply using multiple layered membrane with the subsequent reduction in flux or the use of membranes with inner narrowing of the pores which is effectively the approach used in the membranes studied here. Others studies focus on the evaluation of affinity-type membranes which show a case-by-case virus removal ability [13].

* Corresponding author. Tel.: +34 983423758; fax: +34 983423136.
E-mail address: jicalvo@termo.uva.es (J.I. Calvo).

0376-7388/$ – see front matter © 2011 Elsevier B.V. All rights reserved.
doi:10.1016/j.memsci.2011.02.022

The key parameter to characterize virus filters is their ability to retain viruses of a certain size. This retentiveness is normally expressed as a log reduction value, defined as follows [13]:

$$\mathrm{LRV} = \log_{10}\frac{C_f}{C_p} \quad (1)$$

C_f being the concentration of the retained species in the feed, and C_p being the concentration of this species in permeate. For smaller viruses (as parvovirus) membrane filters provide LRVs of around 3–4. LRVs of above 6 are normally seen for larger viruses (such as a retrovirus). These parameters are typically determined during viral spiking studies, where appropriate virus preparations are used to test the membrane retentiveness.

In order to test filter integrity, particle challenge tests using bacteriophages or gold nanoparticles can be employed. Compared to pathogenic viruses, the advantages of bacteriophages are increased preparation purity, faster and more responsive assays and safer operation.

Working with viruses requires comprehensive safety measures; the procedures are strictly regulated by health agencies that habitually require validation of virus removal steps using actual viruses. This makes those tests very expensive. Even working with bacteriophages like PP7 as a substitute for the small porcine parvovirus, requires substantial safety efforts and laborious work with great detail and complexity. Due to this, it is common to substitute, or at least, to complement virus retention experiments with some tests of dextran retention that give information that can be used to select appropriate membranes to be used for actual virus retentions [2].

Standard air diffusion test are also performed to discard the presence of gross leaks. In contrast to particle tests, which give information on the pore size distribution of the membrane, air diffusion test identify large defects on the membrane surface. In addition, adequate passage of interesting products can be verified in separated tests. For instance, water permeability or buffer solution flows can be of interest for selected applications [4].

A complete characterization of membrane filters to be used for virus clearance is a time consuming and expensive effort. Consequently, there is a strong interest in developing a fast and low cost method of characterization that could provide information that could be correlated to relevant filter parameters, like, e.g., virus retention. Fortunately, now there are porosimetric methods that are able to determine the complete pore size distribution of the analyzed membranes in a short time. The resulting pore size distributions can be linked with membrane performance characteristics. For the case of UF membranes, the most reliable and appropriate porosimetric method is the liquid–liquid displacement porosimetry (LLDP), which is based on the well known bubble point porometry, but uses a liquid–liquid interface to reduce the interfacial tension and to allow an analysis of pores significantly smaller than those determined by usual gas–liquid displacement porosimetry (GLDP).

A fully automated and precise LLDP equipment was developed in the surfaces and porous materials group (SMAP) in Valladolid. This equipment can be used to obtain important information on the structure of UF membranes, including pore size distribution and porosity [14–19]. This equipment has been used in this work to characterize several virus retentive membranes, at a research stage, and the information obtained is correlated and compared with results from other virus membranes characterization methods, to give an idea on how LLDP can be of help to membrane manufacturers and end-users for an appropriate selection of membrane characteristics.

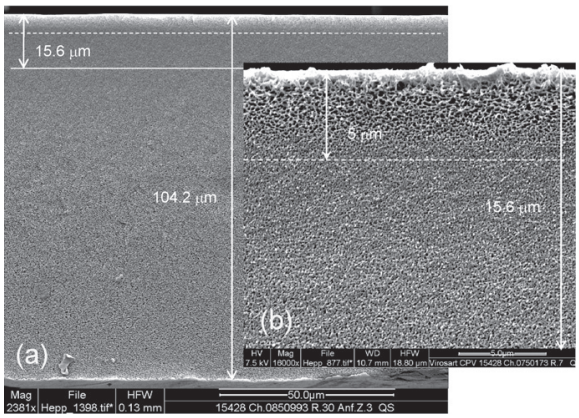

Fig. 1. SEM cross sectional image of a PES virus retentive membrane (a), along with an insert showing the top of previous figure (b). Magnifications are 2381× and 16,000×, respectively. Some characteristic lengths have been marked on it. 5 μm below the top layer is the narrowest pores strip.

2. Experimental

2.1. Membranes

As mentioned previously, the virus retentive membranes used in this work are made of polyethersulphone (PES). PES is a stable polymer that shows a broad pH and temperature range stability, making it possible to sterilize the membrane by either steam or autoclaving. Membrane regeneration, storage and depyrogenation can be accomplished using NaOH even at elevated temperatures. Attending to these features, the PES membrane is ideally suited for biotechnological applications.

The membranes are supposed to have a continuous structure from one side (which could be assimilated to the macroporous support) to the other (more similar to a retentive UF layer [4]). Effectively, the more open structure in the support is gradually tightened to find a minimum size and then continues having a slow transition to the retentive layer of the other side of the membrane. This structure favours virus entrapment which is recognized to improve greatly virus retention capabilities, and it operates in practice as a multi layer membrane. To improve that entrapment phenomenon, membrane filters used for virus filtration are normally operated with membrane support facing the feed stream. The structure of the membrane is shown in Fig. 1, where a cross-sectional picture (a) and a more detailed insert (b) show the membrane morphology.

All membrane samples were manufactured at the R+D department of Sartorius-Stedim. Samples from the same DINA4 sheets were used to perform all characterization tests, including characterization by LLDP.

2.2. Image analysis

We have analyzed cross section images of the PES membranes studied (see for example Fig. 1) from different areas:

- top of the membrane (downstream in usual virus filtration operation),
- central area (around 5 μm below the active layer surface),
- wider pores below this narrow pores central strip (upstream in usual virus filtration operation).

Table 1
Mean pore diameters and standard deviations obtained from image analysis from different areas of cross sections of the membranes studied.

Position	$d_{p,mean}$/nm	σ/nm
Top	123.7	48.4
Center	69.9	33.4
Bottom	88.8	40.2

This kind of microscopic study is able to give insight into the actual mechanism of pore plugging by retained particles, indicating where those particles are plugged [20].

SEM images of membrane cross sections were obtained with a SEM apparatus from FEI (Quanta 2000 FEG). Membrane pieces were water wetted, immersed in liquid nitrogen and then suddenly broken to get a sharp and clean fracture line.

Image analysis was carried out by means of Jandel® ScanPro Software (version 3.00.0030). Each photography is digitalized with a high resolution, and several digital filters and procedures are applied on the resulting image to eliminate parasite changes in grey level due to uneven electron incidence, and to get the maximum contrast and definition [21]. The output of such analysis is shown in Table 1 which summarizes the distributions of Fig. 2.

2.3. Dextran retention tests

Measurements of the retention coefficient for dextran mixtures have been made on each membrane analyzed. The dextran polymer materials were acquired by Serva. The testing mixture of dextrans was obtained by mixing the following single dextrans: 1 kDa, 100–200 kDa, 400–500 kDa and 2000 kDa in the weight proportions (1/6/2/6), the resulting mixture covers approximately the range from 1 to 10,000 kDa (see Fig. 3). This mixture was prepared using 5 L of RO purified water and 0.05 M NaN_3 (3.25 g/L) to get a final dextran concentration of 3 g/L. Resulting solutions have been filtered in Amicon stirred cells type 8200 at 300 rpm and ambient temperature. Filtration was performed by applying a reduced flux of 0.07 mL/min via a syringe pump of Scientific Model 200 series. Taking into account the special features of the membranes analyzed, the solutions have been filtered from bottom to top of the membrane. Five milliliters of dextran solution were discarded, a sample of permeate and retentate solution was subsequently taken and each was analyzed by size exclusion chromatography. SEC analysis was performed with an Agilent 1100 integrated system with RI detector and PSS Suprema columns (100/1000/3000 Å) and aqueous solution of 0.05 M NaN_3 as eluent. This device was calibrated using dextran standards provided by Polymer Standards Service [2].

2.4. Phage retention tests

Bacteriophages are habitually accepted as a model stream for virus retention experiments as previously commented. For the performance characterization of our virus membranes, phages PP7 (ATCC 15692-B2), have been used, with its hosts *Pseudomonas aeruginosa* 1C (ATCC 15692). Bacteria were grown in a liquid nutrient broth culture, in a shaking incubator at 37 °C.

Both permeate and bulk solutions were sampled 1 h after the virus retention test was started. The retentiveness of the membrane has been obtained using Eq. (1). The concentration of the viruses in the seeded bulk solution was 107 108 PFU/mL. The plaque forming units (PFU) are an indicator for the quantity of individual infectious particles (e.g., virus particles) based on the amount of plaque formed per unit volume. Theoretically, the plaque-forming unit includes only the infectious virus particles since a virus particle failing to infect a host cell could not produce a plaque, hence, it should not be counted. PFU rules out possible multiple-hit phenomena and include only the particles capable of infecting cells on their own. Thus, one PFU means one lytic event (or one infectious virus particle). The lowest detection threshold of coliphages is 1–10 PFU/mL.

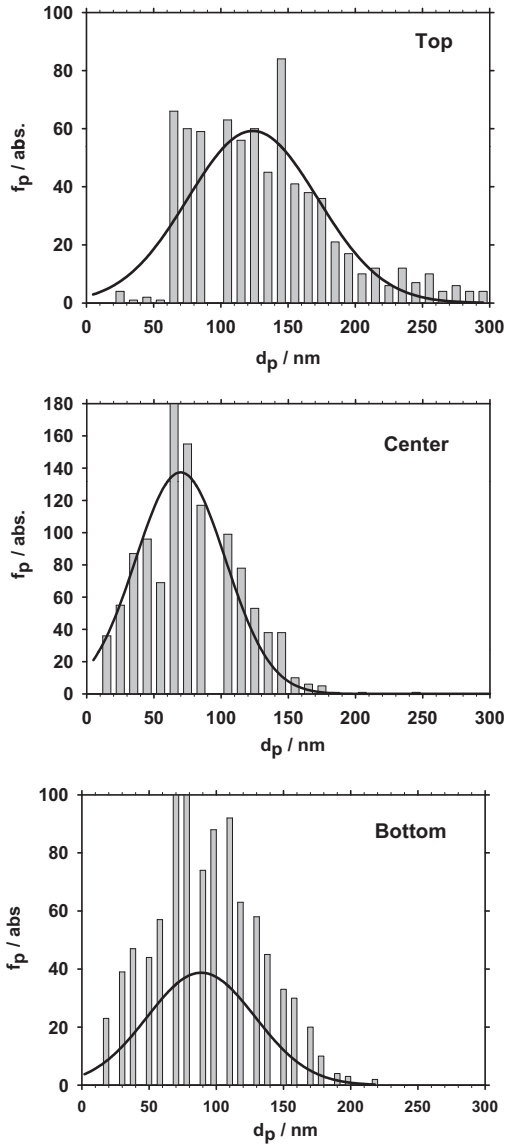

Fig. 2. Pore size distributions at different depths in the membranes analyzed, as obtained from SEM image analysis.

2.5. Filtration characterization

For permeability and phage retention measurements, membranes were assembled into syringe filter holders, exhibiting an effective surface area of 5 cm^2.

The permeability of 0.9% (w/w) NaCl aqueous solution as well as of a potassium phosphate buffer (20 mM Kpi at pH 7.2), have been determined for each membrane sample. The permeability has been measured at a pressure of 0.1 MPa in a dead-end filtration

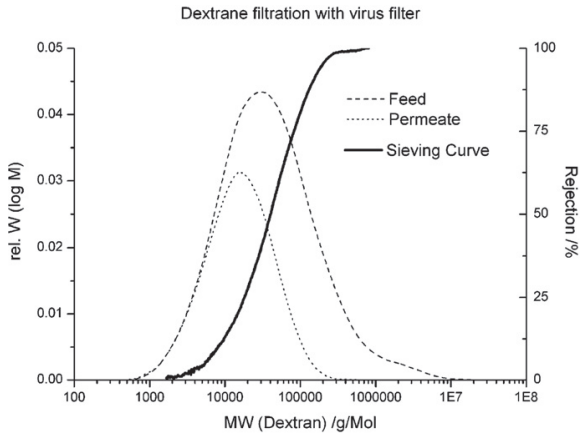

Fig. 3. Weight distributions of the different dextrans used in retention tests.

module. The filter was pre-wet by gravity with the buffer, then the filtration set up was pressurized up to 0.2 MPa and 10 mL of buffer were filtered through the membrane before each measurement.

Air resistance tests have been performed on those cartridges by determining the pressure in mbar occurring at an air flow rate of 100 mL/min trough a membrane area of 5 cm^2.

2.6. Liquid–liquid displacement porosimetry

The porosimeter used in the analysis consists in an automated device developed in the SMAP laboratories in the University of Valladolid [15,19]. A detailed description of the equipment and the experimental procedure can be seen elsewhere [15]. The main feature of the equipment is the use of a precise syringe pump ISCO-250D, allowing accurate and very stable fluxes through a dead end membrane cell, without fluctuations that makes unnecessary any sort of dampening. The experimental procedure allows relating the applied pressure and the corresponding pore radius opened at a given applied pressure according to the Cantor equation, provided that the contact angle between the liquid–liquid interface and the membrane material could be assumed to be zero,

$$P = \frac{2\gamma}{r_p} \tag{2}$$

where P is the applied pressure, γ the interfacial tension and r_p the equivalent pore radius.

By increasing the applied flux stepwise (at a constant rate of 0.025 mL/min), corresponding pore radii and pressure drops, represented as the permeability of the membrane (flow/pressure ratio), are obtained. Therefore, by measuring the equilibrium pressure drop corresponding to each increment of flux, a pore size distribution of the membrane can be evaluated. It should be noted that this pore size corresponds to the narrowest part of the pores found across the whole membrane, independently of the actual pore size gradient appearing within the membrane. The LLDP technique addresses the tightest part of a pore, where capillary forces are the highest and which corresponds to the narrowest region in the membrane cross section. This fact is of importance since this region effectively governs the fluid transport and the corresponding retention.

Several 47 mm diameter flat disk pieces have been used as measuring samples and were previously immersed into the LLDP wetting phase for half an hour under vacuum (150 mmHg) at room temperature to assure complete membrane wetting.

The liquid mixture used to perform the LLDP measurements has been a 1:1 (w/w) mixture of water/isobutanol, with a surface tension of 1.9 mN/m at 25 °C. All alcohols are of reagent grade and have been used as received without further purification. The mixtures were prepared by pouring proper amounts of ultra pure water and alcohol into a separator funnel and shaking it vigorously. The mixtures were then allowed to stand overnight. The separated alcohol-rich phase was drained off and used as the wetting liquid and the aqueous-rich phase was used as the displacing liquid. But these roles could have been interchanged if had been necessary [19] acting the aqueous phase as wetting liquid and the alcoholic one as displacing fluid. This change could be of interest for very hydrophilic membranes, so very prone to wet with water.

3. Results and discussion

An example of porosimetric curve is presented in Fig. 4. We can clearly observe there the features that should be expected for a bubble-point based experiment. Flow does not start until a minimum pressure is established and the wetting liquid starts to penetrate the biggest pores. Subsequently the liquid flow is increased stepwise and pressure in the system increases correspondingly and continues opening pores of decreasing sizes, up to the desired final flux. Once all the pores in the membrane are opened by the pushing liquid, the subsequent points fit very closely to a straight line with a slope corresponding to the membrane permeability of the pure pushing liquid. This asymptotical permeability is marked with a straight line passing through the origin.

For each experimental step of flow-pressure increment, we can evaluate the contribution of the just opened pores to the final permeability as a percentage of such asymptotical permeability. If we plot these percentage contributions to permeability versus the applied pressure in each step, and we use the Cantor equation (Eq. (2)) to label the x-axis in terms of the equivalent pore size (radius) for each equilibrium pressure, we obtain permeability based pore size distributions as shown in Fig. 5 (from data of Fig. 4).

We can fit such distribution to a Gaussian function (the fitted curve is presented as a dashed line) and this fitting gives us the mean pore size of the distribution, $r_{p,\mathrm{mean}}$ (along with the standard deviation). But also maximum and minimum pore sizes can be determined from this sort of distribution. The corresponding values are marked by arrows in Fig. 5. $r_{p,\mathrm{max}}$ is much easier and

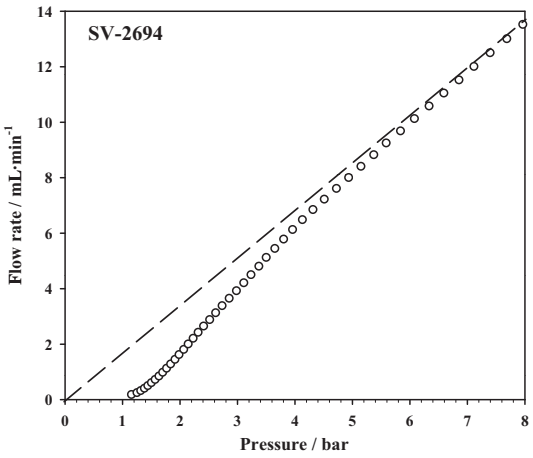

Fig. 4. Example of porosimetric run showing the flux-pressure experimental curve.

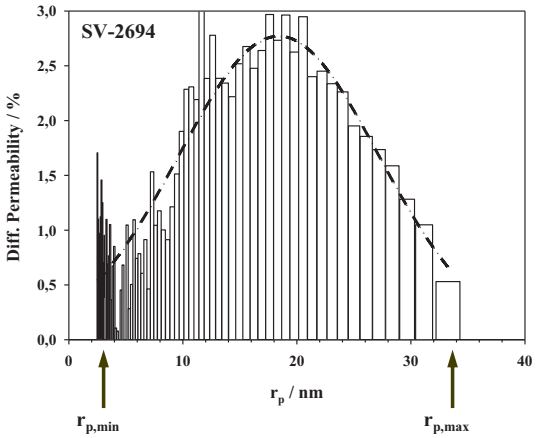

Fig. 5. Permeability distribution obtained from previous curve, along with its Gaussian fitting.

reliable to determine while $r_{p,min}$ is strongly affected by experimental error, which deviate the final points in the porometric run, from theoretical straight line.

Some obtained distributions are not as clearly Gaussian as that of Fig. 5. This is featured in Fig. 6, where the permeability distribution for another different sample is presented. Nevertheless, we decided to fit all distributions to Gaussian functions to assure proper comparison. Even though, it is worth noting that most of the samples show mean pore radii in the range of 20–40 nm, which matches nicely with the mean pore diameters found from image analysis of Fig. 1 (around 70 nm in diameter).

As noted previously, the key parameter for virus filters characterization is the retention of model viruses or, when this is not possible, the retention of test molecules that model appropriately the behaviour of the actual viruses. In our case such molecules were bacteriophages and retentions have been calculated as LRV. High values for LRV have been obtained up to 6.5. Note that attending to the size of the bacteriophages used which size is around 25 nm [22] the retentions obtained should be compared with those typically obtained for parvoviruses that normally, as mentioned are in the range 3–4.

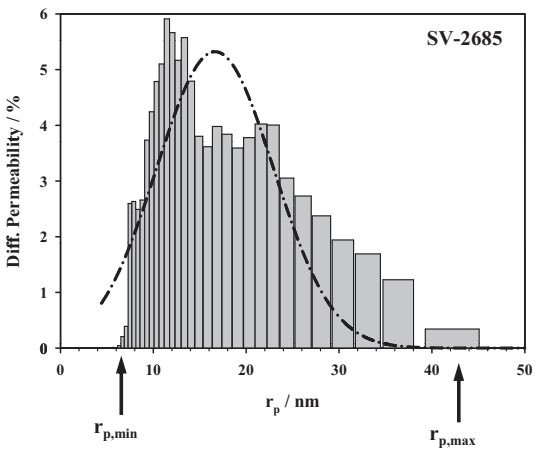

Fig. 6. Another example of permeability distribution fitted to a Gaussian function.

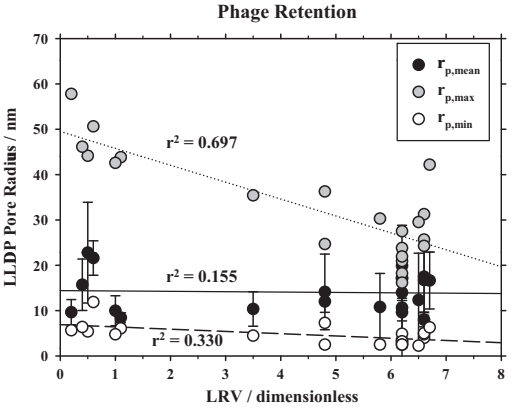

Fig. 7. LLDP results as a function of LRV values obtained from bacteriophages retention tests.

Fig. 7 shows the correlations of LRV with the main LLDP results (mean pore size as obtained from Gaussian fitting, along with maximum and minimum pores sizes directly obtained from the permeability distributions). As could be expected, LRV increases as pore size reduces. This is clearly seen for maximum and minimum pore sizes, while mean pore size shows a less significant correlation, as can be seen in the regression coefficients for all plots. Note that clearly both the maximum and the minimum radii obtained from LLDP behave as expected with higher accuracy in the case of $r_{p,max}$, where almost all the experimental data points are inside the confidence intervals (not shown for the sake of simplicity). Note that $r_{p,max}$ is, among the three parameters studied, the less affected by experimental or calculation errors.

From both these figures we can conclude, that $r_{p,max}$ can be best correlated with the retention of viruses. This advantageous behaviour of $r_{p,max}$ for the prediction of membrane virus retention can well be explained, if we take into account the fundamentals of LLDP. It must be remembered that this technique was originally proposed by Erbe [23] and firstly applied to gas–liquid interfaces, but it is based on the original bubble-point test for Ultrafilters, proposed very early by Bechhold [24] which is still in use as a fast integrity test for MF membranes. It is clear that those methods based on the bubble-point technique are especially accurate to get the maximum pore size present in the distribution, while the rest of the points experimentally obtained, are somehow dependant on the rate of flux (pressure) increase and the quality of the response of the experimental set-up. Also it is important to note that retention is mainly determined by the pores presenting the wider necks so by the larger pore sizes in the most restrictive layer of the membranes.

Once we have demonstrated the good correlation of the maximum pore size with retention capabilities, we can directly expand such correlations for further membrane performance parameters. Such comparisons are presented in Figs. 8–10, where LLDP maximum pore radius for each membrane sample are plotted versus air resistance, water permeability and buffer flow, respectively. The data shows a good correlation of these parameters with $r_{p,max}$, especially for the case of water permeability and buffer flow. All data have been fitted to linear relationships and 95% confidence intervals are included. These well matching results are very reasonable if we consider that LLDP is essentially a flow-based test. It is reasonable to have a worse data correlation for air flow based data (as shown in Fig. 8), since gas flow behaves slightly different than liquid flow. On the other side the fact that correlation is fairly good with permeability (water of buffer) should be due to the quite similar pore size distributions surely characterising all the

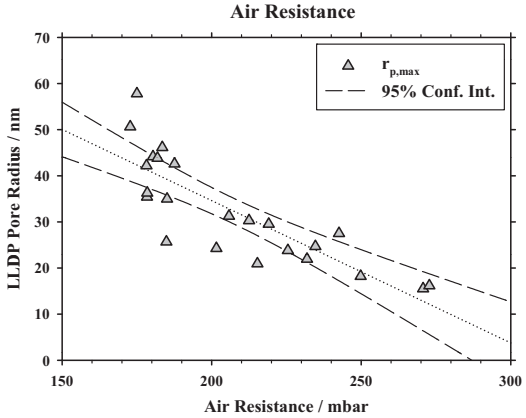

Fig. 8. LLDP maximum radius as a function of air resistance values.

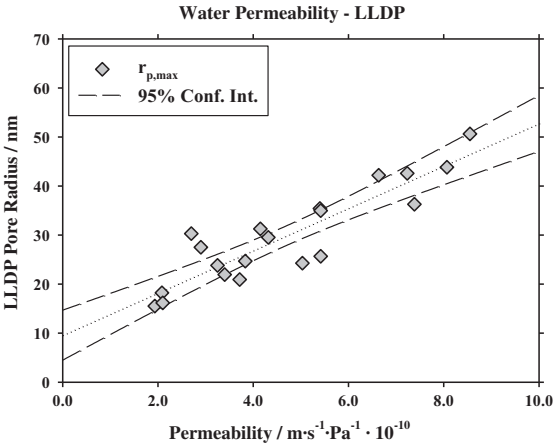

Fig. 9. LLDP maximum radius as a function of water permeability.

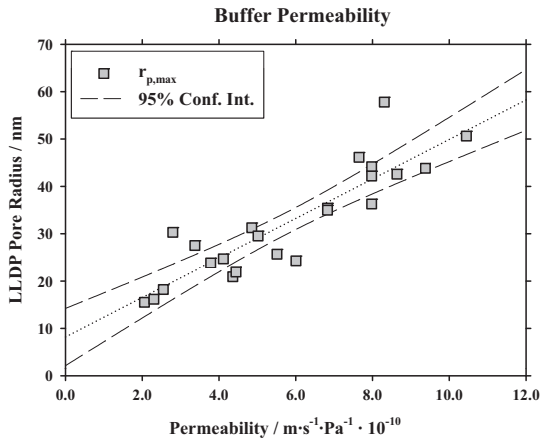

Fig. 10. LDP maximum radius as a function of flow of buffer permeability.

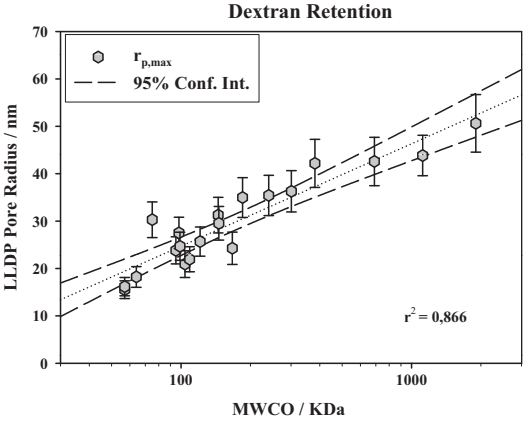

Fig. 11. LLDP maximum radius as a function of MWCO values obtained from dextran retention tests.

analyzed membranes. Actually, they are comparable membranes just manufactured in slightly different ways.

Finally, we have tested the correlation of LLDP with another very important performance related parameter, which is the MWCO as obtained from test molecules retention experiments (dextran molecules in our case). If LRV of virus/phages is more likely to be used for the characterization of virus membranes characterization, dextran retention test is a very commonly used parameter to characterize ultrafiltration membranes. Retention tests of other appropriate molecules are also used for nanofiltration membranes. The sieving curves can be used to calculate a pore size distribution (PSD), which can then be compared to the PSD determined by LLDP and give additional information on how precise/reliable the LLDP method works.

In Fig. 11, we have plotted the LLDP maximum pore radius versus the 90% MWCO obtained from dextran retention experiments for the same samples. The correlation of these magnitudes is remarkably good and allows devising LLDP as a powerful predictive tool for membrane performance characteristics. In this figure also the 95% confidence intervals are presented with almost all data points falling into these prediction lines.

It is important to note that, as commented previously, some virus retentive membranes, as those studied here, present a reduction in the pore size at a certain depth into the membrane. Also, the information coming from LLDP refer, in all cases, to the narrowest portion along each pore. In order to get information on the extent and characteristics of these size profiles along the pore, other complementary methods should be applied. One of such techniques is SEM image analysis of cross sectional viewing of the filters. Nevertheless, the information given by LLDP is basic to assure the retention capabilities for virus or whatever molecule or particle we would like to retain because retention is determined by the pore sizes that LLDP detects; i.e., by the narrowest neck along the pores and especially the largest pores/pathways present in the membrane.

4. Conclusions

We have demonstrated that LLDP experiments can give structural information which can be very reasonably correlated with performance related information, when analysing membranes designed for virus retention.

In this sense, we have shown that the maximum pore size obtained by LLDP distributions can be correlated with performance parameters as relevant as bacteriophages log

retention value (LRV) or dextran test cut-off values. This correlation clearly fits better when using the distribution's maximum pore size instead of minimum or mean pore sizes.

This work allows envisaging possible methods of estimating the retention capabilities of a given filter, without the necessity of performing time consuming and expensive retention experiments (specially in the case of virus membranes where working with active viruses or bacteriophages requires severe control measurements).

The importance of such a straight forward method for the process of development of new filters, adapted for selected applications in the typical pore ranges of ultrafiltration and virus retentive membranes, will surely be recognized by membrane manufacturers and research labs. During the development of appropriate membranes, possible candidates have to be selected. Currently this is done on the basis of results obtained in a battery of time consuming and expensive membrane characterization tests. Instead of these complex methods, LLDP could be used to select the most appropriate candidates on which to perform complete characterizations. This can strongly reduce the number of tests and the cost of characterization experiments. Thus the LLDP method should be recommended for membrane manufacturers and R+D institutions in the first place, moreover it offers a great potential to be developed towards a customer application.

Finally, the good correlation between LLDP maximum pore sizes and the other pore size tests suggest the convenience of a simplification of the technique to the easy and rapid detection of maximum pore sizes.

Acknowledgements

The Spanish authors want to thank the Spanish "Ministerio de Ciencia e Innovación (MCINN)" for financing this work within the frame of the "Plan Nacional de I+D+I" and through the projects CTQ2009-07666 and MAT2008-00619. Also the Spanish "Junta de Castilla y León" has contributed through the project Grupos de Excelencia-GR18.

References

[1] G. Grznárová, M. Viktorin, A. Lang, Characterization of virus retentive membranes by a tailor-made dextran method, Desalination 200 (1–3) (2006) 297–298.
[2] G. Grznárová, M. Viktorin, A. Lang, Characterization of virus retentive membranes by a tailor-made dextran method. Determination of sieving curves and MWCO based on size exclusion chromatography (SEC), in: Proc. Euromembrane, Hamburg, 2006.
[3] T. Urase, K. Yamamoto, S. Ohgaki, Effect of pore structure of membranes and module configuration on virus retention, J. Membr. Sci. 115 (1996) 21–29.
[4] Klaus-Viktor Peinemann, Suzana Pereira Nunes (Eds.), Membranes for Life Sciences, Wiley-VCH, 2007, ISBN 3527314806, 9783527314805.
[5] S.S. Madaeni, A.G. Fane, G.S. Gromann, Virus removal from water and wastewater using membranes, J. Membr. Sci. 102 (1995) 65–75.
[6] J.G. Jacangelo, S.S. Adham, J.-M. Lainé, Mechanism of *Cryptosporidium*, *Giardia*, and MS2 virus removal by MF and UF, AWWA 87 (1995) 107–121.
[7] A.L Zydney, D.M. Bohonak, Compaction and permeability effects with virus filtration membranes, J. Membr. Sci. 254 (2005) 71–79.
[8] C. Shang, H.M. Wong, G. Chen, Bacteriophage MS2 removal by submerged membrane bioreactor, Water Res. 39 (2005) 4211–4219.
[9] B. Kalbfuss, M. Wolff, L. Geisler, A. Tappe, R. Wickramasinghe, V. Thom, U. Reichl, Direct capture of influenza A virus from cell culture supernatant with Sartobind anion-exchange membrane adsorbers, J. Membr. Sci. 299 (2007) 251–260.
[10] L. Fiksdal, T.-O. Leiknes, The effect of coagulation with MF/UF membrane filtration for the removal of virus in drinking water, J. Membr. Sci. 279 (2006) 364–371.
[11] Y. Matsui, T. Matsushita, T. Inoue, M. Yamamoto, Y. Hayashi, H. Yonekawa, Y. Tsutsumi, Virus removal by ceramic membrane microfiltration with coagulation pretreatment, Water Sci. Technol. Water Supply 3 (2003) 93–99.
[12] T. Matsushita, Y. Matshui, N. Shirasaki, Analyzing mass balance of viruses in a coagulation–ceramic microfiltration hybrid system by a combination of polymerase chain reaction (PCR) method and the plaque forming units (PFU) method, in: Proceedings of IWA International Conference on Particle Separation, Seoul Korea, 2005, pp. 487–494.
[13] T. Hongo-Hirasaki, K. Yamaguchi, K. Yanagida, K. Okuyamam, Removal of small viruses (parvovirus) from IgG solution by virus removal filter Planova®20N, J. Membr. Sci. 278 (2006) 3–9.
[14] A. Bottino, J.I. Calvo, P. Prádanos, G. Capannelli, A. Hernández, Characterisation of UF membranes by liquid–liquid displacement porometry and scanning force microscopy, in: Proceedings of Prague Macromolecules Microsymposia, 16–19 July, Prague, Czech Republic, 2001.
[15] J.I. Calvo, A. Bottino, G. Capannelli, A. Hernández, Comparison of liquid–liquid displacement porosimetry and scanning electron microscopy image analysis to characterise ultrafiltration track-etched membranes, J. Membr. Sci. 239 (2004) 189–197.
[16] J.M. Sanz, D. Jardines, A. Bottino, G. Capannelli, A. Hernández, J.I. Calvo, Liquid–liquid porometry for an accurate membrane characterization, Desalination 200 (2006) 195–197.
[17] J.A. Otero, O. Mazarrasa, J. Villasante, V. Silva, P. Prádanos, J.I. Calvo, A. Hernández, Three independent ways to obtain information on pore size distribution of nanofiltration membranes, J. Membr. Sci. 309 (2008) 17–27.
[18] J.I. Calvo, A. Bottino, G. Capannelli, A. Hernández, Pore size distribution of ceramic UF membranes by liquid–liquid displacement porosimetry, J. Membr. Sci. 310 (2008) 531–538.
[19] R. Peinador, J.I. Calvo, P. Prádanos, L. Palacio, A. Hernández, Characterisation of polymeric UF membranes by liquid–liquid displacement porosimetry, J. Membr. Sci. 348 (2010) 238–244.
[20] D.A. Bell, C. Bondy, C. Santeufemio, Examination of fouling and plugging mechanisms of porous polymer membranes by SEM, Microsc. Microanal. 13 (2) (2007) 1494–1495.
[21] A. Hernandez, J.I. Calvo, P. Prádanos, L. Palacio, M.L. Rodríguez, J.A. de Saja, Surface structure of microporous membranes by computerized SEM image analysis applied to anopore filters, J. Membr. Sci. 137 (1997) 89–97.
[22] V.B. Rajal, B.S. McSwain, D.E. Thompson, C.M. Leutenegger, B.J. Kildare, S. Wuertz, Validation of hollow fiber ultrafiltration and real-time PCR using bacteriophage PP7 as surrogate for the quantification of viruses from water samples, Water Res. 41 (2007) 1411–1422.
[23] F. Erbe, The determination of pore distribution according to sizes in filters and ultrafilters, Kolloid Z. 63 (1933) 277–285.
[24] H. Bechhold, The permeability of ultrafilters, Z. Phys. Chem. 64 (1908) 328–342.

Paper four

José Ignacio Calvo, René Israel Peinador, Pedro Prádanos, Laura Palacio, Aldo Bottino, Gustavo Capannelli, Antonio Hernández.
Liquid–liquid displacement porometry to estimate the molecular weight cut-off of ultrafiltration membranes, *Desalination 268 (2011) 174–181*.

Desalination 268 (2011) 174–181

Contents lists available at ScienceDirect

Desalination

journal homepage: www.elsevier.com/locate/desal

Liquid–liquid displacement porometry to estimate the molecular weight cut-off of ultrafiltration membranes

José Ignacio Calvo [a,*], René Israel Peinador [a], Pedro Prádanos [a], Laura Palacio [a], Aldo Bottino [b], Gustavo Capannelli [b], Antonio Hernández [a]

[a] Departamento de Física Aplicada, Facultad Ciencias, Universidad de Valladolid, 47071 Valladolid, Spain
[b] Dipartimento di Chimica e Chimica Industriale, Universitá di Genova, Vía Dodecaneso, 16136, Genova, Italy

ARTICLE INFO

Article history:
Received 21 July 2010
Received in revised form 5 October 2010
Accepted 5 October 2010
Available online 29 October 2010

Keywords:
Molecular weight cut-off
Dextran retention
Pore size distribution
Liquid–liquid porometry

ABSTRACT

Liquid–liquid displacement porometry (LLDP), is proposed to estimate the molecular weight cut-off value of Ultrafiltration (UF) membranes.
Several commercial UF membranes are analysed by using LLDP and their pore size distributions have been used to estimate the molecular weight cut-off as should be obtained by dextran retention.
Results compared reasonably with nominal cut-off values given by manufacturers. The method offers a fast and accurate way to assign cut-off values for UF membranes, without having to perform expensive and time consuming solute retention tests, which bring results very often difficult to compare due to the difficulties in the standardization of such methods.

1. Introduction

In Ultrafiltration (UF), the selectivity is in part determined by the porous structure, which in turn is characterized by the corresponding sieving curve. These curves are obtained from a plot of retention of some selected solutes, called tracers, versus their molecular mass and have reached the category of a "de facto" standard, [1] for the characterization of UF membranes and their classification in terms of the so-called molecular weight cut-off (MWCO). For the membrane manufacturers and for the end-users too, any characterization method should be able to give an adequate idea of the separation range within which the analysed membrane should be more precisely and effectively used. In this sense, the MWCO value is a very valuable parameter because it gives an idea about the molecular weight of species being separated by such membrane.

It is worth mentioning that there are still many points concerning the appropriate tracers and the details of the filtration process that are still far from being established. Many authors, [2–6], have shown that the reported cut-off of a membrane may be very different due to the differences in methodology and test conditions. In effect, operators very often neglect the influence of many factors, not always controlled or clearly stated, on the results of such technique. These factors include the effects of the configuration of the experimental devices and other important operational parameters as, for example, the channel geometry or the degree of turbulence of the feed recirculation on the membrane surface [1].

Actually the results of retention tests cannot be really considered as a characteristic parameter of the membrane because they depend not only on the details of the operation factors during the test but also on the shape, flexibility and molecular weight distribution of the macromolecules used for retention tests. Also the interaction of the macromolecule with the membrane can play a crucial role through concentration polarization and fouling phenomena.

For retention tests, certain types of macromolecules such as dextrans and polyethylene-glycols have been customarily used. These solutes have been used with a broad range of molecular weights, both in a single wide weight distribution or in several single individual narrow molecular weight distributions. Dextrans have several advantages, which have promoted their use as the solute of choice. It is a relatively inert molecule, readily available in a wide range of molecular weights, and its concentration can be easily measured using a refractive index detector. Nevertheless, due to the signal noise, the sensitivity of the assay scarcely detects retentions as low as 0.001. This limitation prevents the use of dextrans in order to characterize retentions at low sieving, [7]. Another limitation of dextran retention tests is its inability to characterize charged UF membranes, which have become increasingly important for high performance tangential flow filtration (HPTFF) applications [7].

Another possibility is to evaluate the pore size distribution of membranes and trying to calculate, from such structural information, which molecules can be retained or passed through membranes. In effect a relationship between retention results and the actual structural

* Corresponding author. Tel.: +34 983423758; fax: +34 983423136.
E-mail address: jicalvo@termo.uva.es (J.I. Calvo).

0011-9164/$ – see front matter © 2010 Elsevier B.V. All rights reserved.
doi:10.1016/j.desal.2010.10.016

characterization of the membrane could be found subjected of course to the real complexity of the retention process itself. Such possible relationship should be investigated at least from a phenomenological point of view in order to help understand the transport phenomena through the membrane, [1,8]. Therefore, knowledge of the actual structure of the pores in the membrane would be really useful because it could be translated to retention terms for each particular solute and each operation condition by a detailed study of the solute–solute and solute–membrane interactions in each application.

Actually the results from retention tests could be in principle far from what might be expected from the actual membrane pore size distribution, [9]. Manufacturers generally specify for their membranes a nominal MWCO corresponding to the molecular mass of the solute that is (or would be) 90% retained by the membrane. However, most UF applications require retentions of 99.9%, or higher, of the product to be processed, [7]. When trying to translate pore size distributions into MWCO data, or vice versa, it is difficult to reach these ranges because there is limited information on the sieving coefficients at high retentions. Most existing models assume spherical neutral solutes passing through cylindrical pores [10,11]. Of course, many refinements have been introduced in the original model, widely used to estimate the pore radii of membranes and to predict or interpret retention, mainly on NF membranes, [12–17]. At present, these correlations are still ambiguous and not totally understood but they already allow correlating approximately retention results with actual pore size distributions.

Many characterization methods like permporometry, thermoporometry, mercury porometry, gas adsorption–desorption, NMR and liquid–liquid porometry, along with several microscopic techniques have been used to characterize the membrane pore and pore size distribution, [18]. Each of these methods has different characteristics and relies on different theoretical considerations to be taken into account to convert the direct results into pore sizes. Actually the information given by all these methods can be considered as complementary and should contribute to a complete picture of the morphology of the pores.

UF membranes usually present pores in the range from some nanometers to 50 nm (0.05 μm) and a proper knowledge of the size distribution of those pores actually open for the flux (active pores) is of great interest to estimate the sort of macromolecules retained. Techniques, such as those based on bubble point test that have gained enormous relevance for the characterization of microfiltration membranes, cannot be properly applied to UF membranes due to the high pressure (more than 10 bar) necessary to evaluate pore with sizes below 0.1 μm, [19]. On the contrary liquid–liquid displacement porometry (LLDP), because it uses a liquid–liquid interface inside the pores, is very suitable for characterizing UF membranes at relatively low applied pressures.

Authors have developed a fully automated and very precise equipment that, making use of LLDP, allows obtaining important information on the structure of UF membranes, including pore size distribution and porosity, [20–24]. This equipment will be used in this work to characterize commercial UF polymeric membranes. In a previous work, [25], it has been demonstrated that LLDP results (especially the maximum pore size present in the distribution) can be reasonably correlated with membrane separation properties as LRV logarithmic reduction value, parameter which is very important in the case filters designed to retain viruses.

In this work, authors will try to examine different empirical correlations that can help to convert structural data, especially those coming from LLDP, into dextran retention data. The resulting equations will be used to estimate the cut-off values for a broad range of commercial membranes. Finally these estimations will be compared with nominal values as given by manufacturers. Then, we will be able to propose a method to accurately assess the membrane retention performance from simple, fast and cheap LLDP experiments.

2. Theory

Several ways to correlate the size of the pores of a membrane with the molecular weight of molecules that can pass through it can be found in the literature. In principle, these approaches are based on empirical relationships between the size of a particular molecule and its molecular weight. Although these relationships exist and are valid in more or less defined ranges, it is worth remembering that they apply well only for specific classes of molecules.

Reiss and Zydney [26] proposed a relationship between the molecular weight of a protein and its Stokes-Einstein radius, derived for a wide range of proteins and given by a 1/3 power:

$$r = 0.88\,\mathrm{MW}^{1/3} \tag{1}$$

Others, [27,28], calculated the mean radius of porous membranes from the MWCO value of dextrans as derived from the following equation:

$$r = 0.33\,\mathrm{M_W}^{0.46} \tag{2}$$

In both Eqs. (1) and (2) M_W is written in Dalton (g/mol) and the particle size (or pore size in Eq. (2)) is given in Angstrom (Å).

Similarly, other authors, [29,30], used a different equation to correlate the hydrodynamic radius values (again in Å) with the molecular weight of dextrans (in Dalton):

$$r = 0.488\,\mathrm{M_W}^{0.437} \tag{3}$$

Schultz et al. [31] obtained data for the osmotic reflection coefficient (σ) for dextrans with weight-average molecular weights from 70 kDa to 500 kDa by using track-etched polycarbonate membranes with uniform cylindrical pores. The dextran sieving coefficients estimated from these results were substantially larger than those predicted by hydrodynamic models for spherical solutes in cylindrical pores. Then, they evaluated an equivalent spherical radius for the studied dextrans from their free solution diffusivities according to the Stokes-Einstein equation:

$$r_S = \frac{k_B T}{6\pi\eta D_\infty} \tag{4}$$

where k_B is the Boltzmann's constant, T the absolute temperature, η the water viscosity and D_∞, the diffusion coefficient of the dextran at infinite dilution in water. They assumed the dextran to be monodisperse.

Chen et al. [32] expressed the diffusion coefficient of dextrans at infinite dilution in water, D_∞ as a function of the molecular weight of the dextran (M) as:

$$\log D_\infty = -4.1154 - 0.47752\log(\mathrm{M}) \tag{5}$$

Eqs. (4) and (5) can be used to get the MWCO corresponding to a given pore size. Actually Eq. (5) should be valid for molecular weights from 21.6 to 526 kDa. Nevertheless, Eqs. (4) and (5) as well as Eqs. (2) and (3) will be tested in a sensibly wider molecular weight range, and results of such equations will be compared with the data on MWCO given by the manufacturers.

The results of the three earlier reported approaches are presented in Fig. 1, where the molecular weight of dextrans is plotted versus their corresponding Stokes radius in a double-log plot. The x-axis scale has been selected to cover the whole UF range, from 1 to 50 nm. It can be observed that a similar trend for all equations, with Eqs. (2), (4) and (5) leading to similar results in the low UF range (under 10 nm). At bigger pore radii (over 10 nm) Eqs. (2) and (3) are much closer to each other.

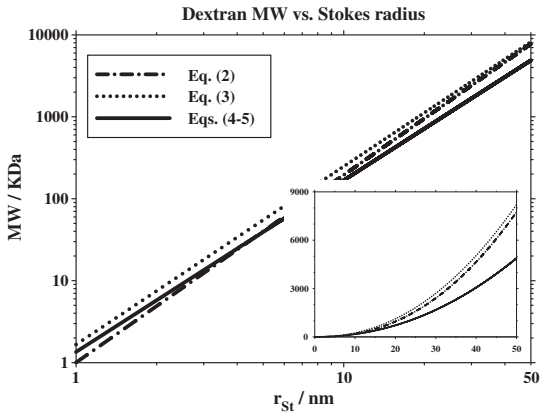

Fig. 1. Comparison of MW of dextran molecules versus Stokes radius of the molecule, using several theoretical equations.

All these equations are normally used to evaluate the mean pore radius from MWCO results. In this work it will be worked in the opposite direction, i.e. using pore size distributions obtained from LLDP experiments, to get the appropriate pore radius which introduced in previous equations will serve to obtain the MWCO of the studied membranes.

2.1. Liquid–liquid displacement porometry

The porometer used in the analysis consists in an automated device developed and improved as part of a collaboration between the University of Valladolid and the University of Genoa, [20]. A detailed description of the equipment and the experimental procedure can be seen elsewhere, [20], and a scheme of the set-up is depicted in Fig. 2.

In the liquid–liquid displacement porometry the membrane is soaked in a liquid (the wetting one) which is subsequently pushed out by another immiscible liquid when the applied pressure increases. The experimental procedure allows correlating the applied pressure and the corresponding pore radius opened at a given applied pressure using the Cantor equation, by assuming the contact angle between the liquid–liquid interface and the membrane material to be zero,

$$\Delta p = \frac{2\gamma}{r_p} \tag{6}$$

where Δp is the applied pressure, γ the interfacial tension and r_p the equivalent pore radius.

By increasing the pressure stepwise, corresponding pore radii and flow values, represented as the permeability of the membrane (L_p = flow/pressure), are obtained. Therefore by measuring the equilibrium pressure drop corresponding to each increment of water flux a pore size distribution of the membrane can be evaluated, where successive values of differential permeability are obtained as:

$$dL_i = \left(\frac{L_i - L_{i-1}}{L_{tot}}\right) \tag{7}$$

being L_{tot}, the final permeability measured at the sample, which corresponds to the permeability once all the pores have been emptied from wetting fluid.

Assuming that the pores are cylindrical, the Hagen–Poiseuille equation can be used to translate permeability pore size distributions to pore number ones, thus correlating the volumetric flow, Q_i, of the pushing liquid and the number of pores, n_k ($k = 1,...,i$) having pore radii, r_k ($< r_i$). For each pressure step, Δp_i, the corresponding measured volume flow is correlated with the number of pores thus opened by:

$$Q_i = \Delta p_i \left(\frac{\pi}{8\eta l} \sum_{k=1}^{i} n_k r_k^4\right) \tag{8}$$

where η is the dynamic viscosity of the displacing fluid and l is the pore length, which roughly corresponds to the membrane thickness in

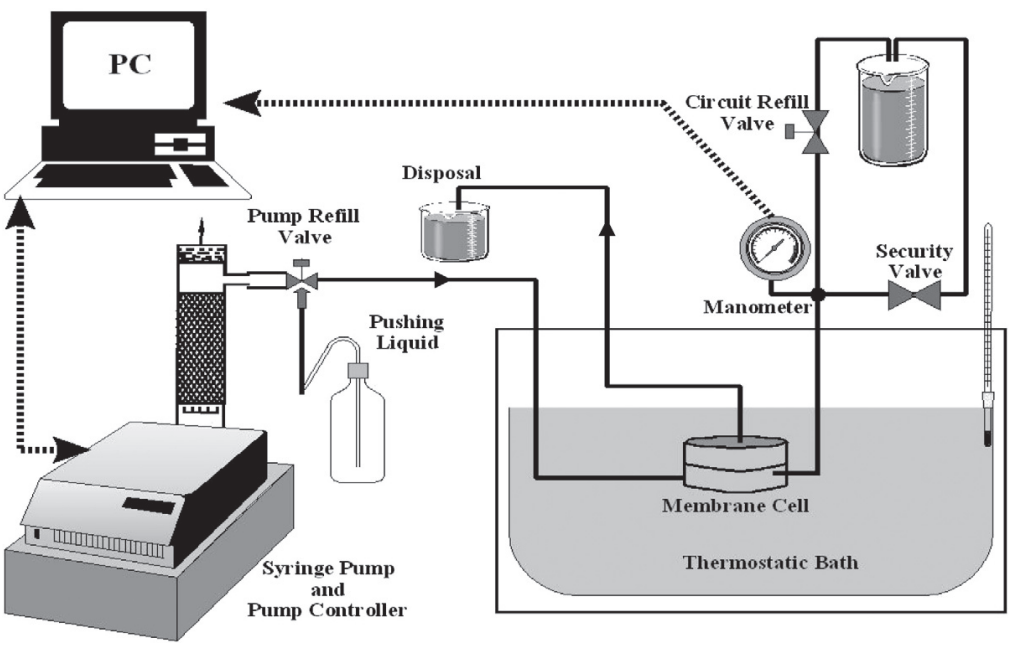

Fig. 2. Scheme of the experimental device.

the case of symmetric membranes, while for asymmetric ones, it should correspond to the active layer thickness, [33].

2.2. Cut-off estimation

In order to estimate the molecular weight cut-off from LLDP measurements for UF membranes, we need to perform a complete LLDP analysis (1–1 1/2 h typically). Then, from the porometric results, it can be obtained, as previously described, both the permeability and number pore size distributions. The number pore size distribution can be presented as cumulative; i.e. plotting the number of pores with radii below each given pore size. In such a representation the biggest pore corresponds to the first one opened while the smallest one should appear theoretically when the 100% of the flux has been reached. Of course it is impossible to be sure that a 100% of the flux has been reached as far as increases of fluxes in these final steps are very slow. Here it will be assumed that the experiment is finished when the experimental fluctuations are higher than the expectable increases in flux due to the opening of very small pores. Then the permeability remains constant or equivalently the flux versus pressure is linear. Afterwards, decrements in permeability could appear due to experimental fluctuations or some membrane compression. In any case, this should mean that the experiment is finished. Then the calculation algorithm does not account for data leading to permeability decrements.

A graphical determination of the pore size such that 90% of the pores are smaller than it and only 10% of the total pores are bigger should define what will be used to estimate the molecular weight cut-off for the membrane. In effect, it can be assumed that if this membrane is used to filter similar spherical molecules, those with sizes up to that corresponding to the 90% of the pores would be retained by 90% of the pores only passing through the remaining 10% pores bigger than the 90% pore size. So it can be considered this value as a reasonable indication of the cut-off pore radius for such a membrane. The only remaining and not easy step is to convert the obtained value from pore size terms to molecular weight units in conditions that could be valid or at least useful for non actually spherical molecules. What is usually done is to use an appropriate equation, among those presented in the theory section; it can be correlated such equivalent or gyration radius with the molecular weight of the corresponding molecules.

3. Experimental

3.1. Membranes and chemicals

A wide representation of commercial UF membranes, having nominal MWCO from 5 to 300 kDa, has been used in this work. The main characteristics of the membranes, including manufacturer, membrane material, configuration and nominal values of MWCO, are listed in Table 1.

Membrane samples were immersed into the LLDP wetting phase for half an hour under vacuum (150 mmHg) at room temperature to assure complete membrane wetting. The liquid mixture used to perform the LLDP measurements was a 1:1 w/w mixture of water and isobutanol. The alcohol was of a reagent grade and was used as received without further purification. The mixture was prepared by pouring proper amounts of Milli-Q grade water and alcohol into a separator funnel and shaking it vigorously. The mixtures were then allowed to stand overnight. The separated alcohol-rich phase was drained off and used as the wetting liquid and the aqueous-rich phase was used as the displacing (pushing) liquid. A statistically significant number of samples of each membrane was analysed and the corresponding outputs were used to obtain mean values and standard deviations.

Table 1
Types, names and characteristics of all membranes used in this study.

Membrane	Name	Material	Manufacturer	Config.	Nom. MWCO/ kDa
Ultracel	PL5	Regen. cellulose	Millipore	Flat	5
	PL10	Regen. cellulose	Millipore	Flat	10
	PL30	Regen. cellulose	Millipore	Flat	30
Biomax	PB5	PES	Millipore	Flat	5
	PB10	PES	Millipore	Flat	10
	PB30	PES	Millipore	Flat	30
Tami	T50	Zirconium oxide	Tami	Tubular	50
	T150	Zirconium oxide	Tami	Tubular	150
	T300	Zirconium oxide	Tami	Tubular	300
Nadir	C030	Cellulose	Microdyn	Flat	30
	C100	Cellulose	Microdyn	Flat	100
	P005	PES	Microdyn	Flat	5
	P020	PES	Microdyn	Flat	20
FS	FS40	Fluoropolymer	DDS	Flat	40
	FS50	Fluoropolymer	DDS	Flat	50
UF-PES	UF-PES-030	PES	Koch	Flat	30
	UF-PES-100	PES	Koch	Flat	100
Minitan	M010	Polysulfone	Millipore	Flat	10
	M030	Polysulfone	Millipore	Flat	30
	M300	Polysulfone	Millipore	Flat	300
GR	GR-60PP	Polysulfone	Alfa Laval	Flat	20
	GR-71PE	Polysulfone	Alfa Laval	Flat	20

4. Results and discussion

Fig. 3 shows a typical LLDP run (which can be called porogram) for an UF-PES-100 sample. It can be seen that an initial increase of permeability appears when the pushing liquid has achieved a high enough pressure to overcome the surface tension of the liquid–liquid-membrane interface and filled pores start to be emptied from the wetting liquid allowing the pushing liquid to start flowing. This starting point (marked with an arrow on the figure) corresponds to the maximum pore size found in the distribution for such sample ($r_{p,max}$). This point is called bubble point in the case of gas–liquid displacement porometry (GLDP). Actually this denomination should not apply here as far as there isn't any gas bubbling through the membrane.

When we continue pushing the liquid against the membrane surface, as pressure increases, more and more pores are being opened and, consequently, permeability increases. This continuous increase leads to a bent up curvature, which means that the number of pores opened at each step is higher than during the previous ones. There should be a point where the number of pores being opened starts to decrease, when the distribution reached the maximum number of pores present in the sample. This fact is related with a change of curvature in the porogram,

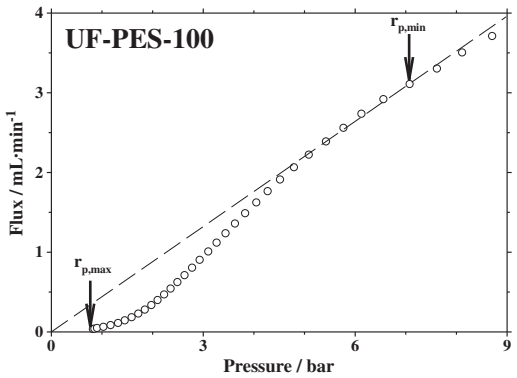

Fig. 3. Typical porosimetric run showing maximum and minimum pore sizes.

which also corresponds to the maximum of the permeability distribution, as shown in Fig. 4. This distribution has been obtained by accounting for the contribution of each experimental step of flow-pressure increment to the overall membrane permeability.

When a linear trend is reached, this fact being assured by fitting the last points to a straight line, the last experimental point before getting a constant permeability is marked in Fig. 3 as $r_{p,\min}$, the corresponding permeability distribution of Fig. 4 does not present any further contributions.

From the permeability distribution (Fig. 4), and taking into account the Hagen–Poiseuille model for convective flux inside capillary tubes, it can be calculated the number of pores which should be necessary for each permeability increase. These values can be plotted as pore number distribution (Fig. 5). This figure is similar to the permeability distribution, but clearly shifted to lower pore sizes, as can be expected due to the 4th power dependence of permeability with pore size.

The main problem with such distributions is that smaller pores need much more number to give similar permeabilities but the experimental values of such smallest pores (or highest pressures) are subjected to larger fluctuations. Due to these usual fluctuations, it is clearly difficult, if not impossible, to get a perfectly straight line at the end of each experiment or porogram. Therefore, pore numbers corresponding to those last points (high pressures and small pores) are not as reliable as those corresponding to lower pressures. Thus, in order to get more standardizable results that could be relatively free from detailed flow assumptions, [34], pore permeability distribution should be used as a more reliable way to get mean pore sizes. Fig. 6 shows cumulative distributions for permeability, pore numbers and pore area corresponding to the previously showed analysis. Only the permeability distribution corresponds to directly measured data while the other two are indirectly obtained as an application of the assumption of purely convective flow through cylindrical pores.

In our case it is needed to use a pore number distribution in order to be able to estimate the MWCO values of the analysed samples by correlating molecular weights of test solutes with pore radius. As commented before, the procedure requires identifying what is the pore size below of which 90% of the total population of pores in our membrane is included. In Fig. 6 this procedure is depicted. The pore size corresponding to the 90% biggest pores is obtained from interception of the cumulative number of pores distribution and a horizontal line placed at the 90% value of the ordinates axis. Then the value of the x-axis corresponding to this intercept is identified as the 90% biggest pore radius.

Using Eqs. (2) and (3) or alternatively Eqs. (4) and (5), this pore size can be converted into the equivalent molecular weight for a dextran molecule which in a typical test retention experiment should lead to a 90% retention. In such way, when using Eqs. (4) and (5) it can be assumed that this dextran molecule is closely spherical, inert and rigid enough to pass through the pores only if they are bigger than the molecule, discarding the possibility of passing due to molecule flexibility or compression. These assumptions, if not completely fulfilled, are used quite often in retention modelling, so we can stand them as empirical basis of our approach. In any case Eqs. (2) and (3) don't require these assumptions since they directly correlate membrane radii with molecular weight cut-offs based on phenomenological correlations.

Such calculations have been done for all the different membranes proposed in the experimental section. After analysing them in the LLDP set-up and obtaining the pore size distributions, they have been plotted the pore number distribution for each sample and obtained the 90% biggest pore, which gave several estimations of cut-off when using Eqs. (2)–(5).

To analyse and discuss the pertinence of each proposed equation, they have been plotted separately the estimations of cut-off arising when using each one as a function of the nominal molecular weight cut-off. In Fig. 7 the corresponding plot for Eqs. (4) and (5) is shown. All the plots give similar trends with fair agreement between nominal and evaluated MWCO. The agreement is slightly better for Eqs. (4), (5) and (2) compared with Eq. (3).

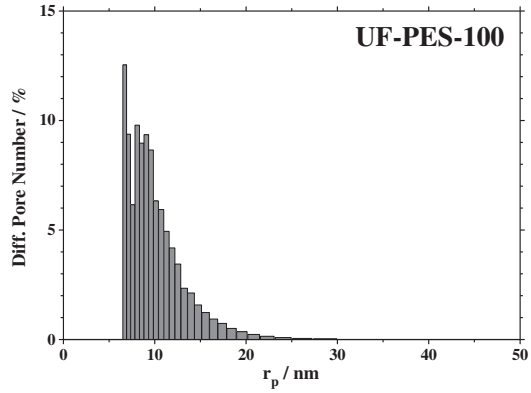

Fig. 5. Pore number distribution obtained using convective transport model.

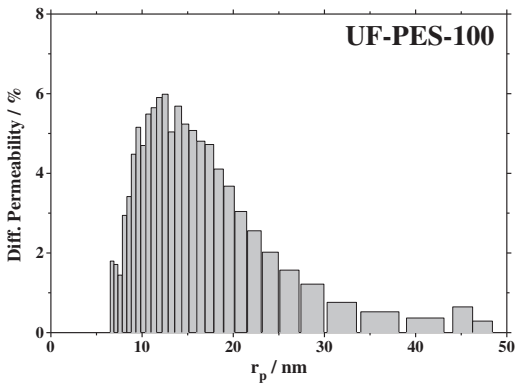

Fig. 4. Permeability distribution evaluated from data of previous figure.

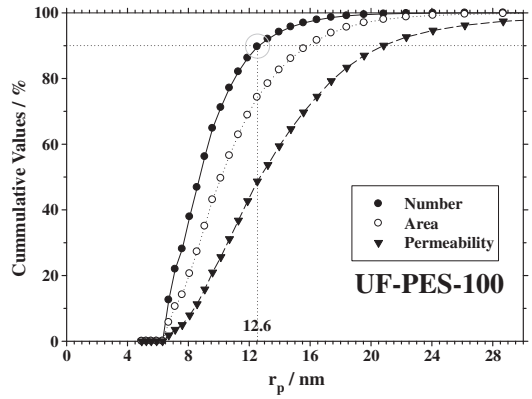

Fig. 6. Accumulative distributions of permeability, pore number and pore area, showing the calculation of the Stokes radius used for cut 90% retention cut-off estimations.

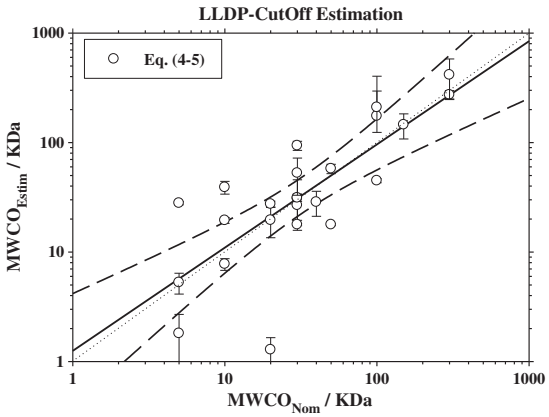

Fig. 7. Cut-off estimations from LLDP versus nominal cut-off values given by the manufacturers, using Eqs. (4) and (5).

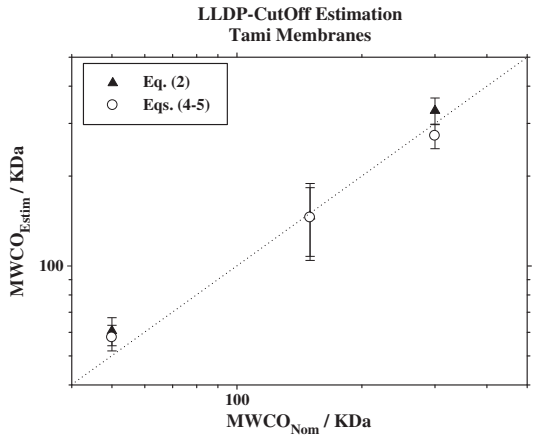

Fig. 9. Cut-off estimations from LLDP versus nominal cut-off values for several Tami Ceram-Inside ceramic membranes.

In Figs. 8 and 9 it has been compared the predictions for some membranes obtained from the same manufacturer. Specifically have been shown are polymeric membranes (Ultracel membranes from Millipore) in Fig. 8 and ceramic ones (Tami tubular membranes) in Fig. 9. It is important to take into account that manufacturers use specific rigs and dextrans to feed the system, and particular module configurations and operation rules to evaluate the cut-off of their membranes. All these explicit procedures can vary strongly from one to another manufacturer, even following the same recommended procedures. Agreement varies from one to another membrane type and manufacturer, but in all cases, Eqs. (4) and (5) seem to lead to values which fit better to the nominal values. It is worth noting that these nominal values could be not the best reference to check the real accuracy of the estimation. Probably performing retention experiments for all the samples and using similar set-up and working conditions, should be the best way to have comparative values of the retention.

Finally, Figs. 10–12 present comparisons of predictions from Eqs. (2), (4) and (5), with nominal cut-off values for several membranes of the same nominal molecular weight cut-off. This comparison is made for membranes covering most of the UF range, from 5 kDa to 100 kDa.

Again, the agreement between estimations and nominal cut-off values is variable, with some membranes leading to quite reasonable agreements. Perhaps some slightly better agreement could be distinguished for high cut-off membranes, with lower dispersions for 30 and 100 kDa, compared with those corresponding to 10 kDa (not shown here) and, especially to 5 kDa. It was already commented in the theoretical section that some of the approaches that have been used to correlate molecular weight and size, namely those given by Eqs. (4) and (5), lose some accuracy when working out of the range they have been empirically fitted for. This could be the reason of the stronger differences found at very low nominal cut-offs that actually correspond more to NF rather than to UF.

5. Conclusions

In conclusion we think that the agreement, between the MWCO evaluated from LLDP experiments and the nominal ones, is reasonable and the slight disagreement is more of a consequence of the lack of definition of the test retention parameters, that probably differ from manufacturer to manufacturer, than due to the LLDP technique.

When one takes into account that the real solution to be fractionated rarely consists in a mixture of dextrans or even have

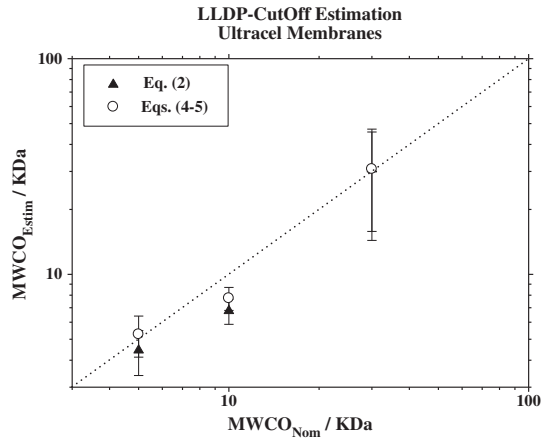

Fig. 8. Cut-off estimations from LLDP versus nominal cut-off values for several Millipore Ultracel membranes.

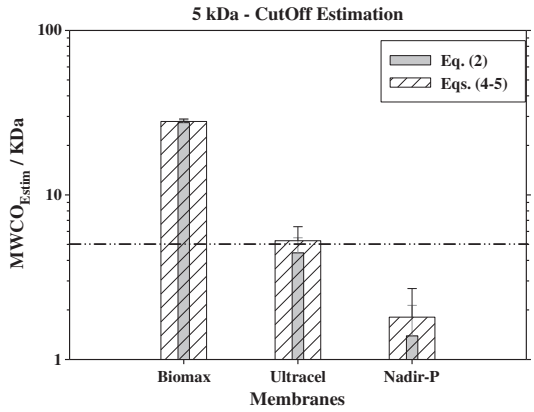

Fig. 10. Cut-off estimations from LLDP versus nominal cut-off values for several 5 kDa membranes from different manufacturers.

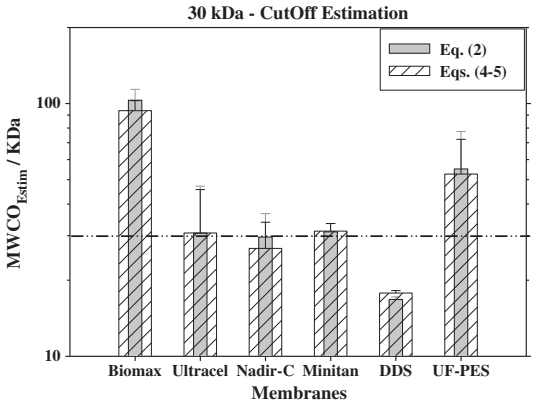

Fig. 11. Cut-off estimations from LLDP versus nominal cut-off values for several 30 kDa membranes from different manufacturers.

similar molecular shapes, aggregation, flexibility or frictional properties; it seems clear that a more easily standardized and controllable method, more directly linked to the structure of active pores, as LLDP, should be recommended to manufacturers of Ultrafiltration membranes in order to characterize them and allowing the end user to compare directly the membranes offered in the market.

This approach is not intended to substitute retention tests as definitive characterization methods for manufacturers deciding the application their membranes are aimed for. On the contrary, LLDP can help them to choose better candidates for selected applications among those developed in the corresponding research labs. Of course, retention test of the real effluents to be separated should be performed on membrane candidates to validate LLDP estimations but this procedure surely should save many expensive experiments.

Finally it must be remarked again that test retention experiments, in spite of being the de facto standard for membrane selection, are not nowadays fully standardized, and then, they can give strongly variable results when performed with different rigs and experimental procedures, in different industrial or research labs. Works in the line of this here presented, could help to define standardizable characterization procedures. Those based on combined information coming from retention tests and LLDP, along with some other possible complementary techniques could lead to clearer and fully comparable characterization results.

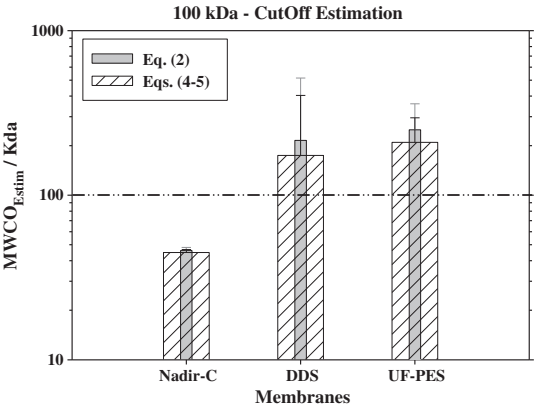

Fig. 12. Cut-off estimations from LLDP versus nominal cut-off values for several 100 kDa membranes from different manufacturers.

Acknowledgements

Spanish authors want to thank the Ministerio de Ciencia e Innovación (MCINN) for financing, under the Plan Nacional de I+D+I through projects: MAT2008-00619 and CTQ2009-07666. Also the Junta de Castilla y León has contributed through the projects BU-03-C3-2 and Grupos de Excelencia-GR18.

References

[1] A.L. Zydney, A. Xenopoulos, Improving dextran tests for ultrafiltration membranes: effect of device format, J. Membr. Sci. 291 (2007) 180–190.
[2] B. Schlichter, V. Mavrov, H. Chmiel, Comparative characterization of different commercial UF membranes for drinking water production, J. Water Supply Res. Technol. AQUA 49.6 (2000) 321–328.
[3] S. Platt, M. Mauramo, S. Butylina, M. Nyström, Retention of pegs in cross-flow ultrafiltration through membranes, Desalination 149 (2002) 417–422.
[4] J.G. Jacangelo, S.S. Adham, J.M. Laîné, Mechanisms of cryptosporidium, giardia and MS2 virus removal by MF and UF, J. AWWA 7 (1995) 107–121.
[5] P. Brown, Assessing the molecular weight cut-off value of UF membranes, Membr. Technol. 61 (1995) 7–9.
[6] K.J. Kim, A.G. Fane, R. Ben Aim, M.G. Liu, G. Jonsson, I.C. Tessaro, A.P. Broek, D. Bargeman, A comparative study of techniques used for porous membrane characterization: pore characterization, J. Membr. Sci. 87 (1994) 35–46.
[7] P. Mulherkar, R. van Reis, Flex test: a fluorescent dextran test for UF membrane characterization, J. Membr. Sci. 236 (2004) 171–182.
[8] B. Van der Bruggen, C. Vandecasteele, Modelling of the retention of uncharged molecules with nanofiltration, Water Res. 36 (2002) 1360–1368.
[9] B. Chakrabarty, A.K. Ghoshal, M.K. Purkait, Effect of molecular weight of PEG on membrane morphology and transport properties, J. Membr. Sci. 309 (2008) 209–221.
[10] J.L. Anderson, J.A. Quinn, Restricted transport in small pores: a model for steric exclusion and hindered particle motion, Biophys. J. 14 (1974) 130–150.
[11] W.M. Deen, Hindered transport of large molecules in liquid-filled pores, AIChE J. 33 (1987) 1409–1425.
[12] C. Causserand, S. Rouaix, A. Akbari, P. Aimar, Improvement of a method for the characterization of ultrafiltration membranes by measurements of tracers retention, J. Membr. Sci. 238 (2004) 177–190.
[13] W.S. Opong, A.L. Zydney, Diffusive and convective protein transport through asymmetric membranes, AIChE J. 37 (1991) 1497–1510.
[14] C. Combe, C. Guizard, E. Aimar, V. Sanchez, Experimental determination of four characteristics used to predict the retention of a ceramic nanofiltration membrane, J. Membr. Sci. 129 (1997) 147–160.
[15] W.R. Bowen, H. Mukhtar, Characterisation and prediction of separation performance of nanofiltration membranes, J. Membr. Sci. 112 (1996) 263–274.
[16] W.R. Bowen, A.W. Mohammad, Diafiltration by nanofiltration: prediction and optimization, AIChE J. 44 (1998) 1799–1812.
[17] A.W. Mohammad, N. Hilal, H. Al-Zoubi, N.A. Darwish, Prediction of permeate fluxes and rejections of highly concentrated salts in nanofiltration membranes, J. Membr. Sci. 289 (2007) 40–50.
[18] A.L. Zydney, D.M. Bohonak, Compaction and permeability effects with virus filtration membranes, J. Membr. Sci. 254 (2005) 71–79.
[19] T.D. Brock, Membrane filtration: a user's guide and reference manual, Science Tecn. Inc., Madison, WI, 1983.
[20] J.I. Calvo, A. Bottino, G. Capannelli, A. Hernández, Comparison of liquid–liquid displacement porosimetry and scanning electron microscopy image analysis to characterise ultrafiltration track-etched membranes, J. Membr. Sci. 239 (2004) 189–197.
[21] J.M. Sanz, D. Jardines, A. Bottino, G. Capannelli, A. Hernández, J.I. Calvo, Liquid–liquid porometry for an accurate membrane characterization, Desalination 200 (2006) 195–197.
[22] J.A. Otero, O. Mazarrasa, J. Villasante, V. Silva, P. Prádanos, J.I. Calvo, A. Hernández, Three independent ways to obtain information on pore size distribution of nanofiltration membranes, J. Membr. Sci. 309 (2008) 17–27.
[23] J.I. Calvo, A. Bottino, G. Capannelli, A. Hernández, Pore size distribution of ceramic UF membranes by liquid–liquid displacement porosimetry, J. Membr. Sci. 310 (2008) 531–538.
[24] R. Peinador, J.I. Calvo, P. Prádanos, L. Palacio, A. Hernández, Characterisation of polymeric UF membranes by liquid–liquid displacement porosimetry, J. Membr. Sci. 348 (2010) 238–244.
[25] R.I. Peinador, J.I. Calvo, K. ToVinh, V. Thom, A. Hernández, Liquid–liquid displacement to characterize retention of virus membranes, submitted to J. Membr. Sci., 2010.
[26] R. van Reis, A. Zydney, Bioprocess membrane technology, J. Membr. Sci. 297 (2007) 16–50.
[27] P. Aimar, M. Meireles, V. Sanchez, A contribution to the translation of retention curves into pore size distributions for sieving membranes, J. Membr. Sci. 35 (1990) 321–338.

[28] T. He, M. Frank, M.H.V. Mulder, M. Wessling, Preparation and characterization of nanofiltration membranes by coating polyethersulfone hollow fibbers with sulfonated poly(ether ether ketone) (SPEEK), J. Membr. Sci. 307 (2008) 62–72.
[29] S.R. Wickramasinghe, S.E. Bower, Z. Chen, A. Mukherjee, S.M. Husson, Relating the pore size distribution of ultrafiltration membranes to dextran rejection, J. Membr. Sci. 340 (2009) 1–8.
[30] D. Venturoli, B. Rippe, Ficoll and dextran vs globular proteins as probes for testing glomerular permselectivity: effects of molecular size, shape, charge and deformability, Am. J. Physiol. Renal. Physiol. 288 (2005) F605–F613.
[31] J.S. Schultz, R. Valentina, C.Y. Choi, Reflection coefficients of homopore membranes: the effect of molecular size and configuration, J. Gen. Physiol. 73 (1979) 49–60.
[32] L.P. Cheng, H.V. Lin, L.W. Chen, T.H. Young, Solute rejection of dextran by EVAL membranes with asymmetric and particulate morphologies, Polymer 39 (1998) 2135–2142.
[33] S. Munari, A. Bottino, G. Capannelli, P. Moretti, Membrane morphology and transport properties, Desalination 53 (1985) 11–23.
[34] CHARMME Network "Harmonization of characterization methodologies for porous membranes", EC Contract SMT4-CT 98-7518.

7 CONCLUSIONES

- Se ha diseñado y automatizado un equipo robusto y fiable de caracterización LLDP. La automatización del software del equipo esta basada en el entorno LabVIEW®, permitiendo su versatilidad y posible implementación en otros equipos similares.

- Se ha optimizado el diseño de celdas de medida adecuadas a membranas planas y tubulares, con buenas características hidrodinámicas, que faciliten la completa interacción entre las diferentes interfases líquidas minimizando la presencia de burbujas que falseen los resultados.

- El equipo diseñado y automatizado ha sido convenientemente testeado con diversas membranas comerciales procedentes de diversos fabricantes, materiales y configuraciones.
En todos los casos se ha conseguido analizar dichos filtros obteniendo de forma fiable y reproducible sus distribuciones de tamaño de poro, así como información estructural complementaria. Todo ello en rangos que van desde la UF mas abierta (centenares de KDa) a la más cerrada (decenas de KDa) o hasta membranas ya en el entorno de NF (cercanas a 1 KDa).

- Se ha comprobado la importancia de la etapa de mojado de la muestra previa a su análisis porosimétrico, etapa que se buscó optimizar con la ayuda del mojado bajo vacío.

- Se han estudiado las diversas mezclas habituales en porosimetría LLDP, intentando optimizar sus prestaciones y rango de trabajo. Se ha comprobado la notable estabilidad de la mezcla isobutanol-agua, preferida en condiciones generales. Además se ha diseñado un protocolo de utilización de la mezcla ternaria, a bajas temperaturas (15ºC) que, minimizando la volatilidad de la muestra, permite bajar sensiblemente el rango de poros analizables, acercándonos al entorno del nanómetro.

- Se ha analizado exhaustivamente la información porosimétrica obtenida por nuestro equipo LLDP, cotejándola siempre que ha sido posible, con información provenientemente de otras técnicas de caracterización tanto estructural como funcional. Se ha comprobado la correlación de la información porosimétrica con datos funcionales de retención.

- Se ha diseñado un protocolo que permite realizar una estimación razonable del MWCO de una membrana a partir únicamente de su análisis porosimétrico. Dicho protocolo se ha comprobado en numerosas membranas comerciales con un notable acuerdo en general.

A continuación se presentan las conclusiones particulares de los diversos artículos publicados como fruto de esta tesis doctoral.

Paper 1

La técnica LLDP ha demostrado precisión y reproducibilidad en la caracterización de varias membranas comerciales de polisulfona y policarbonato. Los experimentos han sido realizados con notable rapidez, dando una visión completa de la estructura de la membrana en algunas horas. Para las membranas presentando poros de forma cilíndrica, el uso de modelos de transporte apropiados permiten obtener con precisión la porosidad y la densidad de poro, mientras que para estructuras no tan regulares (como los que habitualmente se encuentran en la producción de membranas poliméricas asimétricas por inversión de fases) la técnica se puede utilizar fácilmente para estimar el MWCO, un parámetro clave para los fabricantes de membranas, sin la necesidad de realizar experimentos de retención complicados y largos en tiempo.

Paper 2

Dos series de membranas poliméricas planas han sido analizados mediante un dispositivo LLDP automatizado, preciso, exacto y rápido. Los resultados son muy interesantes, con un buen acuerdo entre las diferentes medidas de la misma muestra. También se encontró un óptimo acuerdo para experiencias realizadas utilizando diferentes mezclas líquidas y con datos de otros autores. La porosimetría de RMN es, por supuesto, un método mucho más laborioso e indirecto. Se debe tener en cuenta que la porosimetría de RMN se refiere a todos los poros o huecos presentes dentro de las membranas incluidos aquellos no abiertos al flujo. Este notable acuerdo indica que distribuciones de tamaño de poro similares están presentes tanto entre los poros abiertos como cerrados. La porosimetría de desplazamiento líquido-líquido es una técnica que ofrece no sólo la caracterización precisa de ultrafiltros, sino la flexibilidad suficiente para obtener resultados fiables en condiciones difíciles. Aquí los filtros Biomax™ han sido analizados con la técnica LLDP y la mezcla de agua-isobutanol. Intentos anteriores de utilizar un sistema de isopropanol-agua, fueron infructuosos. La posibilidad de elegir entre diferentes mezclas de líquidos, y también de seleccionar el papel que desempeñan los dos líquidos en el análisis porosimétricos, ofrece una gran ventaja y permite el análisis de muchos filtros diferentes constituidos de materiales diversos y con diversos grados de hidrofililcidad / hidrofobicidad. La técnica permite también la medición en módulos de membrana de diferentes geometrías, incluyendo membranas planas, tubulares o fibras huecas. Es probable que (junto con quizás la permoporometría) sea hoy en día la única técnica capaz de dar información rápida y precisa sobre los poros activos en las membranas de UF.

De todos modos, la técnica de LLDP debería beneficiarse de más trabajo de investigación, principalmente en la determinación de las propiedades relevantes de las mezclas líquidas habituales (por ejemplo, tensión superficial o ángulo de contacto). Especialmente interesante debería dedicarse más esfuerzo a las interesantes propiedades de mezclas ternarias, que permitan analizar los poros más pequeños y sean también menos volátiles y no tan propensas a tener cambios importantes en la composición a lo largo de la duración de la experiencia. Por último, un objetivo muy interesante debería ser correlacionar de forma eficaz la información estructural sobre tamaños de los poros con características de reten-

ción de los filtros analizados, lo que permitiría la predicción de características de rendimiento de los filtros muy eficazmente. Finalmente podemos concluir, que la técnica LLDP se puede considerar hoy en día una técnica precisa capaz de dar la información completa de la distribución de poros (PSD) en tiempos muy razonables (1-1 ½ h para la mayoría de las experiencias).

Paper 3

Hemos demostrado que los análisis LLDP pueden dar información estructural que puede ser muy razonablemente correlacionada con información funcional al analizar membranas diseñadas para la retención de virus. En este sentido, se ha demostrado que el tamaño de poro máximo obtenido por distribuciones LLDP se puede correlacionar con parámetros funcionales tan relevantes como el valor de retención logarítmico de bacteriófagos (LRV) o el más comúnmente usado, el peso molecular de corte en dextranos. Esta correlación se ajusta claramente mejor, cuando se utiliza el tamaño máximo de los poros de la distribución que si en cambio se utiliza el tamaño mínimo o el valor medio de la distribución.

Este trabajo permite prever posibles métodos de estimación de las capacidades de retención de un filtro dado, sin la necesidad de realizar experimentos de retención largos y costosos (especialmente en el caso de las membranas para la retención de virus donde se requieren medidas de control extremadamente seguras). La importancia de un método sencillo, utilizable en el proceso de desarrollo de nuevos filtros, adaptados para las aplicaciones seleccionadas en los rangos típicos de poro de las membranas de ultrafiltración de retención de virus, es reconocido por los fabricantes de membrana y laboratorios de investigación. Durante el desarrollo de nuevas membranas, diversos posibles candidatos para una aplicación dada pueden ser seleccionados. Actualmente esta selección se hace en base a un conjunto de resultados obtenidos, en una batería de ensayos de caracterización largos y costosos. En vez de efectuar estos métodos complejos, la técnica LLDP se podría utilizar para seleccionar los candidatos más adecuados en los que realizar caracterizaciones completas. Esto puede reducir fuertemente el número de pruebas y el costo de los experimentos en caracterización. Así pues, el método LLDP se debe recomendar en primer lugar a los fabricantes de membranas e instituciones de I + D. Aunque también ofrece un gran potencial para ser aplicado por posibles usuarios finales. Finalmente, la buena correlación entre LLDP y los tamaños máximos de poro y las demás pruebas de tamaño de poro, sugieren la conveniencia de una simplificación de la técnica para su detección, fácil y rápida en la detección de tamaños máximo de poro.

Paper 4

En conclusión, creemos que el acuerdo entre el MWCO evaluado a partir de experimentos LLDP y sus valores nominales, es razonable y el pequeño desacuerdo existente es más una consecuencia de la falta de definición de los parámetros de retención de pruebas, que probablemente difieren de un fabricante a otro, que debido a la técnica de LLDP. Cuando se tiene en cuenta que la solución real a tratar rara vez consiste en una mezcla

de dextranos puros o incluso éstos presentan formas moleculares similares, agregación, flexibilidad o propiedades de fricción; parece claro que un método de más fácil estandarización y control, más directamente relacionada con la estructura de los poros activos, como LLDP, se podría recomendar a los fabricantes de membranas de ultrafiltración con el fin de caracterizarlas y permitir que el usuario final pueda comparar directamente las membranas que se ofrecen en el mercado. Este enfoque no pretende sustituir las pruebas de retención como método de caracterización definitivo para el fabricante en la decisión de la aplicación a la que sus membranas están dirigidas. Por el contrario, la técnica LLDP puede ayudar a elegir los mejores candidatos para las aplicaciones seleccionadas entre aquellas membranas desarrolladas en los laboratorios de investigación correspondientes. Por supuesto, tests de retención de los efluentes reales a separar se deben realizar en los potenciales candidatos para validar las estimaciones LLDP pero este procedimiento sin duda permite ahorrar muchos experimentos caros. Por último se debe hacer notar de nuevo que los test de retención, a pesar de constituir el estándar "de facto" para la selección de la membrana, no están en la actualidad plenamente normalizados, y pueden dar resultados muy variables cuando se realizan con diferentes equipos y procedimientos experimentales, en diferentes industrias o laboratorios de investigación. Estudios en la línea del aquí presentado, podrían ayudar a definir los procedimientos de caracterización estandarizables. Los que se basan en la información combinada procedente de las pruebas de retención y LLDP, junto con algunas otras técnicas complementarias posibles podrían conducir a resultados de la caracterización claros y totalmente comparables.

7 CONCLUSIONS

- It has been designed and automated a robust and reliable LLDP characterization setup. The automation of the software in LabVIEW® environment, allows its versatility and possible implementation in other similar equipments.

- It has been optimized the cell design suitable for measuring flat and tubular membranes with good hydrodynamic characteristics that facilitate complete interaction between liquid interfaces and minimizing the presence of bubbles that falsify the results.

- The designed automated equipment has been properly tested with various commercial membranes from different manufacturers, materials and configurations. In all cases it has been able to analyze such filters obtaining in a reliable and reproducible manner their pore size distributions, as well as additional structural information. All within ranges coming from more open UF membranes (hundreds of kDa) to tighter ones (ten KDa) or membranes placed very close to the NF range (around 1 KDa).

- It has shown the importance of the sample wet stage prior to its porosimetric analysis, optimization stage which is sought with the aid of vacuum for a better wetting.

- We have studied the various mixtures usual in LLDP technique, trying to optimize its performance and range. It has been proven the remarkable stability of the isobutanol-water mixture, which is normally preferred for most conditions. Moreover we have designed a protocol using the ternary mixture at low temperatures (15°C), which minimizing the volatility of the sample, it can lower significantly the range of analyzable pores, approaching the value of nanometer.

- It has been thoroughly analyzed the information obtained by our LLDP device, comparing whenever it has been possible with other techniques coming from both structural and functional characterization. It has been proven interesting correlation between porosimetric information and functional data of retention

- We have designed a protocol that provides a reasonable estimate of a membrane MWCO from porosimetric analysis only. This protocol has been proven in many commercial membranes with generally remarkable agreement.

Below are the specific conclusions of the various articles published as a result of this thesis.

Paper one

The LLDP has shown accuracy and reproducibility on the characterization of several commercial polysulfone and polycarbonate membranes. The experiments have been per-formed with nice velocity, giving a complete picture of the membrane structure in some hours. For cylindrical shaped pores, the use of appropriate transport models allow to accurately obtain porosity and pore densities, while for not so regular structures (as those usually found in casting polymeric membranes) the technique can be easily used to estimate MWCO, a key parameter for membrane manufacturers without the necessity to perform complicate and time consuming retention experiments.

Paper two

Two series of polymeric flat membranes have been analysed using a precise, accurate and fast automated LLDP device. The results are very interesting, with a nice agreement between different runs, and also very good agreement was found for experiences performed using different liquid mixtures. A fair agreement with other authors data, have been obtained. The NMR porosimetry is of course a much more laborious and indirect method. Note that, as mentioned, the NMR porosimetry refers to all the pores or voids present within the membranes including those not opened to flux. The fair agreement should mean that similar pore size distributions are present within both open and closed pores. The liquid–liquid displacement porometry is a technique which offers not only accurate characterization of ultrafilters, but enough flexibility to get reliable results in difficult conditions. Here the Biomax™ filters have been analyzed using the LLDP technique and water–isobutanol mixture. As mentioned, previous attempts to use an isopropanol–water system, were unsuccesful. The possibility to choose among different liquid mixtures, and also to select the role that both liquids play in the porosimetric analysis offers a great advantage and allows analysing many different filters made of different material and so presenting diverse degrees of hydrophicility/hydrophobicity. The technique allows also measuring membrane modules in different geometries, including flat, tubular or hollow fibbers. It is probably (along with perhaps permporometry) the only technique nowadays able to give fast and accurate information on active pores in UF membranes.
Anyway, the LLDP technique should benefit from more work of research, mainly in the determination of the relevant properties of the usual liquid mixtures (e.g. surface tension or contact angle). Specially interesting should be to dedicate more effort to the properties of interesting ternary mixtures, that allowing to analyse smaller pores are also less volatile and not so prone to have important changes in composition along the experience duration. Finally a very interesting goal should be to effectively correlate structural information on pore sizes with retention characteristics of the analysed filters, so allowing prediction of performance characteristics of the filters from structural characterization. Finally we can conclude that the LLDP technique can be considered nowadays an accurate technique able to give the complete PSD information in very reasonable times (1–1½ h for most of the experiences).

Paper three

We have demonstrated that LLDP experiments can give structural information which can be very reasonably correlated with performance related information, when analysing membranes designed for virus retention. In this sense, we have shown that the maximum pore size obtained by LLDP distributions can be correlated with performance parameters as relevant as bacteriophages log retention value (LRV) or dextran test cut-off values. This correlation clearly fits better when using the distribution's maximum pore size instead of minimum or mean pore sizes. This work allows envisaging possible methods of estimating the retention capabilities of a given filter, without the necessity of performing time consuming and expensive retention experiments (specially in the case of virus membranes where working with active viruses or bacteriophages requires severe control measurements). The importance of such a straightforward method for the process of development of new filters, adapted for selected applications in the typical pore ranges of ultrafiltration and virus retentive membranes, will surely be recognized by membrane manufacturers and research labs. During the development of appropriate membranes, possible candidates have to be selected. Currently this is done on the basis of results obtained in a battery of time consuming and expensive membrane characterization tests. Instead of these complex methods, LLDP could be used to select the most appropriate candidates on which to perform complete characterizations. This can strongly reduce the number of tests and the cost of characterization experiments. Thus the LLDP method should be recommended for membrane manufacturers and R+D institutions in the first place, moreover it offers a great potential to be developed towards a customer application. Finally, the good correlation between LLDP maximum pore sizes and the other pore size tests suggest the convenience of a simplification of the technique to the easy and rapid detection of maximum pore sizes.

Paper four

In conclusion we think that the agreement, between the MWCO evaluated from LLDP experiments and the nominal ones, is reasonable and the slight disagreement is more of a consequence of the lack of definition of the test retention parameters, that probably differ from manufacturer to manufacturer, than due to the LLDP technique. When one takes into account that the real solution to be fractionated rarely consists in a mixture of dextrans or even have similar molecular shapes, aggregation, flexibility or frictional properties; it seems clear that a more easily standardized and controllable method, more directly linked to the structure of active pores, as LLDP, should be recommended to manufacturers of Ultrafiltration membranes in order to characterize them and allowing the enduser to compare directly the membranes offered in the market. This approach is not intended to substitute retention tests as definitive characterization methods for manufacturers deciding the application their membranes are aimed for. On the contrary, LLDP can help them to choose better candidates for selected applications among those developed in the corresponding research labs. Of course, retention test of the real effluents to be separated should be performed on membrane candidates to validate LLDP estimations but this

procedure surely should save many expensive experiments. Finally it must be remarked again that test retention experiments, in spite of being the defect to standard for membrane selection, are not nowadays fully standardized, and then, they can give strongly variable results when performed with different rigs and experimental procedures, in different industrial or research labs. Works in the line of this here presented, could help to define standardizable characterization procedures. Those based on combined information coming from retention tests and LLDP, along with some other possible complementary techniques could lead to clearer and fully comparable characterization results.